

Cover Page



Universiteit Leiden

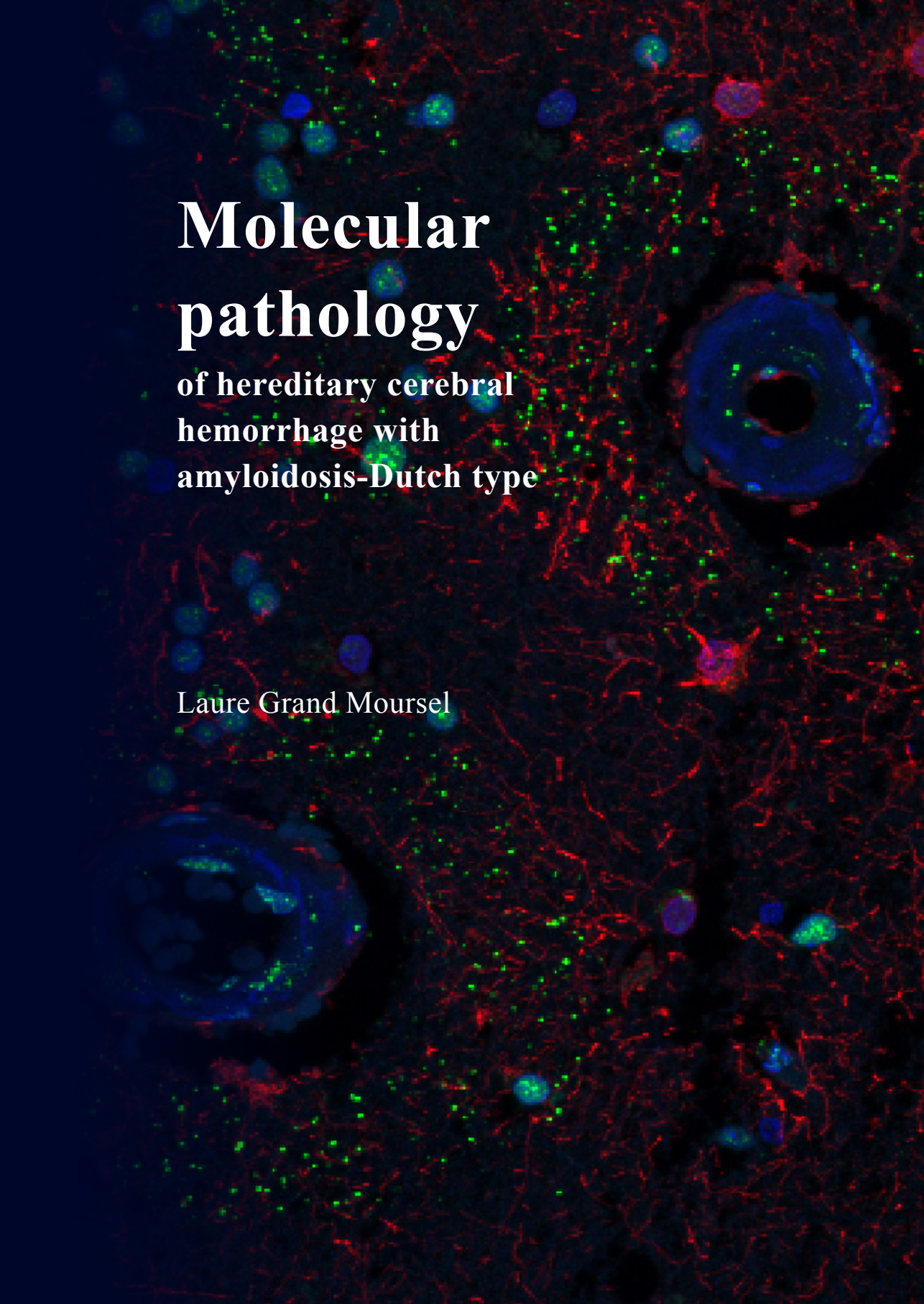


The handle <http://hdl.handle.net/1887/80759> holds various files of this Leiden University dissertation.

Author: Grand Moursel, L.

Title: Molecular pathology of hereditary cerebral hemorrhage with amyloidosis-Dutch type

Issue Date: 2019-11-21

The background of the cover is a fluorescence microscopy image of brain tissue. It features a dense network of red-stained fibers, likely representing the amyloid-beta protein. Scattered throughout are numerous blue-stained circular structures, which are likely neurons or nuclei. Some of these blue structures show internal green or red staining, indicating the presence of specific markers or plaques. The overall appearance is that of a complex, interconnected neural network with significant pathological changes.

**Molecular
pathology**
of hereditary cerebral
hemorrhage with
amyloidosis-Dutch type

Laure Grand Moursel

Molecular pathology of hereditary cerebral hemorrhage with amyloidosis-Dutch type

Laure Grand Moursel

Molecular pathology of hereditary cerebral hemorrhage with amyloidosis-Dutch type

Proefschrift

Ter verkrijging van de graad van Doctor aan de Universiteit Leiden, op gezag van Rector Magnificus Prof. mr. C.J.J.M. Stolker, volgens besluit van het College voor Promoties te verdedigen op

Donderdag 21 November 2019 klokke 10.00 uur.

door

Laure Grand Moursel

geboren te Angoulême, Frankrijk in 1979

© 2019, Laure Grand Moursel
ISBN: 978-94-93184-08-4

Layout and printing: Guus Gijben, proefschrift-aio.nl

Copyrights of published material in chapters 2 to 6 lies with the publisher of the journal listed at the beginning of each chapter.

All rights preserved. No part of this thesis may be reproduced in any form, by print, photocopy, digital file, internet, or any other means without permission of the copyright holder.

Promotor
Prof. dr. M.A. van Buchem

Co-promotores
Dr. L. van der Weerd
Dr. W.M.C. van Roon-Mom

Leden promotiecommissie:
Prof. dr. P. ten Dijke
Prof. dr. Ir. S.M. van der Maarel
Prof. dr. M.J.H. Wermer
Dr. M.M.M. Wilhelmus (VUmc, Amsterdam)
Prof. dr. H.E. de Vries (VUmc, Amsterdam)

The work presented in this thesis was supported by grants from the Bontius stichting (Leiden), the Dutch CAA foundation (Rotterdam) and by the Netherlands Organization for Scientific Research (NWO, The Hague), under research program VIDI, project ‘Amyloid and vessels’, number 864.13.014.

Printing of this thesis was financially supported by Alzheimer Nederland (Amersfoort) and by the Leiden University Medical Center.

Table of contents

Chapter 1: General introduction	7
Chapter 2: Amyloid β in hereditary cerebral hemorrhage with amyloidosis-Dutch type	27
Chapter 3: TGF β pathway deregulation and abnormal phospho-SMAD2/3 staining in hereditary cerebral hemorrhage with amyloidosis-Dutch type	49
Chapter 4: Cerebral amyloid angiopathy with vascular iron accumulation and calcification: a high-resolution MRI-histopathology study	75
Chapter 5: Osteopontin and phospho-SMAD2/3 are associated with calcification of vessels in D-CAA, an hereditary cerebral amyloid angiopathy	91
Chapter 6: Brain Transcriptomic Analysis of Hereditary Cerebral Hemorrhage With Amyloidosis-Dutch Type	111
Chapter 7: General discussion	135
Appendices	153
Summary	153
Nederlandse samenvatting	157
List of publications	161
List of abbreviations	165
Curriculum vitae	169
Acknowledgements	171

Chapter 1

Introduction

Introduction

Hereditary cerebral hemorrhage with amyloidosis-Dutch type (HCHWA-D) is an autosomal dominant hereditary disease caused by a missense mutation on chromosome 21 in the amyloid precursor protein (APP), resulting in a glutamine for glutamic acid substitution (NP_000475.1:p.Glu693Gln, known as APP E693Q) (1). HCHWA-D patients suffer predominantly from hemorrhagic strokes, infarcts, and vascular dementia (2). The so-called APP “Dutch” mutation, originally described in families from small coastal villages in the Netherlands, is characterized by a severe Cerebral Amyloid Angiopathy (CAA) pathology.

The term CAA pathology is first used by Mandybur in 1975 (3) and is defined by the progressive accumulation of amyloid beta ($A\beta$) in the cerebrovasculature, resulting in acellular thickening of the vessel wall (4). CAA pathology is a risk factor for lobar intracerebral hemorrhages (ICH) (5) and for ischemic cerebral infarction (6). Because it disrupts the delicate cerebral vascular homeostasis, it can have both hemorrhagic and/or ischemic consequences (7).

HCHWA-D has been first described as the familial occurrence of ICH (8) but associated with the cerebrovascular pathology of Alzheimer’s disease (AD) only twenty-four years later (9). Shortly after, the Dutch mutation is identified as the first missense mutation associated with the AD phenotype (1), due to the shared pathological brain $A\beta$ deposition. In AD $A\beta$ is aggregating in parenchymal plaques but CAA is also found in 80 to 90% of AD cases from autopsy series (10–17). Therefore the vasculotropic Dutch- $A\beta$ peptide has been extensively studied to unravel the etiology of AD cerebrovascular pathology (references in this chapter).

$A\beta$ is a 4kDa peptide resulting from APP cleavage by processing enzymes (α - and β -secretases cleaving the N-terminal peptide and γ -secretases cutting the C-terminal). Although α -secretase cleavage results in a benign pathway, $A\beta$ peptides produced by β -secretase cleavages can aggregate and form different $A\beta$ species ranging from monomers to fibrils. The Dutch mutation is located near the α -secretase cleavage site of APP, and is thought to affect the APP processing (18). The $A\beta$ peptide with the Dutch mutation is also known as $A\beta$ E22Q, as the modification occurs in position 22 (when using $A\beta$ peptide amino acid numbering). Depending on which cleavage site is used, different $A\beta$ peptides are formed. Most studied isoforms are $A\beta$ (1-40) (or $A\beta$ 40, 40 amino acids) and $A\beta$ (1-42) (or $A\beta$ 42, 42 amino acids) but many N-terminal and C-terminal truncated peptides coexists in HCHWA-D (19), adding complexity to the aggregation process of the peptides.

Clinicopathology of HCHWA-D

White matter lesions (recognized as white matter hyperintensities [WMHs] in magnetic resonance imaging [MRI] scans) are the earliest radiological manifestations in pre-symptomatic mutation carriers (detectable in standard 1.5 Tesla [T] scan). Although more subtle, the grey matter is also affected by cortical thinning in relatively young mutation carriers (mean age 46 years) when compared at 3T MRI to a control group (20). Cortical microinfarcts detected at high resolution 7T MRI are also more prevalent in pre-symptomatic patients than in controls (21). WMHs are located in subcortical areas, and tend to be more severe in the occipital lobe (22). Other radiological manifestations such as microbleeds, intracerebral hemorrhages, superficial siderosis, convexity subarachnoid hemorrhages and microinfarcts, have a higher prevalence in symptomatic patients.

Strokes in HCHWA-D are mostly hemorrhagic but ischemic strokes can also occur. The hemorrhages mostly involve temporal and occipital lobes and occur predominantly in the deeper cortical layers and in subcortical white matter (2) but can be present in the cerebral cortex as well and tend to spare the frontal lobes (23). According to the latest clinical data, the first stroke (mean age onset 54 ± 8 years, $n=58$) is fatal in only 14% of the cases (against two- third of patients 23 years ago; (2)) and the majority of hemorrhages (35%) are located in the occipital lobe followed by the parietal lobe (21%) (24). The mean number of strokes is 3 (range 0-10 strokes) and the mean survival after the first stroke is 10 years (range 0-28 years). Epilepsy occurs in about half of the patients who have suffered from one or more strokes (25). Cognitive decline can precede the onset of hemorrhagic strokes (22) although in a recent study, cognitives abnormalities are not detected in presymptomatic mutation carriers ($n=12$, (21)). Cognitive decline frequently occurs in a stepwise fashion between stroke episodes (26,27).

Neuropathological features of HCHWA-D

CAA pathology in HCHWA-D is widespread and invariably affects cerebral and cerebellar meningeal arteries and cerebrocortical arterioles with a higher severity occipitally (23). The amyloid angiopathy is believed to progress from the leptomeninges towards the neocortex and in most severe cases subcortical white matter and capillaries are involved (vessels anatomy in **Figure 1**). Subcortical white matter shows areas of demyelination, axonal loss, and gliosis (leukoencephalopathy). Tau pathology (one of the neuropathological hallmarks of AD) in HCHWA-D is rare and not associated with dementia (28).

$A\beta$ protein deposition starts at the abluminal basement membrane of vascular smooth muscle cells (VSMCs; grade 1 CAA, **Figure 2A**). At later

stages, amyloid fibrils are observed between VSMCs and in heavily affected vessels, VSMCs are completely displaced by the amyloid (grade 2 CAA, **Figure 2B**). With CAA progression, additional radial layers of A β (one or two) around a layer of homogeneous A β develop in cerebrocortical arterioles at the level of cortical layers II–III of severe cases (absent in leptomeninges and cerebellum) (23,29). Vessels with radial A β are associated with degenerating neurites, reactive astrocytes and activated microglia [30, Maatschieman p227].

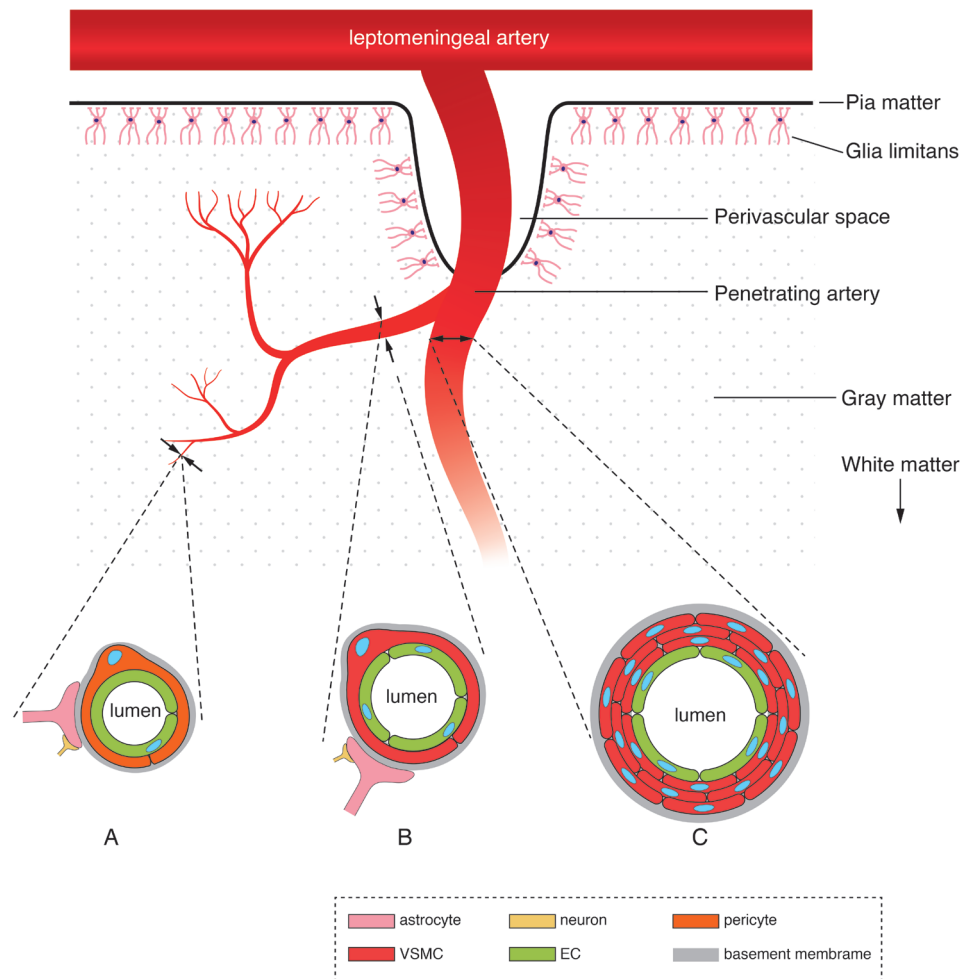


Figure 1: Illustration of the cortical brain vessels anatomy and details of the vascular components in (A) a capillary at the neurovascular unit (NVU), (B) an arteriole and (C) a penetrating artery.

Non-fibrillar A β clouds and fine diffuse plaques in the parenchyma tend to disappear with age and suggests a clearance of non-fibrillar parenchymal A β by glial cells in early stage of the disease (23,31). Indeed, although non-activated glial cells (astrocytes and microglia) are bearing cytoplasmic A β granules, activated glial cells in fibrillar deposits (parenchymal or perivascular associated with CAA) are devoid of A β granules. This suggests that glial response to fibrillar A β is not clearly linked with A β removal (32). Consequently, in contrast to parenchymal A β , CAA severity defined by CAA load and vessel wall thickening tends to intensify with age, even though it might differ considerably between patients of comparable age (28).

Further, disease progression in HCHWA-D is also associated with secondary microvascular degenerations or CAA-associated microvasculopathies such as vascular fibrosis (or hyalinization), microaneurysms, macrophage infiltration, “vessel-within-vessel” configurations (grade 3 CAA in **Figure 2C**), calcifications and vascular thrombi (33). CAA-associated microvasculopathies correlate with the number of cerebrovascular lesions (CAA-associated hemorrhages and/or infarcts; (34)) and with dementia diagnosis (28).

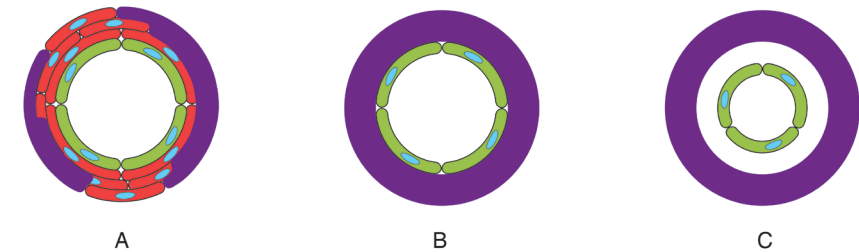


Figure 2: Illustration of CAA severity grading (based on Vonsattel & Greenberg hemorrhage risk scale 1 to 3,(106)). (A) Grade 1 CAA. Start of amyloid deposits (purple colour). (B) Grade 2 CAA. The media of this cortical vessel is fully replaced by amyloid and the wall is thickened. (C) Grade 3 CAA. Example of secondary microvasculopathies classified as grade 3, here a cracking of the vessel wall that creates a “vessel-within-vessel” appearance.

A β -associated proteins found in vascular deposits are investigated in HCHWA-D. Similarly to findings in AD, Amyloid P-component and Apolipoprotein E (ApoE) are identified in vascular and parenchymal A β (35–37). Particularly, APP and CystatinC immunoreactivity are strongly associated with CAA in HCHWA-D (38,39). Inflammatory proteins are not investigated in HCHWA-D brains except for the presence of complement proteins in amorphous plaques (40) and the association of molecular chaperone proteins with CAA (HspB8, Hsp20 and Hsp27), which could

mediate inflammatory reactions (41). The occurrence of other proteins could also vary depending on the type of material used (cryosections vs formalin-fixed and antibodies specificities). As such the presence of heparan sulfate proteoglycans found by van Horssen (42) but not by van Duinen (43), α 1-antichymotrypsin found by Timmers (35), but not by Rozenmuller (40) and low-density lipoprotein receptor-related protein-1 (LRP-1) found by Wilhelmus (44), but not by Deane (45) are a matter of debate.

One characteristic feature in HCHWA-D is the presence extracellular matrix (ECM) parenchymal coarse deposits presenting a strong immunoreactivity for several ECM components (HSPG, laminin, collagen type 3 and 4), clustering around thick-walled A β vessels, but not associated with A β plaques. Collagen type 1 and 3 and fibronectin are associated with strongly A β -laden arterioles (43). Interestingly, lysyl oxidase (LOX) and tissue transglutaminase (tTG), which are enzymes cross-linking ECM-proteins, are associated with angiopathic vessels in HCHWA-D (46,47). Laminin, fibronectin, HSPG, and collagen are substrate for these enzymes whose reaction might participate in CAA formation.

Pathomechanisms of HCHWA-D

In vitro studies in human cerebrovascular cells have largely demonstrated a higher toxicity of the synthetic A β Dutch peptide compared to the wild type peptide (48–54). More precisely, with the Dutch mutation, a charged residue is substituted with an uncharged residue that results in higher oligomer stability favorizing the formation of these non-fibrillar toxic assemblies (55–58). Moreover, Dutch amyloid seeds, have prion-like effect on WT A β and are thus harmful and irreversible (59).

Amyloid deposits in HCHWA-D are a mixture of wild type and Dutch variant (60,61). Whereas CAA in general is mostly composed of A β 40 and to a less extent of A β 42, it is hypothesized that the Dutch mutated A β 42 might seed and trigger the CAA formation. Indeed, both Dutch-mutated A β 40 and wild type A β 40 are present in isolated vessels from brain tissue, but only the Dutch-mutated A β 42, and not the wild-type A β 42 is detected (19). Moreover, histological studies with C-terminal specific antibodies have shown that A β 42 precedes A β 40 deposition in cortical arterioles (23). In addition, electronic microscopy identified non-fibrillar A β 42 as the first species deposited in the basement membrane of capillaries (62).

The vascular pathogenicity of the Dutch mutation is also influenced by an increase in the A β 40:A β 42 ratio (63), as demonstrated in transgenic mice overexpressing in neurons the human APP gene with the E693Q mutation (64). This mouse model, called APP Dutch model, develops an extensive CAA pathology (around 22-25 months) composed of A β 40 predominantly with few diffuse A β 42 parenchymal plaques similar to the neuropathology

of HCHWA-D. Increase in A β 42 concentration by crossing with a PS45 transgenic line (familial AD-causing PS1 mutations) resulted in abundant parenchymal plaque formation at a young age, with limited CAA pathology (64).

So far, no risk factors have been linked with the clinical symptoms of HCHWA-D. In particular, the ApoE genotype (influence on CAA pathology described in the next section) and the polymorphism in the Presenilin (PS) 1 gene, both highly impacting A β transport and processing, have been investigated and did not show any significant association with the disease phenotype (65,66). Only gender may modulate the phenotypic expression of the mutation, indeed the mortality rate is respectively significantly higher for female but lower for individuals with a maternal transmission (67). Nevertheless the reason is unidentified and a recent study on a smaller cohort did not confirm the gender association with the mortality rate (24).

The Dutch mutation can also alter other mechanisms having influence on A β accumulation and clearance from interstitial cerebral fluid. It is suggested from *in vitro* studies that the mutation could enhance the resistance to proteolytic degradation (68,69) thereby reducing the A β turnover rate, while A β production rate seemed unaffected (70–73). Furthermore, altered affinity changes due to the Dutch mutation affects A β transport across the blood-brain-barrier (74). One explanation could be a lower affinity for LRP1 which could affect the LRP-mediated brain capillary clearance (45).

Pathomechanisms such as alteration in vessel wall integrity (VSMCs disappearance), activation of perivascular cell (astrogliosis and microgliosis) and disturbances in peripheral drainage (basement membrane thickening), although more severe in HCHWA-D, are shared features of all CAA pathologies (75–78).

CAA pathology: sporadic CAA (sCAA) and AD with CAA

CAA pathology is frequent in normal ageing, may be asymptomatic in mild cases (79), but is an important cause of spontaneous lobar ICH (80). When taken at any level of severity, in population-based (>85 years) and community-based (median age 88.5) studies, neuropathological evidence of CAA are recorded in respectively 69.6% and 78.9% of autopsied cases (81,82). Earlier studies have related that CAA pathology is related to cognitive impairment and dementia in ageing (83). It is in addition recently proposed that besides being more prevalent among AD patients, CAA might induces an independent cognitive contribution to AD dementia (81,84).

CAA pathology in AD with CAA or in sCAA are intermingled disorders closely resembling at pathological investigation when solely regarding at A β vascular deposition (29). A distinction is made in subjects which rely both on the clinical diagnosis of dementia and on the definite neuropathologic

examination (tau pathology seen as neurofibrillary tangles) presence is a hallmark in AD). Both in AD with CAA and in sCAA, subjects can present an hemorrhagic phenotype which is related to CAA severity. Indeed, in AD with CAA, CAA pathology is predominantly mild to moderate but cases with the higher frequency of hemorrhages had also a more severe CAA (85). Likewise, in sCAA cases presenting lobar ICH, CAA pathology severity is, in general higher (86,87).

Besides ageing, which is the strongest known clinical risk factor for developing CAA pathology (88), certain genetic risk factors have been identified. As in AD, ApoE genotype is strongly associated with CAA pathology and has influence on the pathophysiology of CAA (89–91). ApoE ϵ 2 and ApoE ϵ 4 are related to more severe CAA but only ApoE ϵ 4 is linked with capillary involvement (92,93). Carriers of ApoE ϵ 2 risk are more at risk for CAA-related hemorrhages (87,91,94). Other non-ApoE gene polymorphisms have been compared in a meta-analysis and the strongest association with CAA pathology are found for the transforming growth factor β 1 gene (TGF β 1), the translocase of outer mitochondrial membrane 40 gene (TOMM40) and the complement component receptor 1 gene (CR1) (95).

Interestingly, TGF β 1 expression modulates the CAA phenotype. In transgenic mice, both astrocytic or neuronal overexpression of TGF β 1 resulted in cerebral angiopathy due to an increase in vascular fibrosis (96,97). Moreover, co-overexpression of TGF β 1 and APP in mice resulted in a reduction in parenchymal A β plaque load with CAA increase (98). Multiple studies have shown a role for TGF β 1 in promoting APP and A β production by astrocytes *in vitro* (99–102) but also *in vivo* with increased endogenous APP and A β levels in TGF β 1-astrocytic mouse model (102). However, whether these animal models actually accumulate murine A β is likely mouse strain-dependant (103). In VSMCs, TGF β 1 associated to ApoE4 protein strongly increased the amount of cellular A β (104) and enhances A β internalization in a dose-dependent manner [30, Prior & Urmoneit p255].

Two different CAA grading methods, both based on A β staining, are primarily referred to in neuropathological studies. A first semi-quantitative approach is ranking CAA mostly based on its spreading from leptomeninges to intracortical area (105). A second approach focused on the vessel wall morphology of individual vessel, is assessing a scale ranging from 1 to 3 for hemorrhage risk (106), as illustrated in **Figure 2**. More recently, two similar approaches have been proposed for CAA pathologic assessment (16,107) in an attempt to find a consensus on a single method to assess CAA severity.

HCHWA-D: a model to study biomarkers & therapy for CAA pathology

Totally reliable and noninvasive diagnostic tests of CAA pathology as well as anti-CAA therapy do not exist. Therefore HCHWA-D, as an accepted monogenetic model of CAA pathology, is useful to develop biomarkers (either radiologic imaging or molecular signature) and to find new therapeutic targets.

Neuroimaging biomarkers of CAA pathology at MRI are developed in symptomatic (after first clinically assessed stroke) and pre-symptomatic HCHWA-D patients. In particular, the current diagnostic Boston criteria (based on the pattern of hemorrhagic lesions and superficial siderosis to assess probable CAA during life) have been evaluated and its sensitivity was improved by the inclusion of microbleed counts (108). Lately, two studies identified early imaging biomarkers (before cognitive symptoms and ICH) for CAA pathology diagnosis by inclusion of presymptomatic carriers. In the first study, WMHs and microinfarcts which are ischaemic manifestations of CAA have been detected with high field (3T) and ultra-high field (7T) MRI (21). In the second study measuring regional cerebral blood flow (by Blood-Oxygen-Level Dependent functional MRI or BOLD fMRI), an altered vascular reactivity to visual stimulation in occipital lobe was detected in pre-symptomatic mutation carriers (109). More recently, a striped cortex appearance on 7T MRI (visualized as hypointense lines perpendicular to the pial surface) solely detected in 40% of symptomatic patients (n=15) has for that reason been described as a neuroimaging marker of advanced CAA pathology (110).

Fluid biomarkers, in particular A β , sAPP and Tau (total tau, and phosphorylated tau) protein levels in plasma and cerebrospinal fluid (CSF) are the most common studied biomarkers in amyloid beta related pathologies. In HCHWA-D, A β 42 level in plasma are decreased (111) although no difference are perceived in sCAA (112). In CSF, pronounced decreased levels of A β 40 and A β 42 are measured in HCHWA-D pre-symptomatic mutation carriers (113) and less pronounced but consistent decreased levels are found in sCAA (114,115).

Lastly, other AD specific biomarkers have been tested in an HCHWA-D western Australian family. Pulpil flash response, which is linked to cholinergic deficit in AD, is reduced in mutation carriers and deserves further investigation (116). In the same study, mutation carriers tested with positron emission tomography imaging with Pittsburgh compound B (PiB-PET) showed a higher compound retention, although below the standard threshold for amyloid positivity in AD.

So far, the above mentioned biomarkers can estimate CAA pathology but none of them can precisely determine its severity, nor predict hemorrhagic

risk, nor assess with certainty the efficiency of a therapy. More specific biomarkers are highly needed in clinical trials of A β disease-modifying therapies (117). Although no therapy exist against CAA, besides focusing on amyloid removal therapies uniquely, alternative paths targeting aggravating factors of CAA pathology could help slowing down the CAA build up and delay the onset of symptoms.

Scope and outline of this thesis

The general aim of this thesis is to disentangle the molecular pathogenesis behind CAA formation in HCHWA-D. Since no proven therapeutic treatment exists to prevent or even delay the CAA pathology, understanding the underlying pathomechanisms in HCHWA-D is important and may lead to identification of potential therapeutic targets.

Chapter 2 review the literature on HCHWA-D pathogenesis, combining neuropathological and *in vitro* findings and focusing in particular on the role of ECM in HCHWA-D.

Former research in CAA field indicates the existence of factors able to influence A β to accumulate predominantly in vessels rather than in brain parenchyma, such as TGF β . Identification of aggravating factors of CAA pathology that can interact with currently approved drugs is one area of investigation and therefore we explored in **Chapter 3** TGF β pathway activation in HCHWA-D compared to sCAA.

In order to interpret imaging findings and better evaluate the disease progression **chapter 4 & 5** are dedicated to calcifications in HCHWA-D, a specific CAA-associated microvasculopathy. **Chapter 4** is a histopathological study assessing the histological correlate of a recently discovered MRI radiologic finding in HCHWA-D. **Chapter 5** is exploring the pathomechanisms leading to these abnormalities and tries to assess the relationship of these changes and the TGF β findings from chapter 3.

Chapter 6 is an exploratory transcriptomic study to identify major deregulated pathways in HCHWA-D and broaden our comprehension of molecular pathogenesis.

References

1. Levy E, Carman MD, Fernandez-Madrid IJ, Power MD, Lieberburg I, Van Duinen SG, et al. Mutation of the Alzheimer's disease amyloid gene in hereditary cerebral hemorrhage, Dutch type. *Science* (80-). 1990 Jun 1;248(4959):1124–6.
2. Wattendorff AR, Frangione B, Luyendijk W. Hereditary cerebral hemorrhage with amyloidosis, Dutch type(HCHWA-D): clinicopathological studies. *J Neurol Neurosurg psychiatry*. 1995;58:699–705.
3. Mandybur TI. The incidence of cerebral amyloid angiopathy in Alzheimer's disease. *Neurology*. 1975 Feb;25(2):120–6.
4. Attems J, Jellinger K, Thal DR, Van Nostrand W. Review: Sporadic cerebral amyloid angiopathy. *Neuropathol Appl Neurobiol*. 2011 Feb;37(1):75–93.
5. Kimberly WT, Gilson A, Rost NS, Rosand J, Viswanathan A, Smith EE, et al. Silent ischemic infarcts are associated with hemorrhage burden in cerebral amyloid angiopathy. *Neurology*. 2009 Apr;72(14):1230–5.
6. Cadavid D, Mena H, Koeller K, Frommelt RA. Cerebral beta amyloid angiopathy is a risk factor for cerebral ischemic infarction. A case control study in human brain biopsies. *J Neuropathol Exp Neurol*. 2000 Sep;59(9):768–73.
7. Van Nostrand WE. The influence of the amyloid β -protein and its precursor in modulating cerebral hemostasis. *Biochim Biophys Acta - Mol Basis Dis*. 2015;
8. Luyendijk W, Schoen JH. Intracerebral Hematomas. a Clinical Study of 40 Surgical Cases. *Psychiatr Neurol Neurochir*. 1964;67:445–68.
9. Luyendijk W, Bots GT, Vegter-van der Vlis M, Went LN, Frangione B. Hereditary cerebral haemorrhage caused by cortical amyloid angiopathy. *J Neurol Sci*. 1988 Jul;85(3):267–80.
10. Vinters H V, Gilbert JJ. Cerebral amyloid angiopathy: incidence and complications in the aging brain. II. The distribution of amyloid vascular changes. *Stroke*. 1983;14(6):924–8.
11. Vonsattel JPG, Myers RH, Tessa Hedley Whyte E, Ropper AH, Bird ED, Richardson EP. Cerebral amyloid angiopathy without and with cerebral hemorrhages: A comparative histological study. *Ann Neurol*. 1991 Nov;30(5):637–49.
12. Esiri MM, Wilcock GK. Cerebral amyloid angiopathy in dementia and old age. *J Neurol Neurosurg Psychiatry*. 1986 Nov;49(11):1221–6.
13. Kalaria RN, Ballard C. Overlap between pathology of Alzheimer disease and vascular dementia. *Alzheimer Dis Assoc Disord*. 1999;13 Suppl 3:S115-23.
14. Jellinger KA. Alzheimer disease and cerebrovascular pathology: An update. *J Neural Transm*. 2002 May;109(5–6):813–36.
15. Love S, Miners S, Palmer J, Chalmers K, Kehoe P. Insights into the pathogenesis and pathogenicity of cerebral amyloid angiopathy. *Front Biosci (Landmark Ed)*. 2009 Jan;14:4778–92.
16. Owsley C, McGwin G, Sloane ME, Stalvey BT, Wells J. Timed instrumental activities of daily living tasks: Relationship to visual function in older adults. *Optom Vis Sci*. 2001;78(5):350–9.
17. Arvanitakis Z, Leurgans SE, Wang Z, Wilson RS, Bennett DA, Schneider JA. Cerebral amyloid angiopathy pathology and cognitive domains in older persons. *Ann Neurol*. 2011 Feb;69(2):320–7.

18. De Strooper B, Annaert W. Proteolytic processing and cell biological functions of the amyloid precursor protein. *J Cell Sci.* 2000 Jun;113 (Pt 1):1857–70.
19. Nishitsuji K, Tomiyama T, Ishibashi K, Kametani F, Ozawa K, Okada R, et al. Cerebral Vascular Accumulation of Dutch- Type Ab42 , but Not Wild-Type Ab42 , in Hereditary Cerebral Hemorrhage With Amyloidosis , Dutch Type. *J Neurosci Res.* 2007;2923:2917–23.
20. Fotiadis P, van Rooden S, van der Grond J, Schultz A, Martinez-Ramirez S, Auriel E, et al. Cortical atrophy in patients with cerebral amyloid angiopathy: a case-control study. *Lancet Neurol.* 2016 Jul;15(8):811–9.
21. van Rooden S, van Opstal AM, Labadie G, Terwindt GM, Wermer MJH, Webb AG, et al. Early Magnetic Resonance Imaging and Cognitive Markers of Hereditary Cerebral Amyloid Angiopathy. *Stroke.* 2016 Dec;47(12):3041–4.
22. Bornebroek M, Haan J, Maat-Schieman ML, Van Duinen SG, Roos R a. Hereditary cerebral hemorrhage with amyloidosis-Dutch type (HCHWA-D): I--A review of clinical, radiologic and genetic aspects. *Brain Pathol.* 1996 Apr;6(2):111–4.
23. Maat-schieman M, Roos R, Duinen S Van, van Duinen S. Review Article Hereditary cerebral hemorrhage with amyloidosis- Dutch type. *Neuropathology.* 2005 Dec;25(February):288–97.
24. Van Etten ES, Guroi ME, Van Der Grond J, Haan J, Viswanathan A, Schwab KM, et al. Recurrent hemorrhage risk and mortality in hereditary and sporadic cerebral amyloid angiopathy. *Neurology.* 2016;87(14):1482–7.
25. Bornebroek M, Haan J, Roos RAC. Hereditary cerebral hemorrhage with amyloidosis - Dutch type (HCHWA-D): A review of the variety in phenotypic expression. *Amyloid.* 1999 Sep;6(3):215–24.
26. Bornebroek M, Haan J, Van Buchem MA, Lanser JBK, Simone De Vries-vd Weerd MAC, Zoetewij M, et al. White matter lesions and cognitive deterioration in presymptomatic carriers of the amyloid precursor protein gene codon 693 mutation. *Arch Neurol.* 1996;53(1):43–8.
27. Haan J, Lanser JB, Zijderveld I, van der Does IG, Roos RA. Dementia in hereditary cerebral hemorrhage with amyloidosis-Dutch type. *Arch Neurol.* 1990 Sep;47(9):965–7.
28. Natté R, Maat-Schieman MLC, Haan J, Bornebroek M, Roos RAC, Van Duinen SG. Dementia in hereditary cerebral hemorrhage with amyloidosis-Dutch type is associated with cerebral amyloid angiopathy but is independent of plaques and neurofibrillary tangles. *Ann Neurol.* 2001 Dec;50(6):765–72.
29. Maat-Schieman MLC, Van Duinen SG, Bornebroek M, Haan J, Roos RAC. Hereditary cerebral hemorrhage with amyloidosis-Dutch type (HCHWA-D): II - A review of histopathological aspects. *Brain Pathol.* 1996 Apr;6(2):115–20.
30. Verbeek M, de Waal R, Vinters HV E. Cerebral amyloid angiopathy in Alzheimer's disease and related disorders. Vinters MMV• RMW de W• H V., editor. Dordrecht, the Netherlands: Kluwer Academic Publishers; 2000.
31. Maat-Schieman MLC, Yamaguchi H, Van Duinen SG, Natté R, Roos RAC. Age-related plaque morphology and C-terminal heterogeneity of amyloid β in Dutch-type hereditary cerebral hemorrhage with amyloidosis. *Acta Neuropathol.* 2000 Apr;99(4):409–19.
32. Maat-Schieman MLC, Yamaguchi H, Hegeman-Kleinn IM, Welling-Graafland C, Natté R, Roos RAC, et al. Glial reactions and the clearance of amyloid β protein in the brains of patients with hereditary cerebral hemorrhage with amyloidosis-Dutch type. *Acta Neuropathol.* 2004 May;107(5):389–98.
33. Vinters H V., Natté R, Maat-Schieman MLC, Van Duinen SG, Hegeman-Kleinn I, Welling-Graafland C, et al. Secondary microvascular degeneration in amyloid angiopathy of patients with hereditary cerebral hemorrhage with amyloidosis, Dutch type (HCHWA-D). *Acta Neuropathol.* 1998 Mar;95(3):235–44.
34. Natté R, Vinters H V., Maat-Schieman MLC, Bornebroek M, Haan J, Roos RAC, et al. Microvasculopathy is associated with the number of cerebrovascular lesions in hereditary cerebral hemorrhage with amyloidosis, dutch type. *Stroke.* 1998 Aug 1;29(8):1588–94.
35. Timmers WF, Tagliavini F, Haan J, Frangione B. Parenchymal preamyloid and amyloid deposits in the brains of patients with hereditary cerebral hemorrhage with amyloidosis--Dutch type. *Neurosci Lett.* 1990 Oct;118(2):223–6.
36. Wisniewski T, Frangione B. Molecular biology of Alzheimer's amyloid—Dutch variant. *Mol Neurobiol.* 1992 Mar;6(1):75–86.
37. J Haan, C Van Broeckhoven, C M van Duijn, E Voorhoeve, F van Harskamp, J C van Swieten, M L Maat-Schieman, R A Roos EB. The apolipoprotein E epsilon 4 allele does not influence the clinical expression of the amyloid precursor protein gene codon 693 or 692 mutations. *Ann Neurol.* 1994;36:434–7.
38. Rozemuller AJ, Roos RA, Bots GT, Kamphorst W, Eikelenboom P, Van Nostrand WE. Distribution of beta/A4 protein and amyloid precursor protein in hereditary cerebral hemorrhage with amyloidosis-Dutch type and Alzheimer's disease. *Am J Pathol.* 1993;142(5):1449–57.
39. Haan J, Maat-Schieman ML, van Duinen SG, Jensson O, Thorsteinsson L, Roos R a. Co-localization of beta/A4 and cystatin C in cortical blood vessels in Dutch, but not in Icelandic hereditary cerebral hemorrhage with amyloidosis. *Acta Neurol Scand.* 1994 May;89(5):367–71.
40. Rozemuller JM, Bots GT, Roos R a, Eikelenboom P. Acute phase proteins but not activated microglial cells are present in parenchymal beta/A4 deposits in the brains of patients with hereditary cerebral hemorrhage with amyloidosis-Dutch type. *Neurosci Lett.* 1992 Jun 22;140(2):137–40.
41. Wilhelmus MMM, Boelens WC, Otte-Höller I, Kamps B, Kusters B, Maat-Schieman MLC, et al. Small heat shock protein HspB8: its distribution in Alzheimer's disease brains and its inhibition of amyloid-beta protein aggregation and cerebrovascular amyloid-beta toxicity. *Acta Neuropathol.* 2006 Feb;111(2):139–49.
42. van Horssen J, Otte-Holler I, David G, Maat-Schieman ML, van den Heuvel LP, Wesseling P, et al. Heparan sulfate proteoglycan expression in cerebrovascular amyloid deposits in Alzheimer's disease and hereditary cerebral hemorrhage with amyloidosis (Dutch) brains. *Acta Neuropathol.* 2001 Dec;102(6):604–14.
43. van Duinen SG, Maat-Schieman MLC, Bruijn JA, Haan J, Roos RAC, Wattendorff AR, et al. Cortical Tissue of Patients With Hereditary Cerebral-Hemorrhage With Amyloidosis (Dutch) Contains Various Extracellular-Matrix Deposits. *Lab Investig.* 1995 Aug;73(2):183–9.
44. Wilhelmus MMM, Otte-Höller I, van Triel JJJ, Veerhuis R, Maat-Schieman MLC, Bu G, et al. Lipoprotein receptor-related protein-1 mediates amyloid-beta-mediated cell death of cerebrovascular cells. *Am J Pathol.* 2007 Dec;171(6):1989–99.
45. Deane R, Wu Z, Sagare A, Davis J, Du Yan S, Hamm K, et al. LRP/amyloid β -peptide interaction mediates differential brain efflux of A β isoforms. *Neuron.* 2004 Aug 5;43(3):333–44.

46. De Jager M, van der Wildt B, Schul E, Bol JGJM, van Duinen SG, Drukarch B, et al. Tissue transglutaminase colocalizes with extracellular matrix proteins in cerebral amyloid angiopathy. *Neurobiol Aging*. 2013 Apr;34(4):1159–69.
47. Wilhelmus MMM, Bol JGJM, van Duinen SG, Drukarch B. Extracellular matrix modulator lysyl oxidase colocalizes with amyloid-beta pathology in Alzheimer's disease and hereditary cerebral hemorrhage with amyloidosis-Dutch type. *Exp Gerontol*. 2013 Feb;48(2):109–14.
48. Wisniewski T, Ghiso J, Frangione B. Peptides homologous to the amyloid protein of Alzheimer's disease containing a glutamine for glutamic acid substitution have accelerated amyloid fibril formation. *Biochem Biophys Res Commun*. 1991;179(3):1247–54.
49. Verbeek MM, De Waal RMW, Schipper JJ, Van Nostrand WE. Rapid Degeneration of Cultured Human Brain Pericytes by Amyloid β Protein. *J Neurochem*. 2002 Mar;68(3):1135–41.
50. Davis J, Van Nostrand WE. Enhanced pathologic properties of Dutch-type mutant amyloid β -protein. *Proc Natl Acad Sci*. 1996 Apr 2;93(7):2996–3000.
51. Davis-Salinas J, Saporito-Irwin SM, Cotman CW, Van Nostrand WE. Amyloid β -Protein Induces Its Own Production in Cultured Degenerating Cerebrovascular Smooth Muscle Cells. *J Neurochem*. 1995 Nov 23;65(2):931–4.
52. Eisenhauer PB, Johnson RJ, Wells JM, Long HJ, Simons ER, Davies TA, et al. Toxicity of various amyloid beta peptide species and activated platelets on cultured human blood-brain barrier endothelial cells: Increased toxicity of amyloid dutch type mutant. *Neurobiol Aging*. 2000;21:220.
53. Davis J, Cribbs DH, Cotman CW, Van Nostrand WE. Pathogenic amyloid β -protein induces apoptosis in cultured human cerebrovascular smooth muscle cells. *Amyloid*. 1999 Sep;6(3):157–64.
54. Melchor JP, McVoy L, Van Nostrand WE. Charge alterations of E22 enhance the pathogenic properties of the amyloid β -protein. *J Neurochem*. 2000 May;74(5):2209–12.
55. Miravalle L, Tokuda T, Chiarle R, Giaccone G, Bugiani O, Tagliavini F, et al. Substitutions at codon 22 of Alzheimer's abeta peptide induce diverse conformational changes and apoptotic effects in human cerebral endothelial cells. *J Biol Chem*. 2000 Sep 1;275(35):27110–6.
56. Sian a K, Frears ER, El-Agnaf OM, Patel BP, Manca MF, Siligardi G, et al. Oligomerization of beta-amyloid of the Alzheimer's and the Dutch-cerebral-haemorrhage types. *Biochem J*. 2000;349:299–308.
57. Kassler K, HornAHC, StichtH. Effect of pathogenic mutations on the structure and dynamics of Alzheimer's A beta 42-amyloid oligomers. *J Mol Model*. 2010 May;16(5):1011–20.
58. Ohshima Y, Taguchi K, Mizuta I, Tanaka M, Tomiyama T, Kametani F, et al. Mutations in the β -amyloid precursor protein in familial Alzheimer's disease increase A β oligomer production in cellular models. *Heliyon*. 2018;(October 2017):e00511.
59. Condello C, Lemmin T, Stöhr J, Nick M, Wu Y, Maxwell AM, et al. Structural heterogeneity and intersubject variability of A β in familial and sporadic Alzheimer's disease. *Proc Natl Acad Sci*. 2018;201714966.
60. van Duinen SG, Castano EM, Prelli F, Bots GT, Luyendijk W, Frangione B. Hereditary cerebral hemorrhage with amyloidosis in patients of Dutch origin is related to Alzheimer disease. *Proc Natl Acad Sci*. 1987 Aug;84(16):5991–4.
61. Prelli F, Levy E, van Duinen SG, Bots GTAM, Luyendijk W, Frangione B. Expression of a normal and variant Alzheimer's β -protein gene in amyloid of hereditary cerebral hemorrhage, Dutch type: DNA and protein diagnostic assays. *Biochem Biophys Res Commun*. 1990 Jul;170(1):301–7.
62. Natté R, Yamaguchi H, Maat-Schieman MLC, Prins FA, Neeskens P, Roos RAC, et al. Ultrastructural evidence of early non-fibrillar A β 42 in the capillary basement membrane of patients with hereditary cerebral hemorrhage with amyloidosis, Dutch type. *Acta Neuropathol*. 1999 Dec;98(6):577–82.
63. Herzig MC, Van Nostrand WE, Jucker M. Mechanism of cerebral beta-amyloid angiopathy: murine and cellular models. *Brain Pathol*. 2006 Jan;16(1):40–54.
64. Herzig MC, Winkler DT, Burgermeister P, Pfeifer M, Kohler E, Schmidt SD, et al. A β is targeted to the vasculature in a mouse model of hereditary cerebral hemorrhage with amyloidosis. *Nat Neurosci*. 2004 Oct;7(9):954–60.
65. Bornebroek M, Haan J, Van Duinen SG, Maat-Schieman ML, Van Buchem M a, Bakker E, et al. Dutch hereditary cerebral amyloid angiopathy: structural lesions and apolipoprotein E genotype. *Ann Neurol*. 1997 May;41(5):695–8.
66. Bornebroek M, Haan J, Backhovens H, Deutz P, Van Buchem M a, van den Broeck M, et al. Presenilin-1 polymorphism and hereditary cerebral hemorrhage with amyloidosis, Dutch type. *Ann Neurol*. 1997 Jul;42(1):108–10.
67. Bornebroek M, Westendorp RG, Haan J, Bakker E, Timmers WF, Van Broeckhoven C, et al. Mortality from hereditary cerebral haemorrhage with amyloidosis--Dutch type. The impact of sex, parental transmission and year of birth. *Brain*. 1997 Dec;120 (Pt 1):2243–9.
68. Tsubuki S, Takaki Y, Saido TC. Dutch, Flemish, Italian, and Arctic mutations of APP and resistance of A β to physiologically relevant proteolytic degradation. *Lancet*. 2003 Jun 7;361(9373):1957–8.
69. Morelli L, Llovera RE, Mathov I, Lue L-F, Frangione B, Ghiso J, et al. Insulin-degrading enzyme in brain microvessels: proteolysis of amyloid {beta} vasculotropic variants and reduced activity in cerebral amyloid angiopathy. *J Biol Chem*. 2004 Dec 31;279(53):56004–13.
70. De Jonghe C, Zehr C, Yager D, Prada CM, Younkin S, Hendriks L, et al. Flemish and Dutch mutations in amyloid β precursor protein have different effects on amyloid β secretion. *Neurobiol Dis*. 1998 Oct;5(4):281–6.
71. Watson DJ, Selkoe DJ, Teplow DB. Effects of the amyloid precursor protein Glu693 \rightarrow Gln 'Dutch' mutation on the production and stability of amyloid β -protein. 1999;709:703–9.
72. Nilsberth C, Westlind-Danielsson a, Eckman CB, Condron MM, Axelman K, Forsell C, et al. The "Arctic" APP mutation (E693G) causes Alzheimer's disease by enhanced Abeta protofibril formation. *Nat Neurosci*. 2001;4(9):887–93.
73. Stenh C, Nilsberth C, Hammarback J, Engvall B, Naslund J, Lannfelt L. The Arctic mutation interferes with processing of the amyloid precursor protein. *Neuroreport*. 2002 Oct;13(15):1857–60.
74. Monroe OR, Mackic JB, Yamada S, Segal MB, Ghiso J, Maurer C, et al. Substitution at codon 22 reduces clearance of Alzheimer's amyloid- β peptide from the cerebrospinal fluid and prevents its transport from the central nervous system into blood. *Neurobiol Aging*. 2002;23(3):405–12.
75. Weller RO, Subash M, Preston SD, Mazanti I, Carare RO. Perivascular drainage of amyloid-beta peptides from the brain and its failure in cerebral amyloid angiopathy and Alzheimer's disease. *Brain Pathol*. 2008 Apr;18(2):253–66.

76. Thal DR, Griffin WST, de Vos RAI, Ghebremedhin E. Cerebral amyloid angiopathy and its relationship to Alzheimer's disease. *Acta Neuropathol.* 2008 Jun;115(6):599–609.
77. Zlokovic B V. Neurovascular pathways to neurodegeneration in Alzheimer's disease and other disorders. *Nat Rev Neurosci.* 2011 Dec;12(12):723–38.
78. Nicolakakis N, Hamel E. Neurovascular function in Alzheimer's disease patients and experimental models. *J Cereb Blood Flow Metab.* 2011 Jun;31(6):1354–70.
79. Greenberg SM. Cerebral amyloid angiopathy: prospects for clinical diagnosis and treatment. *Neurology.* 1998 Sep;51(3):690–4.
80. Viswanathan A, Greenberg SM. Cerebral amyloid angiopathy in the elderly. *Ann Neurol.* 2011 Dec;70(6):871–80.
81. Boyle PA, Leurgans S, Wilson RS, Bennett DA. Cerebral amyloid angiopathy and cognitive outcomes in community-based older persons. 2015;
82. Tanskanen M, Mäkelä M, Myllykangas L, Notkola IL, Polvikoski T, Sulkava R, et al. Prevalence and severity of cerebral amyloid angiopathy: A population-based study on very elderly Finns (Vantaa 85+). *Neuropathol Appl Neurobiol.* 2012;38(4):329–36.
83. Greenberg SM, Gurol ME, Rosand J, Smith EE. Amyloid angiopathy-related vascular cognitive impairment. *Stroke.* 2004 Nov;35(11 Suppl 1):2616–9.
84. Vemuri P, Lesnick TG, Przybelski S a., Knopman DS, Preboske GM, Kantarci K, et al. Vascular and amyloid pathologies are independent predictors of cognitive decline in normal elderly. *Brain.* 2015;761–71.
85. Ellis RJ, Olichney JM, Thal LJ, Mirra SS, Morris JC, Beekly D, et al. Cerebral amyloid angiopathy in the brains of patients with Alzheimer's disease: The CERAD experience, part XV. *Neurology.* 1996 Jun;46(6):1592–6.
86. Vinters H V. Emerging Concepts in Alzheimer's Disease. *Annu Rev Pathol Mech Dis.* 2015;10(1):291–319.
87. Charidimou A, Martinez-Ramirez S, Shoamanesh A, Oliveira-Filho J, Frosch M, Vashkevich A, et al. Cerebral amyloid angiopathy with and without hemorrhage: evidence for different disease phenotypes. *Neurology.* 2015;84(12):1206–12.
88. Kövari E, Herrmann FR, Hof PR, Bouras C. The relationship between cerebral amyloid angiopathy and cortical microinfarcts in brain ageing and Alzheimer's disease. *Neuropathol Appl Neurobiol.* 2013;39(5):498–509.
89. Greenberg SM, Rebeck GW, Vonsattel JP, Gomez-Isla T, Hyman BT. Apolipoprotein E epsilon 4 and cerebral hemorrhage associated with amyloid angiopathy. *Ann Neurol.* 1995 Aug;38(2):254–9.
90. Greenberg SM, Briggs ME, Hyman BT, Kokoris GJ, Takis C, Kanter DS, et al. Apolipoprotein E epsilon 4 is associated with the presence and earlier onset of hemorrhage in cerebral amyloid angiopathy. *Stroke.* 1996 Aug;27(8):1333–7.
91. Greenberg SM, Vonsattel JP, Segal AZ, Chiu RI, Clatworthy AE, Liao A, et al. Association of apolipoprotein E epsilon2 and vasculopathy in cerebral amyloid angiopathy. *Neurology.* 1998 Apr;50(4):961–5.
92. Love S, Chalmers K, Ince P, Esiri M, Attems J, Jellinger K, et al. Development, appraisal, validation and implementation of a consensus protocol for the assessment of cerebral amyloid angiopathy in post-mortem brain tissue. *Am J Neurodegener Dis.* 2014;3(1):19–32.
93. Yu L, Boyle P a., Nag S, Leurgans S, Buchman AS, Wilson RS, et al. APOE and cerebral amyloid angiopathy in community-dwelling older persons. *Neurobiol Aging.* 2015;1–8.
94. Nicoll JA, Burnett C, Love S, Graham DI, Dewar D, Ironside JW, et al. High frequency of apolipoprotein E epsilon 2 allele in hemorrhage due to cerebral amyloid angiopathy. *Ann Neurol.* 1997 Jun;41(6):716–21.
95. Rannikmäe K, Samarasekera N, Martínez-González NA, Al-Shahi Salman R, Sudlow CLM. Genetics of cerebral amyloid angiopathy: systematic review and meta-analysis. *J Neurol Neurosurg Psychiatry.* 2013 Aug;84(8):901–8.
96. Wyss-Coray T, Masliah E, Mallory M, McConlogue L, Johnson-Wood K, Lin C, et al. Amyloidogenic role of cytokine TGF-β1 in transgenic mice and in Alzheimer's disease. *Nature.* 1997;389(6651):603–6.
97. Ueberham U, Ueberham E, Brückner MK, Seeger G, Gärtner U, Gruschka H, et al. Inducible neuronal expression of transgenic TGF-β1 in vivo: Dissection of short-term and long-term effects. *Eur J Neurosci.* 2005 Jul;22(1):50–64.
98. Wyss-Coray T, Lin C, Yan F, Yu GQ, Rohde M, Mcconlogue L, et al. TGF-β1 promotes microglial amyloid-β clearance and reduces plaque burden in transgenic mice. *Nat Med.* 2001 May;7(5):612–8.
99. Gray CW, Patel AJ. Regulation of beta-amyloid precursor protein isoform mRNAs by transforming growth factor-beta 1 and interleukin-1 beta in astrocytes. *Brain Res Mol Brain Res.* 1993 Aug;19(3):251–6.
100. Amara FM, Junaid A, Clough RR, Liang B. TGF-β1, regulation of Alzheimer amyloid precursor protein mRNA expression in a normal human astrocyte cell line: mRNA stabilization. *Mol Brain Res.* 1999 Jul;71(1):42–9.
101. Burton T, Liang B, Dibrov A, Amara F. Transforming growth factor-beta-induced transcription of the Alzheimer beta-amyloid precursor protein gene involves interaction between the CTCF-complex and Smads. *Biochem Biophys Res Commun.* 2002 Jul 19;295(3):713–23.
102. Lesné S, Docagne F, Gabriel C, Liot G, Lahiri DK, Buée L, et al. Transforming growth factor-β1 potentiates amyloid-β generation in astrocytes and in transgenic mice. *J Biol Chem.* 2003 May 16;278(20):18408–18.
103. Ueberham U, Zobiak B, Ueberham E, Brückner MK, Boriss H, Arendt T. Differentially expressed cortical genes contribute to perivascular deposition in transgenic mice with inducible neuron-specific expression of TGF-β1. *Int J Dev Neurosci.* 2006;24(2–3):177–86.
104. Mazur-Kolecka B, Frackowiak J, Le Vine H, Haske T, Evans L, Sukontasup T, et al. TGFβ1 enhances formation of cellular Aβ/apoE deposits in vascular myocytes. *Neurobiol Aging.* 2003;24(2):355–64.
105. Olichney JM, Hansen LA, Hofstetter CR, Grundman M, Katzman R, Thal LJ. Cerebral Infarction in Alzheimer's Disease is Associated with Severe Amyloid Angiopathy and Hypertension. *Arch Neurol.* 1995 Jul;52(7):702–8.
106. Greenberg SM, Vonsattel JP. Diagnosis of cerebral amyloid angiopathy. Sensitivity and specificity of cortical biopsy. *Stroke.* 1997 Jul;28(7):1418–22.
107. Deramecourt V, Slade JY, Oakley AE, Perry RH, Ince PG, Maurage CA, et al. Staging and natural history of cerebrovascular pathology in dementia. *Neurology.* 2012;78(14):1043–50.
108. van Rooden S, van der Grond J, van den Boom R, Haan J, Linn J, Greenberg SM, et al. Descriptive analysis of the Boston criteria applied to a Dutch-type cerebral amyloid angiopathy population. *Stroke.* 2009 Sep;40(9):3022–7.

109. van Opstal AM, van Rooden S, van Harten T, Ghariq E, Labadie G, Fotiadis P, et al. Cerebrovascular function in presymptomatic and symptomatic individuals with hereditary cerebral amyloid angiopathy: a case-control study. *Lancet Neurol*. 2017;16(2):115–22.
110. Koemans EA, van Etten ES, van Opstal AM, Labadie G, Terwindt GM, Wermer MJH, et al. Innovative Magnetic Resonance Imaging Markers of Hereditary Cerebral Amyloid Angiopathy at 7 Tesla. *Stroke*. 2018 Apr;
111. Bornebroek M, De Jonghe C, Haan J, Kumar-Singh S, Younkin S, Roos R, et al. Hereditary cerebral hemorrhage with amyloidosis dutch type (A β PP 693): Decreased plasma amyloid- β 42 concentration. *Neurobiol Dis*. 2003 Dec;14(3):619–23.
112. Greenberg SM, Cho HS, O'Donnell HC, Rosand J, Segal AZ, Younkin LH, et al. Plasma beta-amyloid peptide, transforming growth factor-beta 1, and risk for cerebral amyloid angiopathy. *Ann N Y Acad Sci*. 2000 Apr;903:144–9.
113. Van Etten ES, Verbeek MM, Van Der Grond J, Zielman R, Van Rooden S, Van Zwet EW, et al. β -Amyloid in CSF: Biomarker for preclinical cerebral amyloid angiopathy. *Neurology*. 2017;88(2):169–76.
114. Verbeek MM, Kremer BPH, Rikkert MO, Van Domburg PHMF, Skehan ME, Greenberg SM. Cerebrospinal fluid amyloid beta(40) is decreased in cerebral amyloid angiopathy. *Ann Neurol*. 2009 Aug;66(2):245–9.
115. Renard D, Castelnovo G, Wacogne A, Le Floch A, Thouvenot E, Mas J, et al. Interest of CSF biomarker analysis in possible cerebral amyloid angiopathy cases defined by the modified Boston criteria. *J Neurol*. 2012 Nov;259(11):2429–33.
116. Frost S, Kanagasingam Y, Sohrabi H, Taddei K, Bateman R, Morris J, et al. Pupil Response Biomarkers Distinguish Amyloid Precursor Protein Mutation Carriers from Non-Carriers. *Curr Alzheimer Res*. 2013;10(8):790–6.
117. Sperling RA, Jack CRJ, Black SE, Frosch MP, Greenberg SM, Hyman BT, et al. Amyloid-related imaging abnormalities in amyloid-modifying therapeutic trials: recommendations from the Alzheimer's Association Research Roundtable Workgroup. *Alzheimers Dement*. 2011 Jul;7(4):367–85.

Chapter 2

Amyloid β in hereditary cerebral hemorrhage with amyloidosis-Dutch type

Juliette A. Kamp¹, Laure Grand Moursel^{1,2}, Joost Haan^{3,6}, Gisela M. Terwindt³, Saskia A.M.J. Lesnik Oberstein⁴, Sjoerd G. van Duinen⁵, Willeke M.C. van Roon-Mom¹

Departments of: ¹Human Genetics, ²Radiology, ³Neurology, ⁴Clinical Genetics and ⁵Pathology, Leiden University Medical Center.
⁶Department of Neurology, Rijnland Hospital, Leiderdorp.

Adapted from Rev. Neurosci. (2014).

Abstract

Hereditary cerebral haemorrhage with amyloidosis–Dutch type is an autosomal dominant hereditary disease caused by a point mutation in the amyloid precursor protein gene on chromosome 21. The mutation causes an amino acid substitution at codon 693 (E22Q), the ‘Dutch mutation’. Amyloid β , the product after cleavage of the Amyloid Precursor Protein, is secreted into the extracellular space. The Dutch mutation leads to altered amyloid β cleavage and secretion, enhanced aggregation properties, higher proteolysis resistance, lowered brain efflux transporters affinity and enhanced cell surfaces binding. All this results in amyloid β accumulation in cerebral vessel walls, causing cell death and vessel wall integrity loss, making cerebral vessel walls in hereditary cerebral haemorrhage with amyloidosis–Dutch type more prone to rupture and obstruction, leading to haemorrhages and infarcts. Studying effects of altered amyloid β metabolism due to mutations like the ‘Dutch’ provides us with a better understanding of amyloid β toxicity, also in other amyloid β diseases like sporadic Cerebral Amyloid Angiopathy and Alzheimer’s Disease.

Introduction

Hereditary cerebral haemorrhage with amyloidosis–Dutch type (HCHWA-D) is an autosomal dominant hereditary disease caused by a mutation in the Amyloid Precursor Protein (APP) gene on chromosome 21 (1). HCHWA-D patients suffer from haemorrhagic strokes, infarcts and vascular dementia (2). Life expectancy is reduced: the first stroke occurs between the ages of 40 and 65 and is fatal in two thirds of the patients (3,4). The patients that survive the first haemorrhage suffer from recurrent strokes (4).

HCHWA-D is a rare disease and has only been found in three founder families in the Dutch coastal villages of Katwijk and Scheveningen (3,4). A rough estimate is that likely 400-500 persons are at risk in multi-generational offspring families, but no clear data are available at this moment. An affected family described in Western Australia originates from Katwijk (5).

In HCHWA-D, amyloid beta ($A\beta$) accumulates in the cerebral vessels (cerebral amyloid angiopathy; CAA). Especially the meningeal arteries and the cerebrocortical arterioles are affected. The amount of CAA, quantified *ex vivo* using computerized morphometry, is strongly associated with the presence of dementia in HCHWA-D, and this is independent of parenchymal plaque density and age (6). CAA can also be found in at least 80% of Alzheimer’s disease (AD) patients (7). However, in contrast to AD, the presence of intraneuronal neurofibrillary tangles is low in HCHWA-D and does not correlate with dementia (6).

$A\beta$ results from a cascade of proteolytic cleavages of the APP gene product. The most common $A\beta$ isoforms contain either 40 ($A\beta$ -40) or 42 amino acids ($A\beta$ -42), depending on the site of γ -secretase cleavage. In comparison with $A\beta$ -40, $A\beta$ -42 contains more hydrophobic residues and therefore is more prone to aggregation (8). Alternative cleavage of APP within the $A\beta$ fragment by α -secretase prevents the formation of $A\beta$ and leads to the release of the neuroprotective secreted APP (sAPP) (9). After processing of APP, $A\beta$ is released into the extracellular space (10) where it can form parenchymal plaques or accumulate as vascular deposits in the cerebral vessels causing amyloid angiopathy (11). Brains of HCHWA-D patients show few parenchymal plaques, but multiple vascular $A\beta$ deposits.

In this review, it will be described how the $A\beta$ mutation of HCHWA-D patients modifies $A\beta$ properties regarding aggregation, binding to cerebral vessel wall cells, interplay with extracellular matrix, proteolysis and clearance and how these altered characteristics lead to HCHWA-D pathogenesis.

Genetics of HCHWA

Three types of HCHWA are known: Dutch, Icelandic and Italian. The Icelandic type is caused by a mutation in the Cystatin C gene (*CST3*) on chromosome 20 (12). The Dutch and Italian are caused by single point mutations at the A β region of *APP* on chromosome 21 (1,13). There are more known mutations in the *APP* gene, inside and outside the A β region. The mutations in the A β region mainly lead to an AD phenotype, but a mixed pathology (AD and CAA) is also described in patients with the Flemish, Arctic, Iowa, Italian II and II mutations (**Table 1**). The above described mutations are inherited in an autosomal dominant fashion. Recessive pathogenic mutations within the A β region of *APP* are also known, like the Japanese mutation (a deletion of glutamine at A β 's position 22), and the valine substitution for alanine at position 2 (14,15). The point mutation in HCHWA-D, a cytosine for guanine substitution at codon 693 of *APP*, causes an amino acid substitution of glutamine for glutamic acid at position 22 of the A β region of *APP*. The deletion of the glutamine or the substitution of the glutamine for glycine, as present in the Japanese and Arctic types, do not cause the characteristic angiopathy of HCHWA, suggesting that the exact nature of the amino acid substitution is essential for HCHWA pathogenesis. The Dutch (Glu693Gln) and Italian (Glu693Lys) amino acid substitutions lead to a change of charge at A β 's position 22. These changes in charge specifically enable A β 40 to bind to the surface of cerebrovascular smooth muscle cells (SMC) and form amyloid fibrils (16). Moreover, the Dutch mutation makes the A β peptide more resistant to neprilysin-catalysed proteolysis, probably by interfering with the peptide's backbone spatial fitting into neprilysin's catalytic pocket, thereby increasing A β 's half-life (17).

The Dutch mutation is located near the α -secretase cleavage site of *APP* (**Figure 1**), which lies between the lysine at position 16 and the leucine at position 17 of A β (9). Patients with HCHWA-D have reduced levels of sAPP in the cerebral spinal fluid (CSF) (18), which may be caused by an altered processing of the precursor protein or alternatively by increased binding of *APP* to the vessel wall, as described later. Furthermore, the location of the A β mutation appears to influence aggregation properties. When studying the Italian, Dutch, Arctic and Iowa mutations in A β 42 monomers, it was shown that the Italian and Dutch mutation made the A β 42 monomer aggregate quicker than wild type A β 42, while the Arctic and Iowa mutations made the A β 42 monomer aggregate slightly slower than wild type A β 42 (19). This difference in aggregation was attributed to differences in helix propensities in residues 20-23 caused by the mutations: Italian and Dutch mutation increase helix propensity, while Arctic and Iowa mutations slightly decrease helix propensity. It is thought that α -helical intermediates play an important role in amyloid oligomerization (19).

Position A β	Mutation	Phenotype	Alias
2	Ala673Thr	Not pathogenic	
2	Ala673Val*	AD	
6	His677Arg	Not pathogenic	
7	Asp678Asn	AD	
7	Aso678His ¹	Dementia + CAA	
11	Glu682Lys	AD	
16	Lys687Asp ²	AD	
21	Ala692Gly	AD (CAA)	Flemish
22	Glu693Lys	HCHWA	Italian
22	Glu693Gln	HCHWA	Dutch
22	Glu693Gly	AD (CAA)	Arctic
22	Glu693del*	AD	Japanese
23	Asp694Asn	AD (CAA)	Iowa
34	Leu705Val	CAA	Italian II
37	Gly708	Not pathogenic	
42	Ala713Thr	AD (CAA)	Italian III
42	Ala713Val	Not pathogenic	
43	Thr714Ala	AD/Epilepsy	Iranian
43	Thr714Ile	AD	Austrian

Table 1. Mutations within the A β region of *APP* A β = Amyloid β ; *= recessive mutation; AD= Alzheimer's disease; CAA= Cerebral Amyloid Angiopathy. The mutations are shown with the affected amino acid, the affected *APP* codon and, if applicable, the amino acid alteration resulting from the mutation. Mutations were found using the Alzheimer Disease & Frontotemporal Dementia Mutation Database (80) and PubMed: ¹(81); ²(82).

Cerebral amyloid plaques in HCHWA-D

A β deposition in AD is mainly located in the brain parenchyma in the form of plaques. In HCHWA-D, A β deposition is mainly found in the cerebral vessel walls, but also some parenchymal A β deposition in the form of plaques is present, mainly in the form of 'diffuse' plaques, lacking an amyloid core as in AD (20).

A β peptides show different intermediate fibrillization states before plaques and vascular deposits are formed (21). The A β monomers are amphiphatic, with a hydrophilic N-terminal and a hydrophobic C-terminal, and are able to adopt different conformations: α -helices, β -sheets or random coils. After arrangement of dimers and trimers, unstable and toxic oligomers are formed. These oligomers contain up to 50 monomers. Subsequently, the oligomers assemble into protofibrils, which are the relatively flexible and rod-shaped precursors of the mature fibrils. Fibrils contain multiple protofibrils and are the main components of amyloid aggregates.

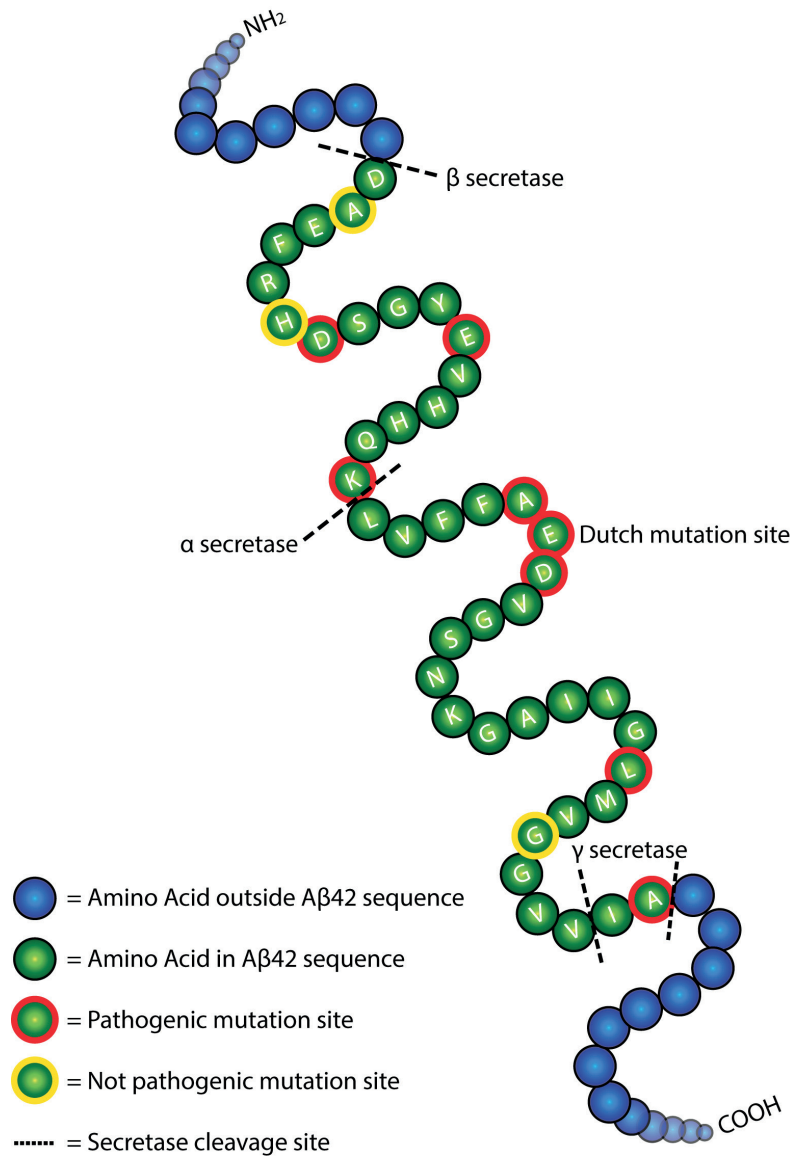


Figure 1: Location of known mutations and secretase cleavage sites in the amyloid beta sequence of the amyloid precursor protein

In the brain parenchyma, there are four different types of parenchymal plaques distinguishable in HCHWA-D: fine diffuse, dense diffuse, coarse and homogeneous. The morphology of these plaques was described by Maat-Schieman and her colleagues (20). Fine diffuse plaques are irregularly shaped, ill-defined, evenly stained, and show finely fibrous A β deposits. Dense diffuse plaques are either irregular, ill-defined or rounded and are stained unevenly. Coarse plaques are clusters of small, coarse and strongly staining deposits and homogeneous plaques are well-defined round shaped plaques. While all plaques show A β 42 staining, A β 40 staining is present in a small subset of dense diffuse and coarse plaques and in all homogeneous plaques. Only plaques containing A β 40 harbour degenerating neurites that showed APP and ubiquitin staining. No tau is present in these degenerating neurites. In addition to the plaques, also clouds of A β 42 were shown to be present throughout the cortex, except around A β containing arterioles (**Table 2**). In addition to ubiquitin, other proteins like amyloid-P, cystatin C and ApoE are known to co-aggregate with amyloid deposition in HCHWA-D (22).

In the initial stages of HCHWA-D, A β deposition in the form of clouds and fine diffuse plaques are present. With age, clouds disappear and plaque density increases from A β 40 negative fine diffuse to A β 40 positive dense plaques (23). Electron microscopy examination showed that A β is non-fibrillar and plasma membrane bound initially, but when the plaques develop, amyloid fibrils accumulate (20). This development can be visualized with Congo red staining that shows increased fluorescent activity *ex vivo*. Non-fibrillar A β is assumed to be cleared by glial cells, thereby limiting the neurotoxic soluble form levels of A β in HCHWA-D patients' brains (23).

		Clouds	Plaques			
			Fine diffuse	Dense diffuse	Coarse	Homogeneous
A β	A β 40	-	-	- to ++	- to ++	++
	A β 42	+	+	++	++	++
DN	APP	-	-	- to +	- to +	±
	Ubiquitin	-	-	- to +	- to +	±
	Tau	-	-	-	-	-

Table 2. Staining intensities of parenchymal clouds and plaques Adapted from (19). Staining intensity: No staining -, few bundles ±, positive staining/small bundles + and strong positive staining/clusters ++. A β = Amyloid beta, DN = Degenerating Neurites.

A β isoforms in HCHWA-D vasculature

While A β 42 is the main A β isoform in parenchymal plaques, A β 40 is the main component of amyloid deposits in the cerebral vessels of HCHWA-D patients (24,25). Amino acid sequencing of amyloid that was isolated from leptomeningeal vascular walls showed that both mutated and wild type A β occurs in the vascular deposits of HCHWA-D patients (26). It has been suggested that it is especially the ratio of A β 40 to A β 42 that is important for vascular amyloid formation (27). Moreover, an important role for mutated A β 42 has been proposed. In vascular amyloid of HCHWA-D, wild type and Dutch mutated A β 40 peptides occur in a 1:1 ratio, while only the Dutch mutated A β 42 and not the wild type A β 42 has been detected, suggesting a possible role for Dutch mutated A β 42 as a seed for the aggregation of A β 40 (24). Importantly, all A β 42 was oxidized at the methionine residue at position 35. The oxidation of Met35 of A β 42 is known to slow down the rate of fibrillation and aggregation of A β 42 (28). However, the Dutch mutation enables A β to fold into different shapes, thereby creating multiple ways to aggregate (28). In addition to A β 40 and A β 42, wild type A β 37, wild type A β 38 and Dutch mutated A β 38 are also present in the vascular amyloid (24). A β 37 and A β 38 are less common isoforms of A β than A β 40 and differ at the C-terminus.

It was shown that neuronal expression of APP with the Dutch mutation was sufficient to induce HCHWA pathology, i.e. CAA, smooth muscle cell degeneration and haemorrhages using a transgenic HCHWA-D mouse model. This indicates that neurons are the main source of Dutch A β in the cerebral vessels. Using this model it was also shown that the Dutch mutation leads to an increased A β 40: A β 42 ratio both in parenchymal and cerebrovascular amyloid deposits and A β 40 was suggested to be inhibitory for parenchymal A β deposition (27). It was discovered in a guinea pig model of the Dutch mutation that A β 40 accumulates around the blood vessels and in the brain due to a reduced clearance from the cerebrospinal fluid and impaired transport over the blood brain barrier, because of the lower affinity for central nervous system efflux transporters (29). Impaired clearance of A β was also shown in a mouse model with the Dutch and Iowa mutation: no detectable plasma A β but abundant A β deposits were present in cerebral vasculature (30). The double mutated A β shows a significant lower affinity to the low-density lipoprotein receptor-related protein 1 (LRP1), which is implicated in A β clearance, in comparison to wild type A β 40 (31). Double mutated A β also seems to down-regulate LRP1 (31). However, in this model, it is not clear how each mutation affects the clearance.

In individuals with and without the Dutch mutation, A β 40 plasma levels were similar (32). On the other hand, the plasma A β 42 concentration of individuals with the Dutch mutation was significantly lower than in the

plasma of their family members that did not carry the mutation (32). Of the 22 individuals with the Dutch mutation, 7 were still asymptomatic. Plasma concentrations of A β 40 and A β 42 in HCHWA-D patients did not correlate with age or severity of the symptoms (32), which indicates that plasma A β does not play a major role in the pathology. It is important to note that the detection method used in this study was only appropriate for soluble A β . Because Dutch mutated A β 42 aggregates more readily than wild type A β 42, the detected decline of A β 42 in plasma of individuals with the Dutch mutation could also be due to the lack of detection of aggregated A β 42. However, reduced A β 42 levels as a consequence of the Dutch mutation were confirmed by *in vitro* experiments that showed a decreased A β 42 concentration in medium of cells with the Dutch mutation, while the A β 40 concentration was unchanged (33).

Decreased A β 42 levels in plasma of HCHWA-D patients and in the cell model with the Dutch mutation suggest that the ratio of A β 40:A β 42 is elevated in HCHWA-D as compared to healthy individuals. The importance of relatively lower A β 42 concentrations in the pathophysiology of HCHWA-D was shown in animal studies. When increasing the A β 42 expression in transgenic HCHWA-D mice by crossing them with A β 42 overexpressing mice, amyloid deposits were redistributed from the cerebral vessels to the parenchyma (27,32).

The nature of the mutation within A β was shown to be crucial in the A β 40:A β 42 ratio in cell models of the Flemish and Arctic mutations, where an increase in A β 42 was present (33). Because the locations of the Dutch, Flemish and Arctic mutations are comparable (Table 1), it is not the actual mutation location but the substitution to glycine that probably affects the A β 40:A β 42 ratio. However, the mechanism behind this altered A β 40:A β 42 ratio is still unknown. Interestingly, haemorrhages are uncommon, whereas parenchymal plaques are abundant in patients with the Flemish and Arctic type mutations (34,35). This supports the role of A β 42 in amyloid accumulation localization, as suggested in animal studies.

A β fibril assembly at cell surfaces

Assembly of A β fibrils to cell surfaces is believed to be crucial in the loss of vessel wall integrity in HCHWA-D. The assembly of A β fibrils has been intensively studied. Both wild type and Dutch mutated A β 40 did not substantially assemble into fibril sheets in solution of 25 μ M A β 40, which is the A β peptides concentration shown to evoke pathological responses in cerebrovascular smooth muscle cells. However, at the same concentration, but in the presence of cultured cerebrovascular smooth muscle cells, Dutch mutated A β 40 did assemble in fibrils (36). This was not the case for wild type A β . So Dutch mutated A β 40 fibril formation is facilitated in the vicinity of smooth muscle cells.

After A β fibrillation, sAPP is able to bind to the A β fibrils at the smooth muscle cell surface (37). The binding of APP leads to the presence of the Kunitz-type protease inhibitor (KPI) domain, which is part of most of the APP isoforms. The KPI domain inhibits coagulant factors XIa and IXa (38), and A β fibrils enhance the anticoagulant property of APP (39). As a consequence, an anticoagulant environment is created, leading to an increased chance of haemorrhages. The binding of sAPP prevents its efflux from the brain, and could thus explain the reduced levels of sAPP in the CSF in HCHWA-D patients (40).

Moreover, A β fibrillation activates an apoptotic pathway in the cerebrovascular smooth muscle cells, leading to cell death (37). The combination of the cell death and the anticoagulant environment induced by A β fibrils in the vessel wall are probably major contributors to the haemorrhages in HCHWA-D patients. Also, Dutch A β induces increased expression and activation of matrix metalloproteinase 2 (MMP-2) in smooth muscle cells and this is believed to contribute to the Dutch A β -induced cell death (41). MMPs are tissue remodelling enzymes and turnover basement membranes. Elevated MMP-2 is known to lead to blood brain barrier disruption and causes cerebral haemorrhage, thus the Dutch A β -induced MMP-2 activation and expression probably contributes to loss of vessel wall integrity and consequent haemorrhagic stroke (41).

In addition to smooth muscle cells, pericytes are also prone to surface Dutch type A β fibril formation. The pericytes are even more vulnerable to the A β -induced degeneration compared to the smooth muscle cells (42). Pericyte degeneration was shown to be dependent on Apolipoprotein E (ApoE) genotype. ApoE is known to be the major risk factor for AD, and carrying one or two ϵ 4 alleles is associated with a dose-dependent increase in AD risk (43).

However, in a study of 36 carriers of the Dutch mutation and 10 related controls, the ApoE ϵ 4 genotype did not influence the age of onset of HCHWA-D, the occurrence of dementia, number of strokes nor the age at death (44). Furthermore, no association between the ApoE ϵ 4 allele and A β plasma levels was found in 22 HCHWA-D patients (32). In contrast with the clinical findings, cultures of human brain pericytes with an ϵ 4/ ϵ 4 genotype showed more Dutch A β -induced cell death than cultures with other ApoE genotypes (45). It is not clear what causes this inconsistency between clinical and *in vitro* studies.

In endothelial cells *in vitro*, A β protofibrils and fibrils induce apoptosis, and these effects are significantly stronger for Dutch mutated A β than wild type A β (46). Thus A β fibril formation in the vessel wall leads to an anticoagulant environment and the degeneration of three different cell types in the cerebral vessel walls, leading to CAA. This CAA leads to the haemorrhages in HCHWA-D.

The role of extracellular matrix components in cerebral amyloid angiopathy

As discussed above, reduction of A β clearance through the vessel wall plays a role in A β accumulation in the vessel wall. A major characteristic of cerebral vessels is the blood brain barrier, which prevents certain molecules to pass through the vessel into the brain and *vice versa*. Extracellular matrix (ECM) properties in the vessel wall are important for this perivascular filter by forming and maintaining basement membranes. The basement membranes are important for regulating cell growth, differentiation and migration and consist of laminins, nidogens, collagen and heparan sulphate proteoglycans (HSPGs) (47). HSPGs co-localize with the vascular deposits in AD and HCHWA-D (48). HSPGs consist of sulphated glycosaminoglycan (GAG) side chains bound to a core protein (49). Heparin and heparan sulphate are GAGs with side chains showing high A β affinity (50). The sulphate moieties of the side chains modulate the aggregation (51). Heparin and heparan sulphate both increase the aggregation of A β 40 with the Dutch mutation, but especially heparin is a very potent aggregation inducer. Moreover, heparin and heparan sulphate both inhibit the cytotoxicity of cerebrovascular cells that is induced by Dutch mutated A β 40, probably because increased aggregation prevents interactions of toxic monomeric, oligomeric or prefibrillar species of Dutch mutated A β 40 (51). So HSPGs are modulators of A β aggregation and inhibitors of Dutch mutated A β 40 cytotoxicity.

There are differences in HSPG subtype expression between AD and HCHWA-D (48) that suggest a different role for these HSPG subtypes in the different disorders. Immunohistochemical examination of AD and HCHWA-D *post mortem* brain tissue showed that the HSPG subtype agrin specifically co-localised with the vascular A β 40 deposits in HCHWA-D, a co-localization that is less frequent in AD. In contrast, another HSPG subtype, syndecan-2 is only present in vascular deposits in AD, but not in HCHWA-D (48). These results suggest that vascular deposits in AD and HCHWA-D arise *via* different mechanisms.

Interestingly, HSPG subtypes that are usually associated with vascular basement membranes were not found in CAA, while CAA associated HSPGs syndecan-2 and glypican-1 are not expressed by vascular cells (48). This indicates that implicated HSPGs are not produced by vascular cells but have other sources and travel towards the vascular wall.

A protein that co-localizes with ECM proteins in CAA is tissue transglutaminase (tTG) (52). tTG is an enzyme involved in posttranslational modifications of proteins, like covalently cross-linked proteins (53). It plays an important role in the remodelling of the ECM after tissue injury and cell stress (54). It is known that tTG mediates A β 40 dimerization through covalent intermolecular cross-linking and thereby seeding aggregation

(55). In early stage CAA, tTG is increased in affected vessel walls and co-localizes with A β deposition. This tTG could originate from endothelial cells or smooth muscle cells around which the A β accumulates. In later stages, co-localization is absent and tTG encloses the A β deposition in an abluminal and a luminal halo as shown in **Figure 2** (56). The tTG in the abluminal halo is assumed to be produced by fibroblasts in leptomeningeal vessels or astrocytes in parenchymal vessels, while tTG in the luminal halo is produced by endothelial cells in all vessel types. Moreover, ECM components fibronectin and laminin colocalize with the tTG in the halos (56). The tTGs cross-link fibronectin and laminin, and thereby stabilize the CAA. In conclusion, tTG might play an important role in the formation of vascular deposits in CAA patient.

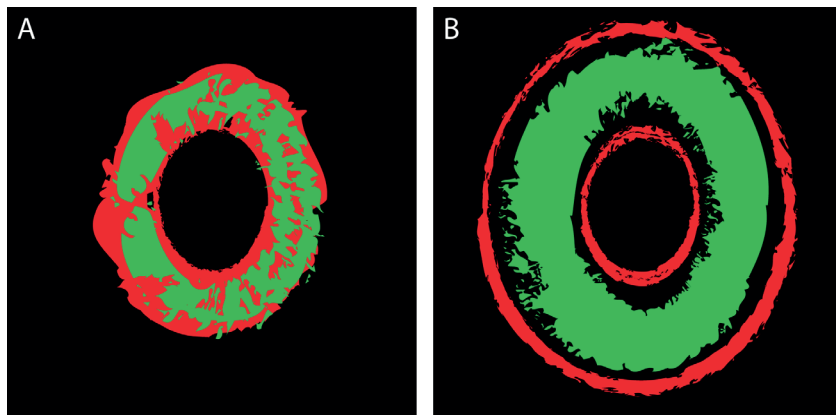


Figure 2 Schematic representation of tissue transglutaminase (tTG) and amyloid- β (A β) localisation in cerebral amyloid angiopathy in the neocortex of HCHWA-D patients. A β is shown in green, tTG in red. A. Early stage CAA: A β and tTG co-localize. B. Late stage CAA: A β and tTG do not co-localize anymore. Two halos of tTG are present: one luminal and one abluminal.

More recently, another important ECM modulator, lysyl oxidase (LOX) has been implicated in HCHWA-D and AD. LOX converts primary amines in peptide chains into aldehydes which interact to form cross-links between proteins. LOX is best known for its cross-linking of elastins and collagens in basement membranes and the ECM to maintain structural integrity (57), but HSPGs are also substrates of LOX (58). LOX is believed to play a role after tissue injury and is secreted by cells that are attracted to the brain injury sites (59). Elevated cross-linking of ECM by LOX increases permeability of the basement membrane, and thus destabilizes the vessels. LOX is present

within reactive astrocytes associated with parenchymal plaques in AD and HCHWA-D and LOX immunoreactivity is significantly increased in CAA affected vessels (58).

Potential therapies for HCHWA-D

Over the past few years, extensive research has been conducted on potential therapies for AD with the main focus on preventing formation and deposition of A β and tau, or increasing their clearance. Strategies reducing A β formation would also be interesting for HCHWA-D. Recent research has shown promising results in reducing A β production using RNA interference. RNA interference is a technique that down regulates gene expression by inducing degradation of targeted mRNA. Allele specific APP down regulation using short interfering RNA improved behaviour in an Alzheimer mouse model carrying the Swedish mutation (60). Using the same model, central and peripheral administration of an antisense oligonucleotide targeting APP, reduced formation of A β and improved the AD phenotype (61). However, APP has multiple morphoregulatory functions, like regulation of neurite outgrowth and complete knock-down of APP expression could lead to major side effects (62). Also the formation of the toxic A β peptides from APP could be prevented by increasing α -secretase activity or inhibiting the β - or γ -secretase activity. Epigallocatechin-gallate (EGCG), a compound that is also found in green tea, upregulates α -secretase and thereby promotes non-amyloidogenic processing of APP (63). Bryostatin 1 promotes α -secretase processing of APP by activating protein kinase C (64) and is currently in phase II clinical trials (Blanchette Rockefeller Neurosciences Institute).

Six small molecule BACE inhibitors are now tested in phase I trials (AZD3293, CTS-21166, E2609, PF-05297909 and TAK-070) and one (MK-8931) in phase II/III (65). Inhibiting γ secretase activity is not the best option, since γ secretase is involved in other pathways, like the Notch pathway (66). However, a “Notch-sparing γ secretase modulator” called Avagacestat has been tested in phase II, but led to worsening cognitive function, just like the phase III γ secretase inhibitor Semagacestat (67). Two other γ secretase targeting compounds (CHF-5074 and NIC5-15) are tested in phase II, but no results have been announced at this moment (67).

Another therapeutic agent that has been investigated for AD and could be interesting for HCHWA-D is *Scyllo*-inositol, an inhibitor of A β aggregation that demonstrated a decrease in CAA in an AD mice model (TgCRND8) after prophylactic administration (68). But clinical efficiency outcomes in a phase two clinical trial of AD patients using 250 mg *Scyllo*-inositol were not significantly different from placebo and higher dose studies were discontinued due to increased infections and mortalities (69).

An important feature of HCHWA-D is assembly of toxic A β fibrils at cell surfaces of cerebrovascular cells. The antioxidant catalase, which binds and degrades A β , was shown to inhibit this A β fibril-induced cell death in human brain pericytes (70).

The heat shock protein HspB8 could also inhibit A β 40 accumulation at the cell surface and this reduced accumulation resulted in reduced death of cerebrovascular cells (71). This made HspB8 an interesting candidate for HCHWA-D therapy. However, more research on heat shock proteins showed that these proteins induce interleukin-6 secretion in HCHWA-D, eventually leading to an inflammatory response (72).

The endogenous bile acid Tauroursodeoxycholic acid (TUDCA) is another agent that shows therapeutic potential by preventing A β accumulation. Administration of TUDCA reduced amyloid deposition and prevented the defects in spatial, recognition and contextual memory in APP/PS1 mice (73) and was shown to prevent Dutch mutated A β -induced apoptosis of cultured cerebral endothelial cells (74).

In HCHWA-D there is a detrimental MMP-2 activation. Using MMP inhibitors, this activation can be diminished and thereby smooth muscle cell viability can be increased (41), which could lead to a lower incidence of cerebral haemorrhages.

As discussed above, ECM components play a major role in CAA. ECM modulators are therefore promising therapeutic targets for HCHWA-D. However, tTG is not a suitable target, since interfering with tTG could lead to destabilization of the vascular A β deposits and consequently enhance the chance for vessel wall rupture and haemorrhages. In contrast, lowering LOX activity could be an interesting therapeutic possibility, since elevated LOX activity in CAA leads to increased permeability of the basement membrane.

Immunotherapy directly targets the toxic A β peptides. Several vaccines have been developed for the treatment of AD, and these vaccines were promising in pre-clinical animal models. However, these vaccines did not lead to clinical improvement in several trials. This must probably be explained by the fact that in these trials participants already showed a (severe) clinical phenotype, whereas the pathogenic mechanism must already have been active for years. It is likely that individuals with 'pre-clinical' AD may benefit more from these vaccines. However, it is still a challenge to identify pre-clinical AD. This is not the case for pre-clinical HCHWA-D, because the majority of individuals with the Dutch mutation will develop symptoms of HCHWA-D.

It should be noted that because aggregated A β is hard to dissolve, it is better to target A β in the soluble state. In addition, dissolving the vascular deposits could also lead to disruption of the vessel wall, increasing the chance of haemorrhages. The clearance of soluble A β could be stimulated by the

widely used drugs caffeine and rifampicin, since these drugs both upregulate the blood brain barrier transporter P-glycoprotein and rifampicin also upregulates LRP1 in wildtype mice (75). Since the proteolytic degradation of soluble A β is stimulated by ApoE, Cramer and colleagues hypothesized that enhancement of ApoE expression with the retinoid X receptor agonist bexarotene could promote A β clearance and microglial phagocytosis. They showed that administration of bexarotene led to a decrease in soluble and insoluble A β 40 and A β 42 levels, a decrease in cortical and hippocampal plaque burden and improved cognitive function of APP/PS1 mice (76). However, although the decrease in soluble A β was replicated (77,78), the decrease in plaque burden could not be replicated (77–80). Moreover, it is still unknown if this treatment would have an effect on CAA.

Conclusion

The Dutch mutation at position 22 of A β leads to multiple altered A β characteristics: charge alteration of the A β peptide leading to enhanced binding to cell surfaces and consequent A β accumulation, resistance to proteolysis and lowering of the affinity to brain efflux transporters.

The Dutch mutated A β is mainly produced in neurons, but forms fibrils at surfaces of cells in the vessel walls, where ECM modulators create an aggregation-promoting environment. The A β and sAPP in the vascular deposits promote cell degeneration and create an anticoagulant environment, which can eventually lead to haemorrhages.

Moreover, the elevated A β 40: A β 42 ratio in HCHWA-D suggests an inhibitory role for A β 40 in parenchymal aggregation, but there is also an important role for A β 42 as a seed for aggregation of A β 40 in the cerebral blood vessels. Studies into HSPG subtypes suggest that vascular deposits in AD and HCHWA-D arise *via* different mechanisms.

Studying HCHWAs and their mutations provides us with a better understanding of the effects of A β and the differences among A β isoforms, which not only gives more insight in HCHWA pathogenesis, but also in other amyloidosis diseases, like sporadic CAA or AD.

References

1. Levy E, Carman MD, Fernandez-Madrid IJ, Power MD, Lieberburg I, Van Duinen SG, et al. Mutation of the Alzheimer's disease amyloid gene in hereditary cerebral hemorrhage, Dutch type. *Science* (80-). 1990 Jun 1;248(4959):1124–6.
2. Wattendorff AR, Frangione B, Luyendijk W, Bots GT, Wattendorff, Frangione, et al. Hereditary cerebral haemorrhage with amyloidosis, Dutch type (HCHWA-D): clinicopathological studies. *J Neurol Neurosurg Psychiatry*. 1995 Aug;58(6):699–705.
3. Luyendijk W, Bots GTAM, Vegter-van der Vlis M, Went LN. Familiaire hersenbloedingen als gevolg van cerebrale amyloide angiopathie.pdf. 1986. p. 1935–40.
4. Wattendorff a R, Bots GT, Went LN, Endtz LJ. Familial cerebral amyloid angiopathy presenting as recurrent cerebral haemorrhage. *J Neurol Sci*. 1982 Aug;55(2):121–35.
5. Panegyres PK, Kwok JBJ, Schofield PR, Blumbergs PC. A Western Australian kindred with Dutch cerebral amyloid angiopathy. *J Neurol Sci*. 2005 Dec 15;239(1):75–80.
6. Natté R, Maat-Schieman MLC, Haan J, Bornebroek M, Roos RAC, Van Duinen SG. Dementia in hereditary cerebral hemorrhage with amyloidosis-Dutch type is associated with cerebral amyloid angiopathy but is independent of plaques and neurofibrillary tangles. *Ann Neurol*. 2001 Dec;50(6):765–72.
7. Yamada M, Naiki H. Cerebral amyloid angiopathy. 1st ed. Vol. 107, Progress in molecular biology and translational science. Elsevier Inc.; 2012. 41-78 p.
8. Jarrett JT, Lansbury PT. Seeding “one-dimensional crystallization” of amyloid: A pathogenic mechanism in Alzheimer's disease and scrapie? Vol. 73, *Cell*. 1993. p. 1055–8.
9. De Strooper B, Annaert W. Proteolytic processing and cell biological functions of the amyloid precursor protein. *J Cell Sci*. 2000 Jun;113 (Pt 1):1857–70.
10. Haass C, Hung AY, Schlossmacher MG, Oltersdorf T, Teplow DB, Selkoe DJ. Normal Cellular Processing of the β -Amyloid Precursor Protein Results in the Secretion of the Amyloid β Peptide and Related Molecules. *Ann N Y Acad Sci*. 1993;695(1):109–16.
11. Probst A, Heitz PU, Ulrich J. Histochemical analysis of senile plaque amyloid and amyloid angiopathy. *Virchows Arch A Pathol Anat Histol*. 1980;388(3):327–34.
12. Levy E, López-Otin C, Ghiso J, Geltner D, Frangione B. Stroke in icelandic patients with hereditary amyloid angiopathy is related to a mutation in the Cystatin C gene, an inhibitor of cysteine proteases. *J Exp Med*. 1989;169(5):1771–1778
13. Bugiani O, Giaccone G, Rossi G, Mangieri M, Capobianco R, Morbin M, et al. Hereditary cerebral hemorrhage with amyloidosis associated with the E693K mutation of APP. *Arch Neurol*. 2010 Aug;67(8):987–95.
14. Di Fede G, Catania M, Morbin M, Rossi G, Suardi S, Mazzoleni G, et al. A recessive mutation in the APP gene with dominant-negative effect on amyloidogenesis. *Science* (80). 2009;323(5920):1473–7.
15. Ovchinnikova OY, Finder VH, Vodopivec I, Nitsch RM, Glockshuber R. The Osaka FAD mutation E22 Δ leads to the formation of a previously unknown type of amyloid β fibrils and modulates A β neurotoxicity. *J Mol Biol*. 2011;408(4):780–91.
16. Melchor JP, McVoy L, Van Nostrand WE. Charge alterations of E22 enhance the pathogenic properties of the amyloid β -protein. *J Neurochem*. 2000 May;74(5):2209–12.
17. Tsubuki S, Takaki Y, Saido TC. Dutch, Flemish, Italian, and Arctic mutations of APP and resistance of A β to physiologically relevant proteolytic degradation. *Lancet*. 2003 Jun 7;361(9373):1957–8.
18. Van Nostrand WE, Wagner SL, Haan J, Bakker E RR. Alzheimers-Disease And Hereditary Cerebral-Hemorrhage With Amyloidosis - Dutch Type Share A Decrease In Cerebrospinal-Fluid Levels Of Amyloid Beta-Protein Precursor. *Ann Neurol*. 1992;32(2):215–8.
19. Lin Y-S, Pande VS. Effects of familial mutations on the monomer structure of A β ₄₂. *Biophys J*. 2012 Dec 19;103(12):L47-9.
20. Maat-Schieman MLC, Yamaguchi H, Van Duinen SG, Natté R, Roos RAC. Age-related plaque morphology and C-terminal heterogeneity of amyloid β in Dutch-type hereditary cerebral hemorrhage with amyloidosis. *Acta Neuropathol*. 2000 Apr;99(4):409–19.
21. Finder VH, Glockshuber R. Amyloid- β aggregation. *Neurodegener Dis*. 2007 Jan;4(1):13–27.
22. Bornebroek M, Haan J, Maat-Schieman ML, Van Duinen SG, Roos R a. Hereditary cerebral hemorrhage with amyloidosis-Dutch type (HCHWA-D): I--A review of clinical, radiologic and genetic aspects. *Brain Pathol*. 1996 Apr;6(2):111–4.
23. Maat-Schieman MLC, Yamaguchi H, Hegeman-Kleinn IM, Welling-Graafland C, Natté R, Roos RAC, et al. Glial reactions and the clearance of amyloid β protein in the brains of patients with hereditary cerebral hemorrhage with amyloidosis-Dutch type. *Acta Neuropathol*. 2004 May;107(5):389–98.
24. Nishitsuji K, Tomiyama T, Ishibashi K, Kametani F, Ozawa K, Okada R, et al. Cerebral Vascular Accumulation of Dutch- Type Ab42 , but Not Wild-Type Ab42 , in Hereditary Cerebral Hemorrhage With Amyloidosis , Dutch Type. *J Neurosci Res*. 2007;2923:2917–23.
25. Ozawa K, Tomiyama T, Maat-Schieman ML, Roos RA, Mori H. Enhanced A β ₄₀ deposition was associated with increased A β _{42/43} in cerebral vasculature with Dutch-type hereditary cerebral hemorrhage with amyloidosis (HCHWA-D). In: *Annals of the New York Academy of Sciences*. 2002. p. 149–54.
26. Prelli F, Levy E, van Duinen SG, Bots GTAM, Luyendijk W, Frangione B. Expression of a normal and variant Alzheimer's β -protein gene in amyloid of hereditary cerebral hemorrhage, Dutch type: DNA and protein diagnostic assays. *Biochem Biophys Res Commun*. 1990 Jul;170(1):301–7.
27. Herzig MC, Winkler DT, Burgermeister P, Pfeifer M, Kohler E, Schmidt SD, et al. A β is targeted to the vasculature in a mouse model of hereditary cerebral hemorrhage with amyloidosis. *Nat Neurosci*. 2004 Oct;7(9):954–60.
28. Hou L, Shao H, Zhang Y, Li H, Menon NK, Neuhaus EB, et al. Solution NMR Studies of the A β (1-40) and A β (1-42) Peptides Establish that the Met35 Oxidation State Affects the Mechanism of Amyloid Formation. *J Am Chem Soc*. 2004;126(7):1992–2005.
29. Monro OR, Mackic JB, Yamada S, Segal MB, Ghiso J, Maurer C, et al. Substitution at codon 22 reduces clearance of Alzheimer's amyloid- β peptide from the cerebrospinal fluid and prevents its transport from the central nervous system into blood. *Neurobiol Aging*. 2002;23(3):405–12.
30. Davis J, Xu F, Miao J, Previti M Lou, Romanov G, Ziegler K, et al. Deficient cerebral clearance of vasculotropic mutant Dutch/Iowa Double A β in human ABPP transgenic mice. *Neurobiol Aging*. 2006 Jul;27(7):946–54.

31. Deane R, Wu Z, Sagare A, Davis J, Du Yan S, Hamm K, et al. LRP/amyloid β -peptide interaction mediates differential brain efflux of A β isoforms. *Neuron*. 2004 Aug 5;43(3):333–44.
32. Bornebroek M, De Jonghe C, Haan J, Kumar-Singh S, Younkin S, Roos R, et al. Hereditary cerebral hemorrhage with amyloidosis dutch type (A β PP 693): Decreased plasma amyloid- β 42 concentration. *Neurobiol Dis*. 2003 Dec;14(3):619–23.
33. Nilsberth C, Westlind-Danielsson a, Eckman CB, Condron MM, Axelman K, Forsell C, et al. The “Arctic” APP mutation (E693G) causes Alzheimer’s disease by enhanced A β protofibril formation. *Nat Neurosci*. 2001;4(9):887–93.
34. Basun H, Bogdanovic N, Ingelsson M, Almkvist O, Näslund J, Axelman K, et al. Clinical and neuropathological features of the arctic APP gene mutation causing early-onset Alzheimer disease. *Arch Neurol*. 2008;65(4):499–505.
35. Brooks WS, Kwok JBJ, Halliday GM, Godbolt AK, Rossor MN, Creasey H, et al. Hemorrhage is uncommon in new Alzheimer family with Flemish amyloid precursor protein mutation. *Neurology*. 2004;63(9):1613–7.
36. Van Nostrand WE, Melchor JP. Disruption of pathologic amyloid beta-protein fibril assembly on the surface of cultured human cerebrovascular smooth muscle cells. *Amyloid*. 2001 Jan;8 Suppl 1(1):20–7.
37. Van Nostrand WE, Melchor J, Wagner M, Davis J. Cerebrovascular smooth muscle cell surface fibrillar A β . *Ann N Y Acad Sci*. 2000 Apr;903(631):89–96.
38. Van Nostrand WE, Schmaier AH, Siegel RS, Wagner SL, Raschke WC. Enhanced plasmin inhibition by a reactive center lysine mutant of the Kunitz-type protease inhibitor domain of the amyloid β -protein precursor. *J Biol Chem*. 1995;270(39):22827–30.
39. Wagner MR, Keane DM, Melchor JP, Auspaker KR, Van Nostrand WE. Fibrillar amyloid β -protein binds protease nexin-2/amyloid β -protein precursor: Stimulation of its inhibition of coagulation factor XIa. *Biochemistry*. 2000;39(25):7420–7.
40. Van Nostrand WE, Schmaier a H, Wagner SL. Potential role of protease nexin-2/amyloid β -protein precursor as a cerebral anticoagulant. *Ann N Y Acad Sci*. 1992;674:243–52.
41. Jung SS, Zhang W, Van Nostrand WE. Pathogenic A β induces the expression and activation of matrix metalloproteinase-2 in human cerebrovascular smooth muscle cells. *J Neurochem*. 2003 May 6;85(5):1208–15.
42. Verbeek MM, De Waal RMW, Schipper JJ, Van Nostrand WE. Rapid Degeneration of Cultured Human Brain Pericytes by Amyloid β Protein. *J Neurochem*. 2002 Mar;68(3):1135–41.
43. Corder EH, Saunders AM, Strittmatter WJ, Schmechel DE, Gaskell PC, Small GW, et al. Gene dose of apolipoprotein E type 4 allele and the risk of Alzheimer’s disease in late onset families. *Science* (80-). 1993;261(5123):921–3.
44. Haan J, Maat-Schieman MLC, Roos RAC. Clinical aspects of cerebral amyloid angiopathy. *Dement Geriatr Cogn Disord*. 1994;5(3–4):210–3.
45. Verbeek MM, Van Nostrand WE, Otte-Höller I, Wesseling P, De Waal RMW. Amyloid- β -induced degeneration of human brain pericytes is dependent on the apolipoprotein E genotype. In: *Annals of the New York Academy of Sciences*. 2000. p. 187–99.
46. Fossati S, Ghiso J, Rostagno A. Insights into caspase-mediated apoptotic pathways induced by amyloid- β in cerebral microvascular endothelial cells. *Neurodegener Dis*. 2012 Jan;10(1–4):324–8.
47. Hawkes C a, Härtig W, Kacza J, Schliebs R, Weller RO, Nicoll J a, et al. Perivascular drainage of solutes is impaired in the ageing mouse brain and in the presence of cerebral amyloid angiopathy. *Acta Neuropathol*. 2011 Apr;121(4):431–43.
48. van Horsen J, Otte-Holler I, David G, Maat-Schieman ML, van den Heuvel LP, Wesseling P, et al. Heparan sulfate proteoglycan expression in cerebrovascular amyloid deposits in Alzheimer’s disease and hereditary cerebral hemorrhage with amyloidosis (Dutch) brains. *Acta Neuropathol*. 2001 Dec;102(6):604–14.
49. Yin X, Zhang J, Wang X. Sequential injection analysis system for the determination of arsenic by hydride generation atomic absorption spectrometry. *Fenxi Huaxue*. 2004;32(10):1365–7.
50. Snow AD, Kinsella MG, Parks E, Sekiguchi RT, Miller JD, Kimata K, et al. Differential Binding of Vascular Cell-Derived Proteoglycans (Perlecan, Biglycan, Decorin, and Versican) to the Beta-Amyloid Protein of Alzheimer’s Disease. *Arch Biochem Biophys*. 1995;320(1):84–95.
51. Timmer NM, Schirris TJJ, Bruinsma IB, Otte-Höller I, van Kuppevelt TH, de Waal RMW, et al. Aggregation and cytotoxic properties towards cultured cerebrovascular cells of Dutch-mutated A β 40 (DA β (1–40)) are modulated by sulfate moieties of heparin. *Neurosci Res*. 2010 Apr;66(4):380–9.
52. De Jager M, van der Wildt B, Schul E, Bol JGJM, van Duinen SG, Drukarch B, et al. Tissue transglutaminase colocalizes with extracellular matrix proteins in cerebral amyloid angiopathy. *Neurobiol Aging*. 2013;34(4):1159–69.
53. Lorand L, Graham RM. Transglutaminases: Crosslinking enzymes with pleiotropic functions. Vol. 4, *Nature Reviews Molecular Cell Biology*. 2003. p. 140–56.
54. Ientile R, Caccamo D, Griffin M. Tissue transglutaminase and the stress response. Vol. 33, *Amino Acids*. 2007. p. 385–94.
55. Schmid AW, Condemi E, Tuchscherer G, Chiappe D, Mutter M, Vogel H, et al. Tissue transglutaminase-mediated glutamine deamidation of β -amyloid peptide increases peptide solubility, whereas enzymatic cross-linking and peptide fragmentation may serve as molecular triggers for rapid peptide aggregation. *J Biol Chem*. 2011;286(14):12172–88.
56. De Jager M, van der Wildt B, Schul E, Bol JGJM, van Duinen SG, Drukarch B, et al. Tissue transglutaminase colocalizes with extracellular matrix proteins in cerebral amyloid angiopathy. *Neurobiol Aging*. 2013 Apr;34(4):1159–69.
57. Kagan HM, Li W. Lysyl oxidase: Properties, specificity, and biological roles inside and outside of the cell. *J Cell Biochem*. 2003;88(4):660–72.
58. Wilhelmus MMM, Bol JGJM, van Duinen SG, Drukarch B. Extracellular matrix modulator lysyl oxidase colocalizes with amyloid-beta pathology in Alzheimer’s disease and hereditary cerebral hemorrhage with amyloidosis-Dutch type. *Exp Gerontol*. 2013 Feb;48(2):109–14.
59. Gilad GM, Kagan HM, Gilad VH. Lysyl oxidase, the extracellular matrix-forming enzyme, in rat brain injury sites. *Neurosci Lett*. 2001;310(1):45–8.
60. Rodríguez-Lebrón E, Gouvion CM, Moore SA, Davidson BL, Paulson HL. Allele-specific RNAi mitigates phenotypic progression in a transgenic model of Alzheimer’s disease. *Mol Ther*. 2009;17(9):1563–73.
61. Farr SA, Erickson MA, Niehoff ML, Banks WA, Morley JE. Central and peripheral administration of antisense oligonucleotide targeting amyloid- β protein precursor improves learning and memory and reduces neuroinflammatory cytokines in Tg2576 (A β PP^{swe}) mice. *J Alzheimer’s Dis*. 2014;40(4):1005–16.

62. Gralle M, Ferreira ST. Structure and functions of the human amyloid precursor protein: The whole is more than the sum of its parts. Vol. 82, *Progress in Neurobiology*. 2007. p. 11–32.
63. Smith A, Giunta B, Bickford PC, Fountain M, Tan J, Shytle RD. Nanolipidic particles improve the bioavailability and α -secretase inducing ability of epigallocatechin-3-gallate (EGCG) for the treatment of Alzheimer's disease. *Int J Pharm*. 2010;389(1–2):207–12.
64. Yi P, Schrott L, Castor TP, Alexander JS. Bryostatin-1 vs. TPPB: Dose-dependent APP processing and PKC- α , - δ , and - ϵ Isoform activation in SH-SY5Y neuronal cells. *J Mol Neurosci*. 2012;48(1):234–44.
65. Yan R, Vassar R. Targeting the β secretase BACE1 for Alzheimer's disease therapy. Vol. 13, *The Lancet Neurology*. 2014. p. 319–29.
66. Sato C, Zhao G, Xenia G, Ilagan M. An Overview of Notch Signaling in Adult Tissue Renewal and Maintenance. *Curr Alzheimer Res*. 2012;9(2):227–40.
67. Mikulca JA, Nguyen V, Gajdosik DA, Teklu SG, Giunta EA, Lessa EA, et al. Potential novel targets for Alzheimer pharmacotherapy: II. Update on secretase inhibitors and related approaches. *J Clin Pharm Ther*. 2014;39(1):25–37.
68. McLaurin JA, Kierstead ME, Brown ME, Hawkes CA, Lambermon MHL, Phinney AL, et al. Cyclohexanehexol inhibitors of A β aggregation prevent and reverse Alzheimer phenotype in a mouse model. *Nat Med*. 2006;12(7):801–8.
69. Salloway S, Sperling R, Keren R, Porsteinsson AP, Van Dyck CH, Tariot PN, et al. A phase 2 randomized trial of ELND005, scyllo-inositol, in mild to moderate Alzheimer disease. *Neurology*. 2011;77(13):1253–62.
70. Rensink AAM, Verbeek MM, Otte-Höller I, Ten Donkelaar HJ, De Waal RMW, Kremer B. Inhibition of amyloid- β -induced cell death in human brain pericytes in vitro. *Brain Res*. 2002;952(1):111–21.
71. Wilhelmus MMM, Boelens WC, Otte-Höller I, Kamps B, Kusters B, Maat-Schieman MLC, et al. Small heat shock protein HspB8: its distribution in Alzheimer's disease brains and its inhibition of amyloid-beta protein aggregation and cerebrovascular amyloid-beta toxicity. *Acta Neuropathol*. 2006 Feb;111(2):139–49.
72. Wilhelmus MMM, Boelens WC, Kox M, Maat-Schieman MLC, Veerhuis R, de Waal RMW, et al. Small heat shock proteins associated with cerebral amyloid angiopathy of hereditary cerebral hemorrhage with amyloidosis (Dutch type) induce interleukin-6 secretion. *Neurobiol Aging*. 2009 Feb;30(2):229–40.
73. Lo AC, Callaerts-Vegh Z, Nunes AF, Rodrigues CMP, D'Hooge R. Tauroursodeoxycholic acid (TUDCA) supplementation prevents cognitive impairment and amyloid deposition in APP/PS1 mice. *Neurobiol Dis*. 2013 Feb;50:21–9.
74. Viana RJS, Nunes a F, Castro RE, Ramalho RM, Meyerson J, Fossati S, et al. Tauroursodeoxycholic acid prevents E22Q Alzheimer's A β toxicity in human cerebral endothelial cells. *Cell Mol Life Sci*. 2009;66(6):1094–104.
75. Qosa H, Abuznait AH, Hill RA, Kaddoumi A. Enhanced brain amyloid- β clearance by rifampicin and caffeine as a possible protective mechanism against Alzheimer's disease. *J Alzheimer's Dis*. 2012;31(1):151–65.
76. Cramer PE, Cirrito JR, Wesson DW, Lee CYD, Karlo JC, Zinn AE, et al. ApoE-directed therapeutics rapidly clear β -amyloid and reverse deficits in AD mouse models. *Science*. 2012 Mar 23;335(6075):1503–6.
77. Fitz NF, Cronican AA, Lefterov I, Koldamova R. Comment on “ApoE-directed therapeutics rapidly clear beta-amyloid and reverse deficits in AD mouse models”. *Science*. 2013 May;340(6135):924–c.
78. Veeraghavalu K, Zhang C, Miller S, Hefendehl JK, Rajapaksha TW, Ulrich J, et al. Comment on “ApoE-directed therapeutics rapidly clear beta-amyloid and reverse deficits in AD mouse models”. *Science*. 2013 May;340(6135):924–f.
79. Price AR, Xu G, Sieminski ZB, Smithson LA, Borchelt DR, Golde TE, et al. Comment on “ApoE-directed therapeutics rapidly clear beta-amyloid and reverse deficits in AD mouse models”. *Science*. 2013 May;340(6135):924–d.
80. Tesseur I, Lo AC, Roberfroid A, Dietvorst S, Van Broeck B, Borgers M, et al. Comment on “ApoE-directed therapeutics rapidly clear beta-amyloid and reverse deficits in AD mouse models”. *Science*. 2013 May;340(6135):924–e.
81. Cruts M, Theuns J, Van Broeckhoven C. Locus-specific mutation databases for neurodegenerative brain diseases. *Hum Mutat*. 2012;33(9):1340–4.
82. Lan MY, Liu JS, Wu YS, Peng CH, Chang YY. A novel APP mutation (D678H) in a Taiwanese patient exhibiting dementia and cerebral microvasculopathy. *J Clin Neurosci*. 2014;21(3):513–5.
83. Kaden D, Harmeier A, Weise C, Munter LM, Althoff V, Rost BR, et al. Novel APP/A β mutation K16N produces highly toxic heteromeric A β oligomers. *EMBO Mol Med*. 2012;4(7):647–59.

Chapter 3

TGFβ pathway deregulation and abnormal phospho-SMAD2/3 staining in hereditary cerebral hemorrhage with amyloidosis-Dutch type

Laure Grand Moursel^{1,2}, Leon P. Munting^{1,2}, Linda M. van der Graaf^{1,2}, Sjoerd G. van Duinen³, Marie-Jose T.H. Goumans⁴, Uwe Ueberham⁵, Remco Natté³, Mark A. van Buchem², Willeke M.C. van Roon-Mom¹, Louise van der Weerd^{1,2}

¹ Department of Human Genetics, Leiden University Medical Center

² Department of Radiology, Leiden University Medical Center

³ Department of Pathology, Leiden University Medical Center

⁴ Department of Molecular Cell Biology, Leiden University Medical Center

⁵ Paul Flechsig Institute of Brain Research, University of Leipzig

Adapted from Brain Pathol. (2017).

Abstract

Hereditary cerebral hemorrhage with amyloidosis-Dutch type (HCHWA-D) is an early onset hereditary form of cerebral amyloid angiopathy (CAA) pathology, caused by the E22Q mutation in the amyloid β (A β) peptide. Transforming Growth Factor β 1 (TGF β 1) is a key player in vascular fibrosis and in the formation of angiopathic vessels in transgenic mice. Therefore we investigated whether the TGF β pathway is involved in HCHWA-D pathogenesis in human postmortem brain tissue from frontal and occipital lobes. Components of the TGF β pathway were analyzed with quantitative RT-PCR. TGF β 1 and TGF β Receptor 2 (TGFBR2) gene expression levels were significantly increased in HCHWA-D in comparison to the controls, in both frontal and occipital lobes. TGF β -induced pro-fibrotic target genes were also upregulated. We further assessed pathway activation by detecting phospho-SMAD2/3 (pSMAD2/3), a direct TGF β down-stream signaling mediator, using immunohistochemistry. We found abnormal pSMAD2/3 granular deposits specifically on HCHWA-D angiopathic frontal and occipital vessels. We graded pSMAD2/3 accumulation in angiopathic vessels and found a positive correlation with the CAA load independent of the brain area. We also observed pSMAD2/3 granules in a halo surrounding occipital vessels, which was specific for HCHWA-D. The result of this study indicates an upregulation of TGF β 1 in HCHWA-D, as was found previously in AD with CAA pathology. We discuss the possible origins and implications of the TGF β pathway deregulation in the microvasculature in HCHWA-D. These findings identify the TGF β pathway as a potential biomarker of disease progression and a possible target of therapeutic intervention in HCHWA-D.

Introduction

Sporadic cerebral amyloid angiopathy (sCAA) is a disease of the elderly and is due to amyloid β (A β) deposition in cerebral leptomeningeal and cortical vessels and it is associated with intracerebral hemorrhages. CAA pathology is a common feature in Alzheimer's Disease (AD) and is also a defining pathological feature in hereditary cerebral hemorrhage with amyloidosis-Dutch type (HCHWA-D; (22)). HCHWA-D is caused by a Gln-to-Glu substitution at codon 693 of the Amyloid Precursor Protein (APP) gene leading to the formation of the A β E22Q peptide, a particularly aggregation-prone and toxic variant of the A β peptide (17). The Dutch mutation results in severe CAA pathology with loss of vascular smooth muscle cells and intracerebral hemorrhage typically between the ages of 40 and 65. Although the correlation between HCHWA-D carrier status, reduced cerebrovascular function and the clinical phenotype has been studied (40), the exact mechanisms underlying A β accumulation in the vessel wall are still largely unknown.

Some earlier studies of HCHWA-D *post mortem* brain material have focused on A β clearance and deposition in the vasculature by the induction and modification of extracellular matrix (ECM) proteins (39,15). Transforming Growth Factor β 1 (TGF β 1) has a key role in vascular fibrosis by inducing ECM production in vessels. In postmortem AD brain material, TGF β 1 mRNA levels correlate positively with the extent of CAA pathology (46). Moreover, mouse models of TGF β 1 overexpression in astrocytes or neurons demonstrated that high TGF β 1 levels lead to vascular fibrosis (47,36). Whether these animal models actually accumulate murine A β in the CAA pathology-like vascular plaques remains controversial, but many *in vitro* studies have shown a role for TGF β 1 in promoting APP and A β production by astrocytes (12,1,21,4). Interestingly, TGF β 1 astrocytic overexpression in APP-overexpressing mice results in a CAA increase with a reduction in parenchymal A β plaque load (46).

TGF β 1, 2 and 3 isoforms are expressed in mammals and mediate their cellular effects through the TGF β type I (TGFBR1) and type II (TGFBR2) receptors. TGF β is present in an inactive form bound to the ECM and is activated by consecutive cleavage of the latent-associated-protein and pro-domain. Once activated, TGF β binding to TGFBR2 induces transphosphorylation of the TGFBR1 kinase, which subsequently recruits and phosphorylates the receptor regulated Smad (homolog of *Drosophila* mothers against decapentaplegic) signal transducing proteins, SMAD2 and/or SMAD3. Phospho-SMAD2/3 (pSMAD2/3) interacts with the common Smad, SMAD4, and translocate into the nucleus to regulate target gene expression. Genes related to ECM synthesis such as plasminogen activator inhibitor-1 (PAI-1), fibronectin

(FN1) and collagen (Type I Col1A1 and Type III Col3A1 for example) are typical TGF β target genes, and evidence is mounting that an increase in ECM production is linked to CAA pathology (14,44).

Accordingly, the aim of this study was to investigate in postmortem material whether the TGF β pathway is involved in the pathogenesis of HCHWA-D, based on gene expression levels and histological observations. We specifically investigated in HCHWA-D if there is a correlation between the deregulation of the TGF β pathway and the extent of CAA pathology.

Material and methods

Experimental design

HCHWA-D, healthy controls and sCAA brain material was used in the study as summarized in Table 1. Both frontal and occipital cortex were used in all studies, based on the assumption that the CAA pathology seems more severe in the occipital lobes in HCHWA-D (23) which therefore is expected to represent a more advanced disease stage compared to the frontal lobe. sCAA individuals were included to investigate whether the Dutch mutation in HCHWA-D results in a different effect on TGF β signaling compared to CAA pathology in general. As TGF β signaling increases with age (9), the control group was age-matched to the HCHWA-D patients. sCAA patients were significantly older (see Table 1).

We evaluated TGF β pathway activation by immunohistochemistry in HCHWA-D brain tissue, staining for the dually phosphorylated pSMAD2 and/or pSMAD3 indicative of active TGF β receptor signaling. These studies were performed in 11 HCHWA-D (age 60.5 years \pm 10.7 years), 11 control (age 69.2 years \pm 14.9 years) and 10 sCAA (age 74.8 years \pm 8.0 years) cases. We also analyzed gene expression levels for several pathway components (RT-PCR, see Table 2) in a sub-set of these patients of whom frozen brain was available: 7 HCHWA-D patients (age 56.4 years \pm 7.7 years) and 7 age-matched controls individuals (age 59.1 years \pm 0.1 years). Frozen sCAA material was not available for this measurement.

Brain tissue

Frontal and occipital human *post mortem* brain tissue was obtained from the Netherlands Brain Bank (NBB) and from our hospital (LUMC). Written informed consent was obtained for each donor and all material and data were handled in a coded fashion maintaining patient anonymity according to Dutch national ethical guidelines (Code for Proper Secondary Use of Human Tissue, Dutch Federation of Medical Scientific Societies). The study was approved by the local Ethics Committee.

Table 1 Demographics of cases and material used in this study

Diagnosis	Source	Code	Age	Gender	PMD ^a	RTqPCR ^b	IHC ^c	IF ^d
NDC	LUMC	C1	70	M	6	X	X	X
NDC	LUMC	C9	53	F	15			X
NDC	LUMC	C10	69	M	n.a.			X
NDC	LUMC	C11	51	M	15			X
NDC	LUMC	C12	67	M	29			X
NDC	LUMC	C13	78	F	n.a.			X
NDC	NBB	C2	61	F	10	X	X	X
NDC	NBB	C3	64	F	6	X	X	X
NDC	NBB	C4	56	M	9	X	X	X
NDC	NBB	C5	55	M	8	X	X	X
NDC	NBB	C6	51	M	8	X	X	X
NDC	NBB	C7	57	F	8	X	X	X
NDC	NBB	C14	91	F	4		X	
NDC	NBB	C15	89	F	7		X	
NDC	NBB	C16	83	M	5		X	
NDC	NBB	C17	84	F	6		X	
sCAA	LUMC	S1	68	M	n.a.		X	X
sCAA	LUMC	S2	67	M	n.a.		X	X
sCAA	LUMC	S3	68	M	n.a.		X	
sCAA	LUMC	S4	78	F	n.a.		X	
sCAA	LUMC	S5	73	F	n.a.		X	
sCAA +AD	LUMC	S6	69	F	n.a.		X	
sCAA	LUMC	S7	81	M	n.a.		X	
sCAA	LUMC	S8	74	F	n.a.		X	
sCAA	LUMC	S9	84	M	n.a.		X	
sCAA	LUMC	S10	89	F	n.a.		X	
HCHWA-D	NBB	H7	71	M	6	X	X	X
HCHWA-D	NBB	H6	61	M	7	X	X	X
HCHWA-D	LUMC	H4	55	F	15	X	X	X
HCHWA-D	LUMC	H5	50	M	19	X	X	X
HCHWA-D	LUMC	H1	48	M	11	X	X	X
HCHWA-D	LUMC	H2	57	M	3	X	X	X
HCHWA-D	LUMC	H3	53	F	6	X	X	X
HCHWA-D	LUMC	H8	51	M	3		X	X
HCHWA-D	LUMC	H11	81	F	n.a.		X	
HCHWA-D	LUMC	H9	67	F	n.a.		X	
HCHWA-D	LUMC	H10	71	M	n.a.		X	

NDC non-demented control, sCAA sporadic cerebral amyloid angiopathy, HCHWA-D hereditary cerebral hemorrhage with amyloidosis-Dutch type, NBB Netherlands Brain Bank, LUMC Leiden University Medical Center, n.a. not available. HCHWA-D subjects clinical history in Supplementary Table 2

^a Postmortem delay (in hours)

^b Quantitative RT-PCR

^c Immunohistochemistry for pSMAD2/3 quantification

^d Immunohistofluorescence for double staining

Table 2 Primer list used for qRT-PCR

Genebank Acc. Num.	Name	Primers	Target
NM_000660	TGFB1	5'-TACCTGAACCCGTGTTGCTC-3' 5'-GTATCGCCAGGAATTGTTGC-3'	Intron-spanning (exons 2-3)
NM_003238	TGFB2	5'-CAATGCCAACTTCTGTGCTG-3' 5'-ATATAAGCTCAGGACCCTGCTG-3'	Intron-spanning (exon 6-7)
NM_005901	SMAD2	5'-GTTTTGAAGCCGTCTATCAGC-3' 5'-TTGTTACCGTCTGCCTTCG-3'	Intron-spanning (exon 10-11)
NM_005902	SMAD3	5'-GAAGATGGAGAAACCAGTGACC-3' 5'-ATTCCGGGATAGGTTTGGAG-3'	intron-spanning (exons 4-5)
NM_005359	SMAD4	5'-TGGAGCTCATCCTAGTAAATGTG-3' 5'-AGGAAATCCTTCCGACCAG-3'	Intron-spanning (exon 2-3)
NM_005904	SMAD7	5'-AGGGGGAACGAATTATCTGG-3' 5'-TCGTCTTCTCCTCCAGTATG-3'	Intron-spanning (exon 3-4)
NM_001130916	TGFBR1	5'-CGTGCTGACATCTATGCAATG-3' 5'-TCAACTGATGGGTCAGAAGG-3'	Intron-spanning (exon 7-8)
NM_001024847	TGFBR2	5'-CTGTGTCGAAAGCATGAAGG-3' 5'-AGTCAACGTCTCACACACCATC-3'	intron-spanning (exon 6-7)
NM_000602	PAI-1	5'-CAACTGCTTGGGAAAGGAG-3' 5'-CGTCTGATTGTGGAAGAGG-3'	Intron-spanning (exons 3-4)
NM_212482	FN1	5'-GCAGTGGCTGAAGACACAAG 5'-CCTGCCATTGTAGGTGAATG	Intron-spanning (exon 7-8)
NM_000088	Col1A1	5'-ATGACGTGATCTGTGACGAGAC 5'-TTCTTGGTCGGTGGGTGAC	Intron-spanning (exons 2-3)
NM_000090	Col3A1	5'-GACCTGAAATTCTGCCATCC 5'-GCATGTTTCCCCAGTTTCC	Intron-spanning (exons 48-49)
NM_003194	TBP	5'-CGCCGAATATAATCCAAGC-3' 5'-GAAAATCAGTGCCGTGGTTC-3'	intron-spanning _ reference gene
NM_000983	RPL22	5'-TCGCTCACCTCCCTTTCTAA-3' 5'-TCACGGTGATCTTGCTCTTG-3'	intron-spanning _ reference gene
NM_000190	HMBS	5'-GCAACGGCGGAAGAAAA-3' 5'-CGAGGCTTCAATGTTGCC-3'	intron-spanning _ reference gene

Quantitative RT-PCR

Frozen brain tissue was cut with a sliding microtome (Leica SM2010 R), homogenized with ceramic MagNA lyser beads (Roche) and grinded using a Bullet Blender (Next Advance). RNA was extracted immediately with Aurum Total RNA Mini Kit (Biorad), including removal of remaining genomic DNA by an on-column DNaseI treatment for 25 min. Total RNA was eluted in 60 µl of provided buffer and the RNA content was measured with Nanodrop at 260 nm. All RNA extractions were performed in duplicate and cDNA was synthesized directly after extraction with the Transcriptor First Strand cDNA Synthesis Kit (Roche) using Random Hexamer primers

at 65 °C. The cDNA was then adjusted and aliquoted at 20 ng/µL. Evaluation of RNA Integrity was performed with on-chip electrophoresis using an RNA 6000 Nano kit and a Bio-Analyzer 2100 (Agilent Technologies).

Intron-spanning primers targeting TGFβ pathway components (indicated in Table 2) were designed for qPCR using Primer3 Plus software (38). Primer pairs were first spotted into the wells (2.5 pmol of each in 2 µl). The qPCR was performed in a 384 wells plate using 6 ng of cDNA in a PCR master mix (Roche; 1 time PCR buffer with MgCl₂, 0.2 mM dNTPs, 0.28 U FastStart Taq DNA Polymerase) containing 1 time EvaGreen-qPCR dye (Biotum) and PCR grade water to a final volume of 8 µl per well. All samples were run in duplicate on the same plate along with three reference genes: Hydroxymethylbilane Synthase (HMBS), Ribosomal Protein L22 (RPL22) and TATA-Box Binding Protein (TBP). The amplification was performed on a LightCycler 480 (Roche) with an initial denaturation of 10 minutes at 95°C, followed by 45 cycles of 10 seconds denaturation at 95°C, 30 seconds annealing at 60°C and 20 seconds elongation at 72°C. Relative expression of the transcript levels was calculated using LinRegPCR v11.1 (32) with the raw fluorescence values as input. Transcript levels were calculated with the Geomean of the biological and technical repeat (4 points) normalized with two of the reference genes (HMBS and RPL22). The third reference gene (TBP) was used to check the normalization efficiency and the inter-plate variance. Changes in relative transcript levels were analyzed in GraphPad Prism version 6.00 using an unpaired two-sided Student's *t* test. Differences between groups were considered significant when *p*<0.05.

Immunohistochemical staining and quantification of pSMAD2/3 in blood vessels

Formalin-fixed, paraffin-embedded blocks of brain tissue were cut into serial 5 µm thick sections and mounted on coated glass slides (SuperFrost® Plus, VWR). Deparaffinization in xylene and rehydration through a series of ethanol concentrations were followed by antigen retrieval by cooking for 40 minutes at 0.76 bar steam pressure (Steba DD 1 ECO) in an acidic pH 6 solution (H-3300, Vector labs). Sections were then blocked for endogenous peroxidase with 3 % H₂O₂ in dH₂O for 10 minutes and for unspecific epitopes binding with blocking buffer [1 % BSA suspension in washing buffer (0.1 % Tween 20 in Phosphate Buffer Saline pH 7.4)] for 1 hour at room temperature. After, the sections were incubated with rabbit anti-pSMAD2/3 antibody (#3101S, Cell Signaling, 1:500 dilution) overnight at 4°C in the blocking buffer. Incubation with secondary anti-Rabbit HRP was followed by a DAB reaction kit (SK-4100, Vector lab) and mounting with Entellan® New (107961, Merck). Sections were scanned (Philips Ultra Fast Scanner 1.6 RA) for grading.

The grading of pSMAD2/3 staining was reproduced on scanned sections by two independent researchers (LvdG; JMdJ) blinded to the clinical diagnosis of each case. Six fields throughout gray matter areas of the slides were randomly selected at 100x magnification (2.016 mm² per field view). Per area, radially crosscut parenchymal angiopathic arterioles were counted. CAA load is defined here as the average number of angiopathic arterioles, identified by a typical thickened vessel wall, per mm². Presence of A β in angiopathic arterioles was checked on a consecutive slide (data not shown, not used for the grading). pSMAD2/3 deposits in the tunica media of angiopathic arterioles was determined for each vessel at 400x magnification. Difference in CAA load between frontal and occipital cortex was assessed with GraphPad Prism version 6.00 using a paired two-sided Student's *t* test. Differences between groups were considered significant when *p*<0.05.

Immunohistofluorescent double staining and pSMAD2/3 specificity

Formalin-fixed, paraffin-embedded frontal and occipital cortex 5 μ m sections were used from patient material as specified in Table 1. Deparaffinization, antigen retrieval and blocking steps were identical to the immunohistochemical staining. Rabbit anti-pSMAD2/3 antibody (#3101S, Cell Signaling; 1:500 dilution) was incubated overnight at 4°C with mouse antibodies (references and dilutions in Supplementary Table 1). The antibodies were visualized with anti-rabbit Alexa Fluor® 488 and anti-mouse Alexa Fluor® 594 respectively (1 hour at RT). Alternatively, Tyramide Signal Amplification (TSA® biotin detection kit, NEL700A001KT, Perkin Elmer) followed by streptavidin, Alexa Fluor® 488 conjugate was used when specified in the text (Supplementary Table 1). Nuclei were stained with DAPI (1 μ g/mL) during the secondary antibody incubation step. After each incubation, the slides were extensively washed in washing buffer. Sections were mounted in Pro Long Diamond (Life technologies). Images of the fluorescent staining were acquired using a confocal laser-scanning microscope (Leica SP8, Leica Microsystems). The specificity of pSMAD2/3 staining was assessed either with calf intestine alkaline phosphatase treatment removing the phosphor-epitopes (adapted from (37), details in Supplementary Figure 1) and by using different phospho-antibodies for the same epitope (Supplementary Figure 1 and Supplementary Table 1). No cross-reactivity were observed with anti-pSMAD1/5/9 (data not shown). A granular perivascular pSMAD2/3 staining was also detected by Dr Ueberham.

Results

TGF β 1 and TGFBR2 are upregulated in HCHWA-D

From literature we know that the SMAD-dependent signaling TGF β pathway is activated upon binding of TGF β 1 or TGF β 2 to TGFBR2, followed by phosphorylation of SMAD2 and 3 by TGFBR1. To assess TGF β pathway implication we measured gene expression levels of TGF β 1, TGF β 2, TGFBR1, TGFBR2, SMAD2, SMAD3, SMAD4 and SMAD7 by qRT-PCR. The relative gene expression levels of TGF β 1 and TGFBR2 were significantly higher in the frontal and occipital lobes of HCHWA-D patients compared to age-related controls (Figure 1). TGFBR1 followed a similar trend, but did not reach statistical significance. TGF β 2 levels were significantly higher in the frontal lobe of HCHWA-D samples, especially in the two eldest patients from the gene expression study (H6 and H7); (Figure 1). Interestingly, these two samples also present the highest level of the inhibitory Smad, SMAD7, suggesting an enhanced TGF β pathway activation compared to the other HCHWA-D patients (Supplementary Figure 2). Other signaling effectors of the canonical SMAD pathway (SMAD2, SMAD3, SMAD4 and SMAD7) were further not significantly different (Supplementary Figure 2).

Plasminogen activator inhibitor-1 (PAI-1), fibronectin1(FN1), Col1A1 and Col3A1 are known SMAD-dependent downstream targets of TGF β . PAI-1 and FN1 gene expression level were both significantly higher in frontal and occipital cortex of HCHWA-D patients. Col3A1 and Col1A1 were upregulated in both brain area, but reach statistical significance in the frontal cortex only (Figure 2).

pSMAD2/3 is accumulating in HCHWA-D, but not in sCAA

To evaluate TGF β pathway activation by immunohistochemistry in HCHWA-D brain tissue, we stained for the TGF β 1 down-stream signaling effector dually phosphorylated pSMAD2/3. Frontal and occipital cortex of controls, sCAA and HCHWA-D cases were assessed for pSMAD2/3 staining. In all the observed cases, pSMAD2/3 labelling was predominantly located in nuclei of neurons, with little or no cytoplasmic staining detected in both brain areas.

Both in frontal and occipital cortex, pSMAD2/3 staining in amyloid-laden vessels were found uniquely in HCHWA-D cases. The staining pattern showed distinct granules in the tunica media as well as diffuse staining covering the entire vessel wall. Examples of these granular deposits are given in Figure 3A. pSMAD2/3-positive and negative vessels were not morphologically different. Notably, pSMAD2/3 deposits were mainly found in parenchymal arterioles with A β covering the entire vessel circumference (double staining with anti-A β antibodies, Figure 3B),

corresponding to an advanced CAA grade (grade 2 or 3 based on the A β content as defined by Greenberg and Vonsattel (13)). Nevertheless these granular deposits in the tunica media were not colocalized with the smooth muscle actin (SMA) staining, and we could observe in some angiopathic vessels an accumulation of pSMAD2/3 granules in vacuoles believed to be the remains of vascular smooth muscle cells (Supplementary Fig 3).

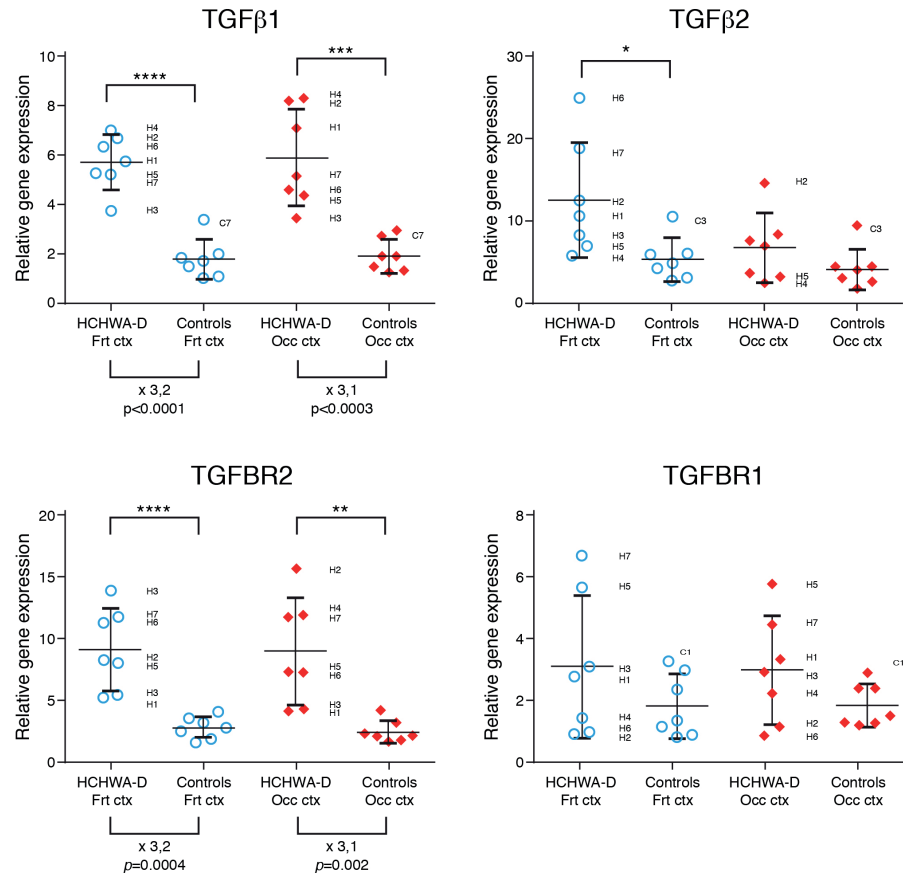


Figure 1: Significant upregulation of TGFβ1 and TGFBR2 gene levels (*left panel*; *x* indicates the time fold change) in HCHWA-D frontal (Frt) and occipital (Occ) cortex compared to age-related controls. Transcript expression levels in postmortem brain cortex were normalized with two reference genes and represented in a dot plot with mean ± SD of 7 samples; **p*<0.05, ***p*<0.01, ****p*<0.001 and *****p*<0.0001 as determined by a two-tailed unpaired Student's *t* test

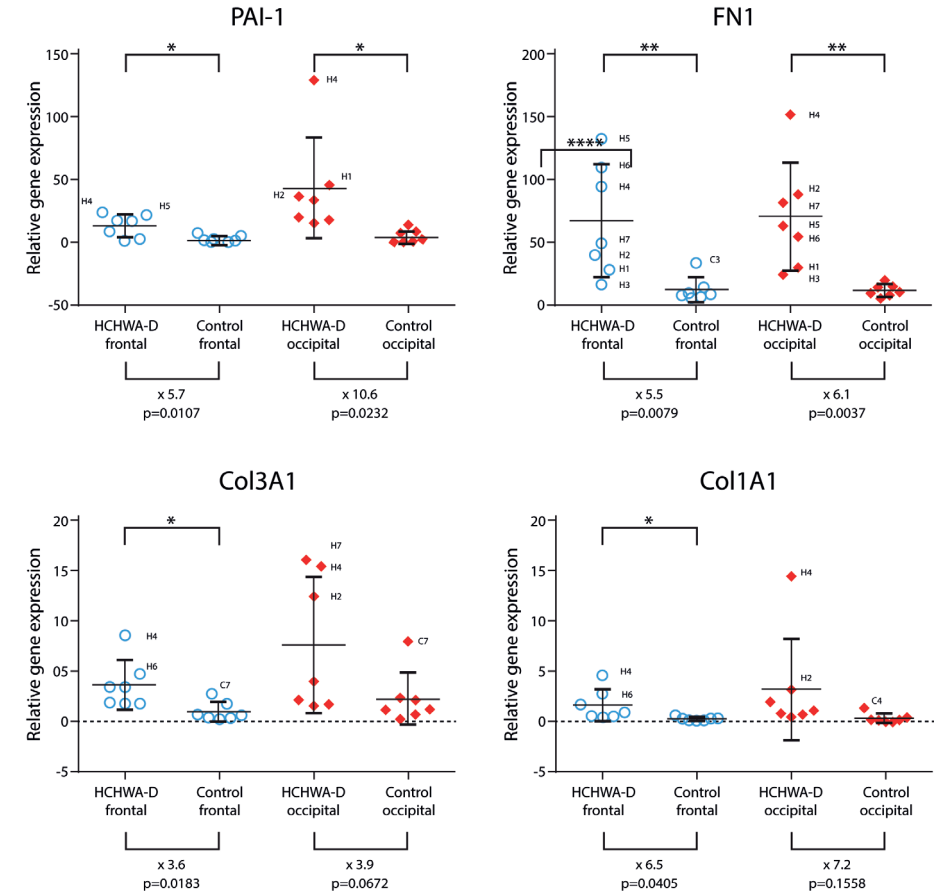


Figure 2: Significant upregulation of PAI-1 and FN1 gene levels (*upper panel*; *x* indicates the time fold change) in HCHWA-D frontal (Frt) and occipital (Occ) cortex compared to age-related controls. Col3A1 and Col1A1 increase reach statistical significance in frontal cortex only. Transcript expression levels in postmortem brain cortex were normalized with two reference genes and represented in a dot plot with mean ± SD of 7 samples; **p*<0.05, ***p*<0.01, ****p*<0.001 and *****p*<0.0001 as determined by a two-tailed unpaired Student's *t* test

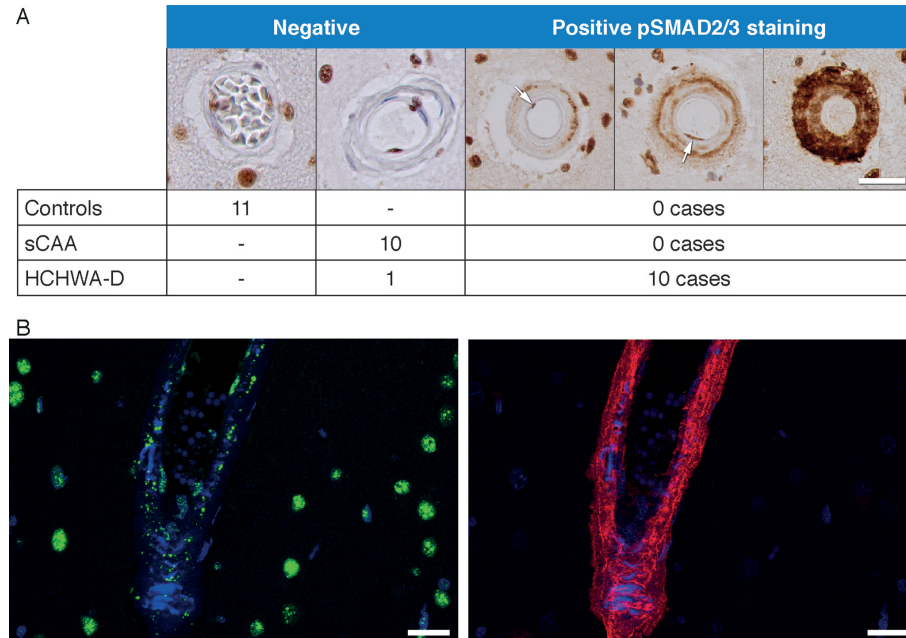


Figure 3: pSMAD2/3 granular deposits in angiopathic vessel walls. **(A)** Examples of immunohistochemical pSMAD2/3 staining graded as negative and positive. pSMAD2/3 deposits were found in 10 out of 11 HCHWA-D cases (at least one positive vessel per slide), none were found in controls or sCAA cases. Staining of endothelial cell nuclei are not counted (see the “negative” example). (*arrows* illustrate nuclei of endothelial cells in luminal position). **(B)** Immunohistofluorescent double staining with pSMAD2/3 TSA (*green*), A β 6E10 (*red*) and nuclei (*blue*). pSMAD2/3 deposits in parenchymal angiopathic arterioles, with A β covering the entire vessel circumference. HCHWA-D H2 patient-occipital cortex, merged confocal stack. *Scale bar (A, B) 25 μ m*

pSMAD2/3 accumulation is correlated with CAA load, but less with age

Entire tissue sections were graded to assess pSMAD2/3 staining in HCHWA-D samples. For the same sections, the CAA load was measured as the number of angiopathic arterioles in a defined area. We found no significant differences in CAA load between frontal and occipital cortex (Figure 4A). However, a significant positive correlation between pSMAD2/3-positive angiopathic vessels and CAA load was found independently of the brain area studied (Figure 4B). This confirmed that pSMAD2/3 deposits are only present once the CAA pathology becomes more severe. In areas with a high CAA load, most angiopathic vessels are pSMAD2/3-positive. Although there is a strong correlation between pSMAD2/3 and CAA pathology

severity, CAA load in itself is only moderately dependent on the age of the patients (Fig 4C and 4D). In particular, the 81-years-old patient, who reached an unusual age for HCHWA-D, was much less affected than expected.

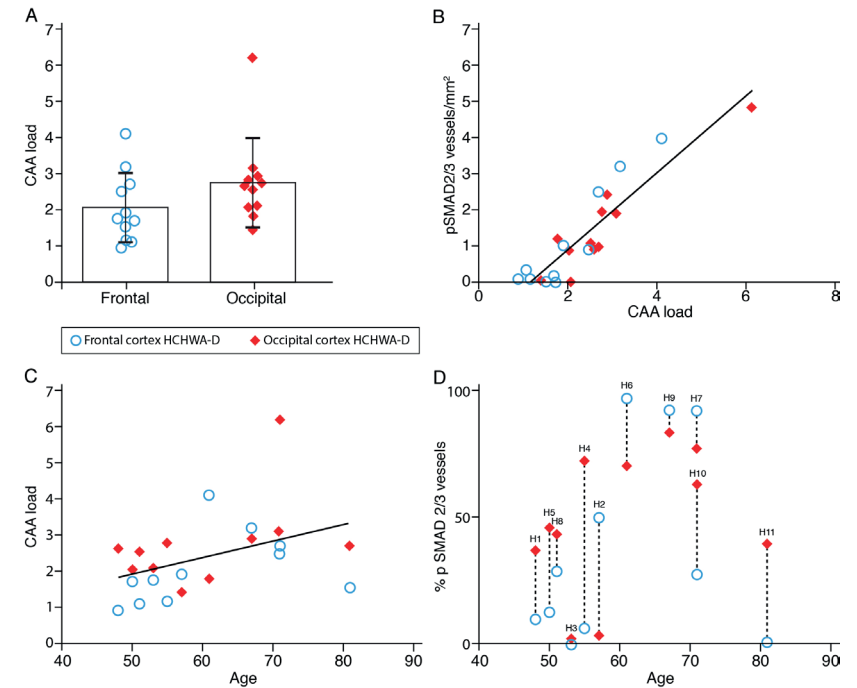


Figure 4: Quantification of CAA load and relationship with pSMAD2/3 accumulation in HCHWA-D. **(A)** CAA load was higher in occipital cortex but did not reach statistical difference (two-tailed paired Student’s *t* test; the graph represents the mean \pm SD of angiopathic vessels per mm²). **(B)** Angiopathic pSMAD2/3 vessel wall deposits were correlated positively with CAA load (both expressed as number of vessel per mm²; $r^2=0.8220$, $p<0.0001$). **(C)** CAA load was weakly correlated with age ($r^2=0.1702$; not statistically significant). **(D)** Proportion of angiopathic vessels in HCHWA-D subjects with pSMAD2/3 vessel wall deposits (*dashed lines* link brain parts of the same subject; *H numbers* refer to Table 1)

Perivascular pSMAD2/3 granules are present in occipital cortex of HCHWA-D

Apart from granules localized on angiopathic vessels in HCHWA-D, pSMAD2/3 granules were also found in the parenchyma. These were observed as perivascular parenchymal rings (see Figure 5A and B) in the occipital cortex in about 50 % of the cases (Supplementary Table 2), but

never in the frontal cortex of HCHWA-D brains or in sCAA and control cases. Perivascular rings were found both around angiopathic and non-angiopathic vessels, as well as around capillaries, and were found in clusters with a predilection for the first and last cortical layer of the gray matter. SMAD4 binding to pSMAD2/3 is a prerequisite for SMAD2/3 to enter the nucleus and initiate gene transcription. However, in our samples, SMAD4 was neither co-localized with granular vascular, nor with perivascular halo of pSMAD2/3 staining (Supplementary Figure 4); suggesting that these granules are probably not participating in the active signalling.

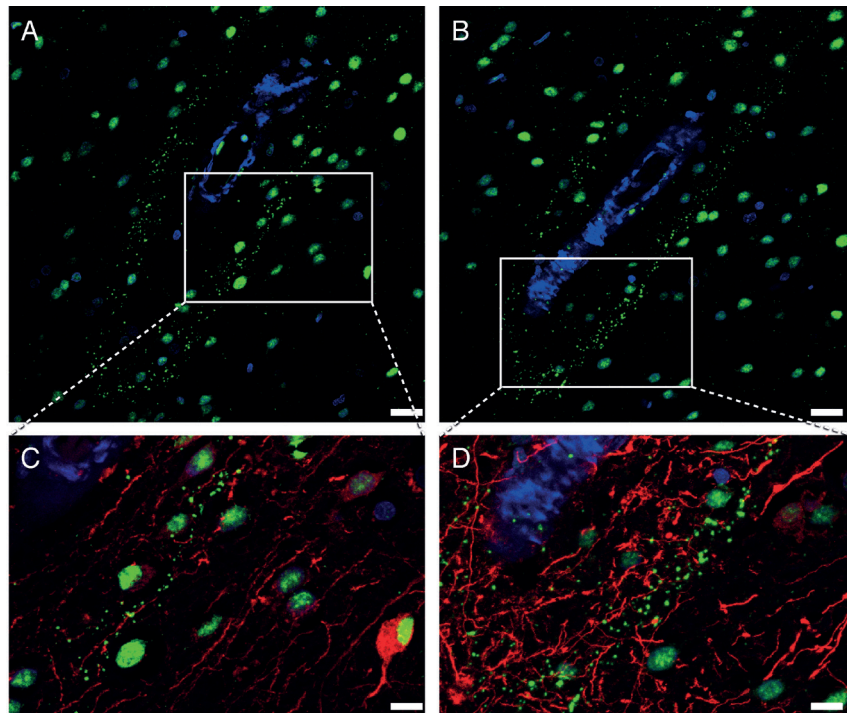


Figure 5: Perivascular pSMAD2/3 granules showed a linear alignment in a vessel with a longitudinal cut in HCHWA-D occipital cortex. Immunohistochemical double staining with neuronal (MAP-2) and astrocytic (GFAP) cytoskeleton markers. (A-B) pSMAD2/3 TSA (green) and nuclei (blue) channels. (C-D) detail including MAP-2 (red; C) or GFAP (red; D). Presence of perivascular pSMAD2/3 granules along the neuronal MAP-2 dendrites (C), and never colocalizing with GFAP processes (D). Consecutive sections of HCHWA-D H1 patient occipital cortex, merged confocal stack. Scale bar (A-B) 25 μ m; (C-D) 10 μ m

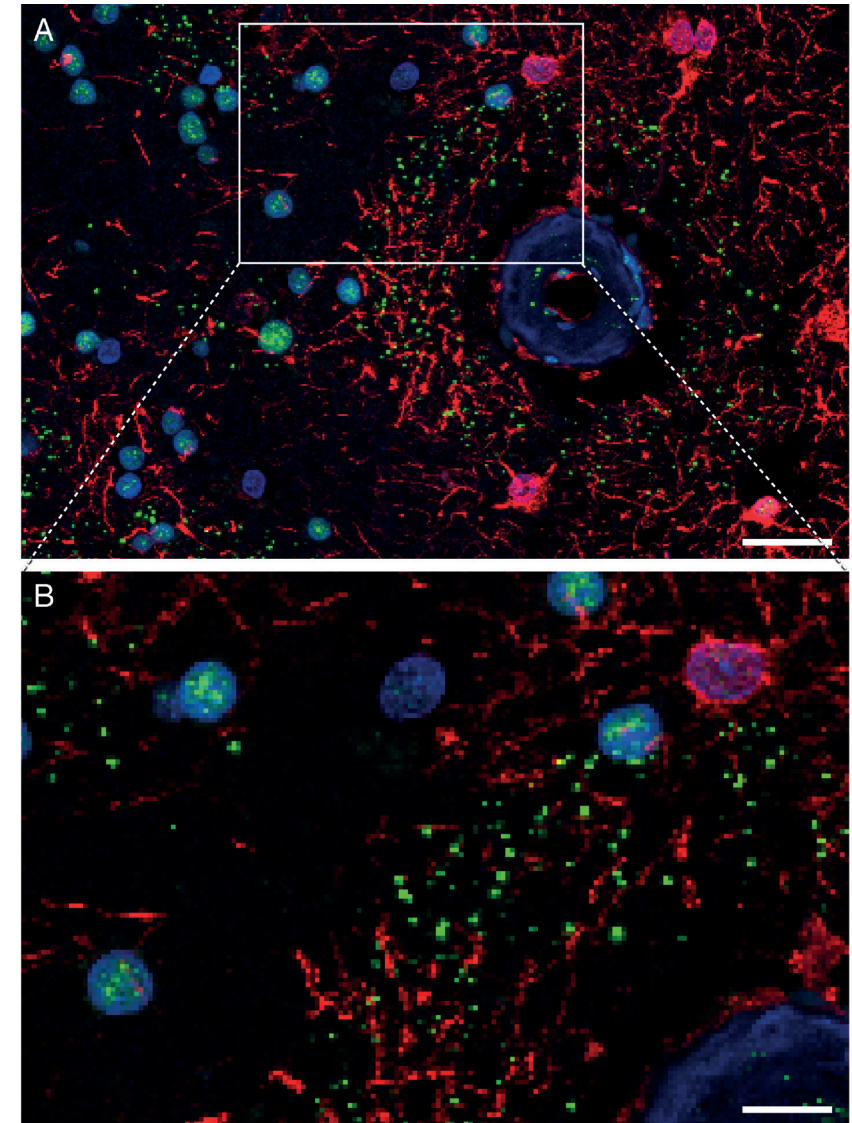


Figure 6: Perivascular ring of pSMAD2/3 granules limited to the area of GFAP-positive astrocytes. Immunohistochemical double staining with pSMAD2/3 (green), GFAP (red) and nuclei (blue). (B) detail of (A). HCHWA-D H1 patient occipital cortex, merged confocal stack. Scale bar (A) 25 μ m; (B) 10 μ m

Perivascular pSMAD2/3 granules do not co-localize with studied cell types or neuropathological features

Since perivascular pSMAD2/3 granules were arranged in a linear alignment, reminiscent of cytoskeletal filaments (Figure 5), we investigated whether the granules co-localized with a particular cell type using neuronal and astrocytic cytoskeleton markers. MAP-2 staining revealed a presence of the granules along perivascular dendrites (Figure 5C) without co-localization within the neuronal processes. pSMAD2/3 granules never aligned with GFAP processes (Figure 5D) but were topographically restricted to GFAP-positive perivascular areas, as depicted in Fig 5. Further, parenchymal cytoplasmic pSMAD2/3 granules were incidentally identified in neurons in some HCHWA-D individuals (Supplementary Figure 5).

Previous HCHWA-D studies reported perivascular ubiquitinated and phosphorylated neurites associated with preamyloid and amyloid deposits around angiopathic vessels (33,24). Therefore, we examined in HCHWA-D occipital samples whether the pSMAD2/3 perivascular granules were co-localized with any of these previously reported deposits. No co-localization of pSMAD2/3 granules was found in the perivascular rings with A β , hyperphosphorylated Tau (pTau, AT-8 antibody) and ubiquitin. Likewise, we stained for perivascular coarse deposits of ECM as described previously for HCHWA-D using collagen IV and laminin antibodies (39). Although we found these coarse deposits, they did not co-localize with pSMAD2/3 granules (Figure 7A and B). Furthermore, an extracellular pSMAD2/3 deposition with amyloid deposits and neuritic plaques was described in AD (37,6). Even though a similar co-localization with diffuse parenchymal A β plaques in HCHWA-D was occasionally detected, these extracellular pSMAD2/3 deposits had a fibrous-like and diffuse staining that is different from the bright round-shaped dots composing the pSMAD2/3 granular rings (Supplementary Figure 6).

Discussion

Our findings suggest that TGF β is implicated in the pathogenesis of HCHWA-D. We found an upregulation in gene expression of several components of the TGF β pathway and its direct downstream signaling targets as well as a strong correlation of pSMAD2/3 deposits with CAA load.

Based on previous studies in HCHWA-D describing an increased CAA pathology in the occipital cortex compared to the frontal cortex (23), we hypothesized that the CAA load and the associated vascular pathology in the occipital lobe would represent a more advanced disease stage. However, in our HCHWA-D samples, individual perforating arterioles presented a

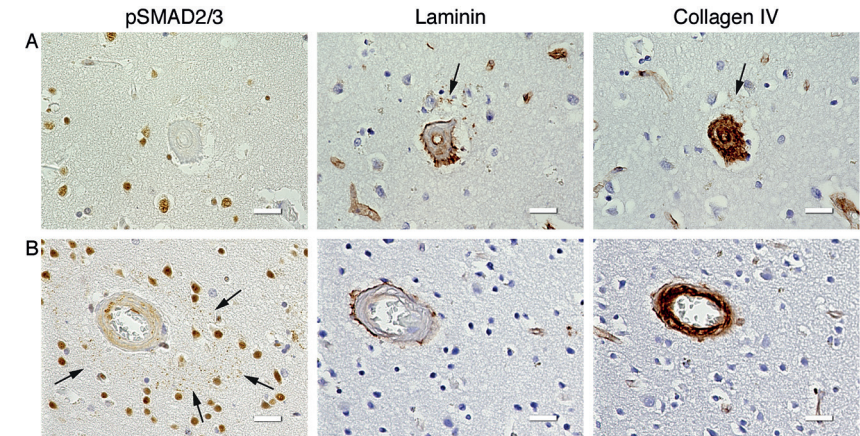


Figure 7: ECM coarse deposits did not spatially correspond to the pSMAD2/3 granules. Immunohistochemical staining of consecutive slides with pSMAD2/3, laminin and collagen IV antibodies. (A) Laminin coarse deposit (and weak Collagen IV colocalization; arrows) without presence of pSMAD2/3 granules; HCHWA-D H5 patient-occipital cortex. (B) pSMAD2/3 perivascular ring of granules (arrows) without perivascular ECM deposits; HCHWA-D H1 patient-occipital cortex. Scale bar 25 μ m

consistent moderate to severe CAA grade (grade 2 to 3), irrespective of the brain area studied. Furthermore, the CAA load, based on the number of angiopathic vessels per mm², was not significantly different in the two lobes (Figure 4A). A possible explanation for this finding is that the higher CAA load in the occipital cortex compared to the frontal cortex in previous studies is influenced by the presence of angiopathic capillaries (25). Capillary CAA is typically a feature of aged patients, while our cohort was relatively young. Additionally, the high occipital CAA load in the occipital cortex was in most cases confined to the end of the occipital horn (28), whereas our samples were obtained from diverse occipital area.

Although we did not find a difference in CAA severity between occipital and frontal lobes, we found a high correlation between the CAA load and the presence of pSMAD2/3 granules. Strikingly, these granules were only found in HCHWA-D patients, but not in sCAA cases, even in similarly affected vessels. The association of CAA pathology with pSMAD2/3, which is a direct TGF β down-stream signaling effector, suggests an involvement of TGF β on the vessel wall pathology. TGF β is thought to be a key mediator of vascular remodelling (31) that is found in sporadic small-vessel diseases (34). TGF β deregulation in the vessel wall is a central mechanism common to several hereditary brain microvasculopathies, like cerebral autosomal dominant arteriopathy with subcortical infarcts and leukoencephalopathy

(CADASIL; (18)) or cerebral autosomal recessive arteriopathy with subcortical infarcts and leukoencephalopathy (CARASIL, (48,3)). TGF- β signaling was recently proposed as a common denominator of several forms of cerebral small-vessel diseases (26). Common microvasculopathies include microaneurysms, fibrinoid necrosis, obliterative intimal changes, and hyaline thickening. Interestingly, these secondary structural microvasculopathies, are found more frequently in HCHWA-D in comparison to sCAA (41) and are correlated to CAA load (28). This aggravated remodeling may be due to a fast progression of the disease in HCHWA-D or to a direct effect of Dutch-type A β binding to TGFBR2, directly activating the signaling pathway (16). Accumulation of pSMAD2/3 granules in the vessel wall in HCHWA-D supports the hypothesis that TGF β deregulation contributes to secondary microvascular remodeling.

TGF β 1 was upregulated in our HCHWA-D *post mortem* brain tissue, similar to a previous study where a correlation was found in the cerebrovascular pathology of AD (45). Although part of the observed result is possibly influenced by differences in the cellular composition of HCHWA-D cortex, normalization per cell type cannot be achieved, nor is commonly done in RT-qPCR. We corrected for the total amount of transcript per sample with stably expressed reference genes. Another potential confounder in our study is that all patients suffered one or more hemorrhagic strokes before death, which influences TGF β 1 expression. It is known that the expression of TGF β 1 increases rapidly after brain injury to restrict brain damage and as part of the healing process (11,9). Still, we found consistent upregulation in all patients in our cohort, despite very different survival times after hemorrhage (from days to several years), variable hemorrhage sites and even unrelated causes of death. This suggests that the TGF β upregulation we found cannot solely be explained by an acute response after stroke, but is likely linked to the CAA pathology itself, as evidenced by the histological spatial correlation described above. We also found TGFBR2, the ligand-binding receptor, upregulated in HCHWA-D occipital and frontal cortex. Previous studies have also found high levels of TGFBR2 in a mouse model of traumatic cerebral injury and stroke in the chronic phase (10,30). These findings indicate that TGFBR2 upregulation is not an acute response. Lastly, the upregulation of TGF β -induced pro-fibrotic target genes such as PAI-1, FN1, Col1A1 and Col3A1 indicate that the TGF β signaling pathway is likely activated.

TGF β upregulation is a double-edged sword with both protective and deleterious consequences. The vascular remodeling and fibrosis induced by TGF β might have a protective effect in CAA pathology, due to the cross-linked increased ECM and basement membrane which might prevent the weakening of the vessel wall (49,8). Despite this protective effect in

terms of stroke survival and prevention of hemorrhage, persistent TGF β upregulation is also thought to have a major downside. The resultant ECM synthesis which modifies the composition of basement membrane impairs perivascular drainage, thereby triggering further amyloid deposition and aggravating the CAA (42,5). This was demonstrated in mouse models of both inducible neuronal- and astrocytic-TGF β overexpression, where perivascular astrogliosis is preceding and promoting the vascular angiopathy (36,47).

In our study we found a perivascular ring of pSMAD2/3 granules around vessels in the occipital lobe of HCHWA-D samples. Comparable pSMAD2/3 granules were found in other neurodegenerative disorders, such as AD, Pick's syndrome, progressive supranuclear palsy and corticobasal degeneration (7,6,2). Typically, in AD the granules were found intracellularly and associated with neuronal aggregates of pTau or granulovacuolar inclusion of ubiquitin (37,20,2,27). This aberrant cytoplasmic dislocation of pSMAD2/3 could impair the normal TGF β signaling pathway by sequestration of this transcription factor (37,6,2,27). In our study, we did not find pTau, ubiquitin or A β colocalization with the perivascular ring of pSMAD2/3 granules, which is not surprising considering the general lack of neuronal degeneration and pTau involvement in HCHWA-D. Nevertheless, the granular sequestration of pSMAD2/3 may point to a similar deregulation of the TGF β pathway.

In the current study, we often found that the perivascular granules were positioned following a linear pattern, reminiscent of astrocytic processes. In a recent study, a decrease in cerebrovascular reactivity in the occipital cortex of HCHWA-D was described as an early biomarker of the disease (40) and astrocytes are key mediators in this process (19). In transgenic mice with cerebral angiopathy due to overexpression of TGF β or APP, the cerebrovascular reactivity was impaired, due to neurovascular decoupling (35,29). This decoupling is the result of retraction of astrocyte end feet from the vessel wall. Similar underlying mechanisms likely occur in HCHWA-D patients. Such perivascular astrocytic remodeling has been linked in AD mouse models with CAA pathology severity and astrocytic phenotypic switch, defined by a loss of GFAP-positivity (43). The perivascular granules could be the remnants of astrocytic cytoskeletal remodeling.

In summary, our results indicate a possible contribution of TGF β to the amyloid angiopathy and the resulting vascular remodeling seen in HCHWA-D. Future studies into the early involvement of TGF β in the amyloid angiopathy pathogenesis should be determined in ongoing longitudinal studies in HCHWA-D.

Acknowledgments

The authors thank the Netherlands Brain Bank (Amsterdam, The Netherlands) for supplying brain tissue. We acknowledge I.M. Hegeman for the preparation of sections and J.M. de Jong for her contribution to the work. We are grateful to collaborators from the Department of Molecular Cell Biology (LUMC): Dr. P. ten Dijke for valuable discussion, Dr. B.P.T. Kruithof for technical support, and J.C.A.G. Wiegant and A.M.A. Boonzaier-vd Laan for assistance with the confocal microscopy. This work was supported by the Bontius stichting (Leiden, The Netherlands) and by the Netherlands Organisation for Scientific Research (NWO), under research program VIDI, project ‘‘Amyloid and vessels’’, number 864.13.014.

Compliance with ethical standards

Conflicts of interest: The authors declare they have no conflicts of interest.

Ethical approval: All procedures performed in this study involving human participants were in accordance with the ethical standards of the institutional and/or national research committee and with the 1964 Helsinki declaration and its later amendments or comparable ethical standards.

Informed consent: Informed consent was obtained from all individual participants included in the study.

Supplementary Material

The Supplementary Material for this article can be found online at: <https://onlinelibrary.wiley.com/doi/full/10.1111/bpa.12533>

References

- Amara FM, Junaid A, Clough RR, Liang B (1999) TGF-beta(1), regulation of alzheimer amyloid precursor protein mRNA expression in a normal human astrocyte cell line: mRNA stabilization. *Brain Res Mol Brain Res* 71:42-49.
- Baig S, van Helmond Z, Love S (2009) Tau hyperphosphorylation affects Smad 2/3 translocation. *Neuroscience* 163:561-570.
- Beaufort N, Scharrer E, Kremmer E, Lux V, Ehrmann M, Huber R, Houlden H, Werring D, Haffner C, Dichgans M (2014) Cerebral small vessel disease-related protease HtrA1 processes latent TGF-beta binding protein 1 and facilitates TGF-beta signaling. *Proc Natl Acad Sci U S A* 111:16496-16501.
- Burton T, Liang BH, Dibrov A, Amara F (2002) Transforming growth factor-beta-induced transcription of the Alzheimer beta-amyloid precursor protein gene involves interaction between the CTCF-complex and Smads. *Biochem Biophys Res Commun* 295:713-723.
- Carare RO, Hawkes CA, Jeffrey M, Kalaria RN, Weller RO (2013) Review: cerebral amyloid angiopathy, prion angiopathy, CADASIL and the spectrum of protein elimination failure angiopathies (PEFA) in neurodegenerative disease with a focus on therapy. *Neuropathol Appl Neurobiol* 39:593-611.
- Chalmers KA, Love S (2007) Neurofibrillary tangles may interfere with Smad 2/3 signaling in neurons. *J Neuropathol Exp Neurol* 66:158-167.
- Chalmers KA, Love S (2007) Phosphorylated Smad 2/3 colocalizes with phospho-tau inclusions in Pick disease, progressive supranuclear palsy, and corticobasal degeneration but not with alpha-synuclein inclusions in multiple system atrophy or dementia with Lewy bodies. *J Neuropathol Exp Neurol* 66:1019-1026.
- de Jager M, van der Wildt B, Schul E, Bol JG, van Duinen SG, Drukarch B, Wilhelmus MM (2013) Tissue transglutaminase colocalizes with extracellular matrix proteins in cerebral amyloid angiopathy. *Neurobiol Aging* 34:1159-1169.
- Doyle KP, Cekanaviciute E, Mamer LE, Buckwalter MS (2010) TGFbeta signaling in the brain increases with aging and signals to astrocytes and innate immune cells in the weeks after stroke. *J Neuroinflammation* 7:62.
- Fee DB, Sewell DL, Andresen K, Jacques TJ, Piaskowski S, Barger BA, Hart MN, Fabry Z (2004) Traumatic brain injury increases TGF beta RII expression on endothelial cells. *Brain Res* 1012:52-59.
- Flanders KC, Ren RF, Lippa CF (1998) Transforming growth factor-betas in neurodegenerative disease. *Prog Neurobiol* 54:71-85.
- Gray CW, Patel AJ (1993) Regulation of beta-amyloid precursor protein isoform mRNAs by transforming growth factor-beta 1 and interleukin-1 beta in astrocytes. *Brain Res Mol Brain Res* 19:251-256.
- Greenberg SM, Vonsattel JP (1997) Diagnosis of cerebral amyloid angiopathy. Sensitivity and specificity of cortical biopsy. *Stroke* 28:1418-1422.
- Hawkes CA, Hartig W, Kacza J, Schliebs R, Weller RO, Nicoll JA, Carare RO (2011) Perivascular drainage of solutes is impaired in the ageing mouse brain and in the presence of cerebral amyloid angiopathy. *Acta Neuropathol* 121:431-443.

15. Horssen J, Otte-Höller I, David G, Maat-Schieman ML, Heuvel LP, Wesseling P, Waal RM, Verbeek MM (2001) Heparan sulfate proteoglycan expression in cerebrovascular amyloid β deposits in Alzheimer's disease and hereditary cerebral hemorrhage with amyloidosis (Dutch) brains. *Acta Neuropathol* 102:604-614.
16. Huang SS, Huang FW, Xu J, Chen S, Hsu CY, Huang JS (1998) Amyloid beta-peptide possesses a transforming growth factor-beta activity. *J Biol Chem* 273:27640-27644.
17. Kamp JA, Grand Moursel L, Haan J, Terwindt GM, Lesnik Oberstein SA, van Duinen SG, van Roon-Mom WM (2014) Amyloid beta in hereditary cerebral hemorrhage with amyloidosis-Dutch type. *Rev Neurosci* 25:641-651.
18. Kast J, Hanecker P, Beaufort N, Giese A, Joutel A, Dichgans M, Opherk C, Haffner C (2014) Sequestration of latent TGF-beta binding protein 1 into CADASIL-related Notch3-ECD deposits. *Acta Neuropathol Commun* 2:96.
19. Lecrux C, Hamel E (2011) The neurovascular unit in brain function and disease. *Acta Physiol* 203:47-59.
20. Lee HG, Ueda M, Zhu X, Perry G, Smith MA (2006) Ectopic expression of phospho-Smad2 in Alzheimer's disease: uncoupling of the transforming growth factor-beta pathway? *J Neurosci Res* 84:1856-1861.
21. Lesne S, Docagne F, Gabriel C, Liot G, Lahiri DK, Buee L, Plawinski L, Delacourte A, MacKenzie ET, Buisson A, Vivien D (2003) Transforming growth factor-beta 1 potentiates amyloid-beta generation in astrocytes and in transgenic mice. *J Biol Chem* 278:18408-18418.
22. Luyendijk W, Bots GT, Vegter-van der Vlis M, Went LN, Frangione B (1988) Hereditary cerebral haemorrhage caused by cortical amyloid angiopathy. *J Neurol Sci* 85:267-280.
23. Maat-Schieman M, Roos R, van Duinen S (2005) Hereditary cerebral hemorrhage with amyloidosis-Dutch type. *Neuropathology* 25:288-297.
24. Maat-Schieman ML, Yamaguchi H, Hegeman-Kleinn IM, Welling-Graafland C, Natté R, Roos RA, van Duinen SG (2004) Glial reactions and the clearance of amyloid beta protein in the brains of patients with hereditary cerebral hemorrhage with amyloidosis-Dutch type. *Acta Neuropathol* 107:389-398.
25. Maat Schieman MLC, Van Duinen S, Natté R, Roos R (2000) Neuropathology of Hereditary Cerebral Hemorrhage with Amyloidosis-Dutch Type. In: Verbeek MM, de Waal RMW, Vinters HV (eds) *Cerebral amyloid angiopathy in Alzheimer's disease and related disorders*. Kluwer Academic Publishers, pp 223-236.
26. Müller K, Courtois G, Ursini MV, Schwanager M (2017) New Insight Into the Pathogenesis of Cerebral Small-Vessel Diseases. *Stroke* 48:520-527.
27. Nakamori M, Takahashi T, Yamazaki Y, Kurashige T, Yamawaki T, Matsumoto M (2012) Cyclin-dependent kinase 5 immunoreactivity for granulovacuolar degeneration. *Neuroreport* 23:867-872.
28. Natté R, Maat-Schieman MLC, Haan J, Bornebroek M, Roos RAC, van Duinen SG (2001) Dementia in hereditary cerebral hemorrhage with amyloidosis-Dutch type is associated with cerebral amyloid angiopathy but is independent of plaques and neurofibrillary tangles. *Ann Neurol* 50:765-772.
29. Nicolakakis N, Aboukassim T, Aliaga A, Tong XK, Rosa-Neto P, Hamel E (2011) Intact memory in TGF-beta1 transgenic mice featuring chronic cerebrovascular deficit: recovery with pioglitazone. *J Cereb Blood Flow Metab* 31:200-211.
30. Pál G, Lovas G, Dobolyi A (2014) Induction of transforming growth factor beta receptors following focal ischemia in the rat brain. *PLoS One* 9:e106544.
31. Pardali E, Ten Dijke P (2012) TGFbeta signaling and cardiovascular diseases. *Int J Biol Sci* 8:195-213.
32. Ruijter JM, Ramakers C, Hoogaars WM, Karlen Y, Bakker O, van den Hoff MJ, Moorman AF (2009) Amplification efficiency: linking baseline and bias in the analysis of quantitative PCR data. *Nucleic Acids Res* 37:e45.
33. Tagliavini F, Giaccone G, Bugiani O, Frangione B (1993) Ubiquitinated neurites are associated with preamyloid and cerebral amyloid beta deposits in patients with hereditary cerebral hemorrhage with amyloidosis Dutch type. *Acta Neuropathol* 85:267-271.
34. Thompson CS, Hakim AM (2009) Living beyond our physiological means: small vessel disease of the brain is an expression of a systemic failure in arteriolar function: a unifying hypothesis. *Stroke* 40:e322-330.
35. Tong XK, Nicolakakis N, Kocharyan A, Hamel E (2005) Vascular remodeling versus amyloid beta-induced oxidative stress in the cerebrovascular dysfunctions associated with Alzheimer's disease. *J Neurosci* 25:11165-11174.
36. Ueberham U, Ueberham E, Bruckner MK, Seeger G, Gartner U, Gruschka H, Gebhardt R, Arendt T (2005) Inducible neuronal expression of transgenic TGF-beta1 in vivo: dissection of short-term and long-term effects. *Eur J Neurosci* 22:50-64.
37. Ueberham U, Ueberham E, Gruschka H, Arendt T (2006) Altered subcellular location of phosphorylated Smads in Alzheimer's disease. *Eur J Neurosci* 24:2327-2334.
38. Untergasser A, Cutcutache I, Koressaar T, Ye J, Faircloth BC, Remm M, Rozen SG (2012) Primer3--new capabilities and interfaces. *Nucleic Acids Res* 40:e115.
39. van Duinen SG, Maat Schieman MLC, Bruijn JA, Haan J, Roos RAC (1995) Cortical Tissue of Patients with Hereditary Cerebral-Hemorrhage with Amyloidosis (Dutch) Contains Various Extracellular-Matrix Deposits. *Lab Invest* 73:183-189.
40. van Opstal AM, van Rooden S, van Harten T, Ghariq E, Labadie G, Fotiadis P, Gurol ME, Terwindt GM, Wermer MJ, van Buchem MA, Greenberg SM, van der Grond J (2017) Cerebrovascular function in presymptomatic and symptomatic individuals with hereditary cerebral amyloid angiopathy: a case-control study. *Lancet Neurol* 16:115-122.
41. Vinters HV, Natté R, Maat-Schieman ML, van Duinen SG, Hegeman-Kleinn I, Welling-Graafland C, Haan J, Roos RA (1998) Secondary microvascular degeneration in amyloid angiopathy of patients with hereditary cerebral hemorrhage with amyloidosis, Dutch type (HCHWA-D). *Acta Neuropathol* 95:235-244.
42. Weller RO, Boche D, Nicoll JA (2009) Microvasculature changes and cerebral amyloid angiopathy in Alzheimer's disease and their potential impact on therapy. *Acta Neuropathol* 118:87-102.
43. Wilcock DM, Vitek MP, Colton CA (2009) Vascular amyloid alters astrocytic water and potassium channels in mouse models and humans with Alzheimer's disease. *Neuroscience* 159:1055-1069.
44. Wilhelmus MM, Bol JG, van Duinen SG, Drukarch B (2013) Extracellular matrix modulator lysyl oxidase colocalizes with amyloid-beta pathology in Alzheimer's disease and hereditary cerebral hemorrhage with amyloidosis--Dutch type. *Exp Gerontol* 48:109-114.
45. Wyss-Coray T, Lin C, Sanan DA, Mucke L, Masliah E (2000) Chronic overproduction of transforming growth factor-beta1 by astrocytes promotes Alzheimer's disease-like microvascular degeneration in transgenic mice. *Am J Pathol* 156:139-150.

46. Wyss-Coray T, Lin C, Yan F, Yu GQ, Rohde M, McConlogue L, Masliah E, Mucke L (2001) TGF-beta1 promotes microglial amyloid-beta clearance and reduces plaque burden in transgenic mice. *Nat Med* 7:612-618.
47. Wyss-Coray T, Masliah E, Mallory M, McConlogue L, Johnson-Wood K, Lin C, Mucke L (1997) Amyloidogenic role of cytokine TGF-beta1 in transgenic mice and in Alzheimer's disease. *Nature* 389:603-606.
48. Yamamoto Y, Craggs L, Baumann M, Kalimo H, Kalaria RN (2011) Review: molecular genetics and pathology of hereditary small vessel diseases of the brain. *Neuropathol Appl Neurobiol* 37:94-113.
49. Zipfel GJ, Han H, Ford AL, Lee JM (2009) Cerebral amyloid angiopathy: progressive disruption of the neurovascular unit. *Stroke* 40:S16-19.

Chapter 4

Cerebral amyloid angiopathy with vascular iron accumulation and calcification: a high-resolution MRI-histopathology study

Marjolein Bulk^{1,2}, Laure Grand Moursel^{1,2}, Linda M. van der Graaf^{1,2}, Susanne J. van Veluw³, Steven M. Greenberg³, Sjoerd van Duinen⁴, Mark van Buchem¹, Sanneke van Rooden¹, Louise van der Weerd^{1,2}

¹ Department of Radiology, Leiden University Medical Center

² Department of Human Genetics, Leiden University Medical Center

³ Department of Neurology, Massachusetts General Hospital and Harvard Medical School, Boston

⁴ Department of Pathology, Leiden University Medical Center

Adapted from Stroke (2018).

Abstract

Background and Purpose: Previous studies of symptomatic and asymptomatic hereditary cerebral amyloid angiopathy (CAA) patients offered the possibility to study the radiologic manifestations of CAA in the early stages of the disease. Recently, a ‘striped cortex’, observable as hypointense lines perpendicular to the pial surface on T2*-weighted 7T MRI, was detected in 40% of the symptomatic hereditary CAA patients. However, the origin of these MRI contrast changes is unknown. This study aimed at defining the underlying pathology associated with the *in vivo* observed striped pattern.

Methods: Formalin-fixed *post mortem* brain material including the occipital lobe of four Hereditary Cerebral Haemorrhage with Amyloidosis-Dutch type (HCHWA-D) cases and six sporadic CAA (sCAA) cases were selected from local neuropathology tissue collections. Depending on the availability of the material, intact hemispheres or brain slabs including the occipital lobe of these patients were screened for the presence of a striped cortex. Regions containing the striped cortex were then subjected to high-resolution 7T MRI and histopathological examination.

Results: We found two HCHWA-D cases and one sCAA case with striped patterns in the occipital cortex resembling the *in vivo* signal. Histopathological examination showed that the striped pattern in the cortex at 7T MRI is due to iron accumulation and calcification of penetrating arteries. The presence of both non-heme iron and calcification on penetrating arteries causes signal loss and hence the abnormal striped patterns in the cortical ribbon on T2*-weighted MRI.

Conclusion: We identified iron accumulation and calcification of the vessel wall in HCHWA-D as the histopathological correlates of the striped cortex observed on *in vivo* 7T MRI.

Introduction

Hereditary Cerebral Haemorrhage with Amyloidosis-Dutch type (HCHWA-D) is a genetic disorder caused by a point mutation in the Amyloid Precursor Protein (APP; p.Glu693Gln mutation), resulting in severe cerebral amyloid angiopathy (CAA) characterized by recurrent haemorrhagic strokes with midlife onset (1, 2). Since sporadic CAA (sCAA) is also a disease of the elderly and a common feature in Alzheimer’s disease, the diagnostic point mutation makes HCHWA-D a useful model to study CAA *in vivo* (2).

Previous studies of symptomatic and asymptomatic HCHWA-D mutation carriers offered the possibility to study the radiologic manifestations of CAA pathology during the course of the disease. A ‘striped cortex’, observable as hypointense lines perpendicular to the pial surface on T₂*-weighted 7T MRI, was detected in 40% of the symptomatic mutation carriers, specifically in the occipital lobe (3). This pattern was only seen in advanced disease stages and not in asymptomatic patients. However, the underlying pathology of this pattern is unknown.

The feasibility of investigating histopathological correlates of MRI abnormalities have been previously shown in *post mortem* brain tissue (4-6). In the context of CAA, high-resolution *ex vivo* 7T MRI scanning allowed the detection of microvascular lesions, including microhaemorrhages, microinfarcts, and CAA-related vasculopathies (6).

The aim of this study was to define the underlying pathology associated with the *in vivo* observed striped pattern. Therefore, we screened *post mortem* brain material of four HCHWA-D donors from our local neuropathology tissue collection using 7T MRI. In two cases, striped patterns in the occipital cortex resembling the *in vivo* signal were detected. These areas were subjected to high-resolution 7T MRI to study the pattern in greater detail. Based on our hypothesis that the observed MRI contrast might be due to calcification, we added a micro computed tomography (μCT) scan as this modality is the most sensitive and specific imaging tool allowing for the identification of calcifications (7). Serial sections of the identified areas were further subjected to histological investigation to examine the histopathological correlates of the distinctive striped MRI pattern. Since HCHWA-D serves as a model for sCAA, we additionally retrospectively screened previously acquired whole hemisphere *ex vivo* 3T MRI scans of six sCAA cases. In one case (with severe CAA) a striped pattern was observed in the occipital cortex. Brain samples from that area were then subjected to 7T MRI and subsequent histopathological examination.

Material and Methods

The data that support the findings of this study are available from the corresponding author upon reasonable request.

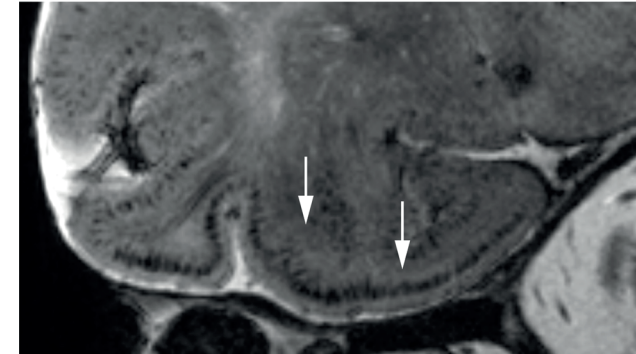
Study design

Formalin-fixed *post mortem* brain material including the occipital lobe of four HCHWA-D cases were selected from the neuropathology tissue collection of the Leiden University Medical Center (LUMC) in Leiden (The Netherlands) (see workflow in Fig. 1). Depending on the availability of the material, intact hemispheres or brain slabs including the occipital lobe of these patients were scanned at 7T MRI. The 7T MR images were visually inspected by two experienced observers (SvR, LvdW) and screened for a striped cortical pattern defined as hypointense lines perpendicular to the pial surface (3). Two cases showed a striped cortex on 7T MR images and smaller tissue blocks from these cases were further investigated on high-resolution 7T MRI and histology. Based on our hypothesis that the observed MRI contrast might be due to calcification, we added an μ CT scan as this modality is the most sensitive and specific imaging tool allowing for the identification of calcifications (7). In addition, *ex vivo* 3T MRI scans from six sCAA cases, acquired at the Massachusetts General Hospital (MGH) in Boston (MA, USA) were retrospectively screened for the presence of a striped cortex. This pattern was observed in one sCAA case, which was then subjected to 7T MRI and histopathological examination. Case characteristics of screened HCHWA-D and sCAA cases are presented in Table 1.

Table 1: Characteristics of screened HCHWA-D and sCAA cases.

	Age	Sex	<i>Post mortem</i> delay (hours)	Striped cortex detected
HCHWA-D #1	70	Female	5	Yes
HCHWA-D #2	57	Male	2,5	Yes
HCHWA-D #3	50	Female	16	No
HCHWA-D #4	50	Male	19	No
sCAA #1	70	Male	16	Yes
sCAA #2	80	Male	Unknown	No
sCAA #3	76	Male	27	No
sCAA #4	65	Male	14	No
sCAA #5	81	Male	Unknown	No
sCAA #6	70	Female	Unknown	No

Striped cortex in vivo in symptomatic HCHWA-D patients observed at 7T MRI³



Step 1: Detection of the striped cortex on *ex vivo* MRI

Post mortem formalin-fixed hemispheres/brain slabs of HCHWA-D (n=4) cases stored in the local neuropathology tissue collection were scanned and screened

Step 2: High-resolution 7T MRI and μ CT of positive cases (HCHWA-D 2 cases, sCAA 1 case)

A small tissue block corresponding to a striped pattern area was resected and imaged with high resolution 7T MRI and CT

Step 3: Investigation of the histopathological correlates of the cortical changes detected at 7T MRI

Tissue blocks from step 2 were paraffin embedded. Tissue sectioning was guided by the *post mortem* MRI and based on anatomical landmarks such as the grey-white matter border, vessels, and the orientation of the striped pattern.

Histopathological assessment included staining for: iron, calcification, A β , H&E

Figure 1: Study design and flowchart.

Brain samples and preparation

Formalin-fixed intact hemispheres or brain slabs of HCHWA-D patients were obtained from the local neuropathology tissue collection of the LUMC. Written informed consent for the HCHWA-D patients was obtained for each donor and all material and data were handled in a coded fashion maintaining patient anonymity according to Dutch national ethical guidelines (Code for Proper Secondary Use of Human Tissue, Dutch Federation of Medical Scientific Societies). Formalin-fixed intact hemispheres of the sCAA cases were obtained through an ongoing *post mortem* brain MRI study for the evaluation of MRI markers in the context of sporadic CAA at the MGH in Boston (MA, USA). Informed consent was obtained from a legal

representative prior to brain autopsy. This study was approved by the local Ethics Committees of the respective institutions.

Before MRI, the formalin-fixed brain material of the HCHWA-D patients was washed with phosphate buffered saline (PBS) for 24 h to partially restore the relaxation parameters (8). The hemisphere or brain slabs were placed in a plastic bag containing a proton-free fluid (Fomblin®, LC08, Solvay). To minimize the amount of trapped air bubbles, a vacuum was applied overnight. Before scanning, the plastic bag was sealed and fixed on a plastic plateau or using foam padding in the coil.

After scanning the intact hemisphere and brain slabs, the scans were inspected for the presence of a striped cortex by two experienced observers (SvR, LvdW). If positive, a small tissue block of approximately 20x15x15 mm was resected from the area containing the striped cortex and placed in a regular 15 ml tube (Greiner Bio-One). Before MRI, the tissue block was washed with PBS (for 24 h) to partially restore the relaxation parameters (8). Next, the 15 ml tube containing the tissue block was filled with Fomblin® (LC08, Solvay). Care was taken to avoid trapped air bubbles.

Post mortem MRI acquisition

The HCHWA-D hemispheres were scanned at the LUMC (Leiden, the Netherlands) on a whole-body human 7T MR system (Philips Healthcare, Best, the Netherlands) using a quadrature transmit and 32-channel receiver head coil. The hemisphere was positioned with the frontal lobe in the head direction and the occipital lobe in the feet direction of the scanner. A 2D T_2^* -weighted gradient echo scan was acquired with a total imaging duration of 13 minutes. Imaging parameters were: repetition time (TR)/echo time (TE) 3146/25 ms, flip angle 60°, slice thickness 1.0 mm with a 1.1 mm interslice gap and a spatial resolution of 0.21x0.21 mm.

The HCHWA-D brain slabs and smaller tissue blocks were also scanned at the LUMC (Leiden, the Netherlands), but on a 7T horizontal bore Bruker MRI system equipped with a 23 mm receiver coil (Bruker Biospin, Ettlingen, Germany). The smaller tissue blocks were scanned with a Multiple Gradient Echo (MGE) sequence using the following parameters: (TR)/(TE) 75/12.5, 23.2, 33.9 and 44.6 ms, flip angle 25°, at 100 μ m isotropic resolution with 20 signal averages.

Brain slabs of one sCAA case that demonstrated a striped pattern on previously acquired whole hemisphere *ex vivo* 3T MRI scans, were subsequently scanned at 7T MRI. Scanning was performed at the Athinoula A. Martinos Center for Biomedical Imaging (MGH, Charlestown, MA, USA), on a whole-body human 7T MR Siemens MAGNETOM scanner, using a custom built 32-channel head coil, as described previously (6).

Slabs were stacked on top of each other in a glass beaker, filled with 10% formalin. A multi-echo T_2^* -weighted MRI scan was acquired using the following parameters: one run each of three flip angles (10°, 20°, and 30°), TE = 8, 18, 28, and 38 ms, at 200 μ m isotropic resolution.

The most similar MRI slice with respect to the given histology was selected based on the physical location of the section in the tissue block, measured by counting the number of sections taken starting at the block surface. At this approximate location, the most similar MRI slice was chosen by visual comparing clearly detectable landmarks (contours, vasculature, tears etc.) allowing comparison of the MRI with histology.

Post mortem μ CT

For the HCHWA-D cases, MRI acquisition was followed by μ CT to detect the presence of calcifications. The 15 ml tube containing the tissue block in Fomblin was imaged on a Skyscan 1076 *in vivo* μ CT (Bruker Biospin, Ettlingen, Germany) using the following settings: 40-48 kV, 200-250 μ A, 0.5 mm filter, 2-10 averages. The same approach as described above for the MRI slice selection was used to select the most similar μ CT image.

Histology and immunohistochemistry

The resected tissue blocks used for both MRI and μ CT were next subjected to detailed histopathologic examination. Each tissue block was embedded in paraffin, and subsequently cut in 5 μ m-thick serial sections on a microtome. The sectioning was guided by the *post mortem* MRI scans based on anatomical landmarks such as the grey-white matter border, vessels, and the orientation of the striped pattern.

The first section was stained for A β (anti-human A β , 6F/3D DakoCytomation, Glostrup, Denmark): endogenous peroxidase activity was blocked with 0.3% H₂O₂ in methanol followed by an antigen retrieval step using formic acid and trypsin. The primary antibody was incubated overnight at room temperature. The secondary antibody was incubated for one hour followed by a 30 minutes incubation with avidin-biotin complex (ABC, Vector Labs, CA, USA). Signal enhancement was completed by immersion in 3,3'-Diaminobenzidine (DAB). Finally, sections were counterstained with Harris Haematoxylin.

Adjacent sections were stained with the Von Kossa technique to detect calcification and a standard hematoxylin & eosin (H&E) staining. For the detection of iron, two protocols were used. For each case one section was stained using the classic Perls' Prussian blue iron stain. In addition, one section was stained according to an in-house protocol of a modified Meguro staining (9). In short, sections were incubated for 30 minutes in 1% potassium ferrocyanide, washed, followed by 60 minutes incubation in

methanol with 0.01 M NaN_3 and 0.3% H_2O_2 . Subsequently, sections were washed with 0.1 M phosphate buffer followed by 30 minutes incubation in a solution containing 0.025% 3'3-DAB-tetrahydrochloride (DakoCytomation) and 0.005% H_2O_2 in 0.1 M phosphate buffer. The reaction was stopped by washing in demi water.

Tissue blocks from the sCAA case were processed in a similar fashion. Sections underwent histological staining with H&E, Perls' Prussian blue iron, and Von Kossa, and immunohistochemistry against $\text{A}\beta$ (6F/3D, Dako).

All slides were digitized using an automatic bright field microscope (Philips Ultra Fast Scanner, Philips, Netherlands) for microscopic evaluation. All stained sections were independently evaluated by LGM, MB and SvV for the amount of $\text{A}\beta$, iron and calcium positive vessels. For both HCHWA-D subjects one area with the striped cortex, one area without the striped cortex and one area with some contrast changes were scored. Percentages were calculated for the amount of vessels positive and negative for iron and calcium with respect to the total number of $\text{A}\beta$ positive vessels.

Results

Detection of the striped cortex *ex vivo*

Post mortem brain material of four HCHWA-D were scanned at 7T and in two out of four HCHWA-D cases a striped pattern was found *ex vivo* in the occipital cortex, similar to the *in vivo* MRI observation (Fig. 2A). In both HCHWA-D cases, also areas with normal contrast were observed on high-resolution *ex vivo* 7T MRI. In one out of six cases with sCAA screened for this study, a similar striped pattern as in the HCHWA-D cases was observed in the occipital cortex (Fig. 3A).

μCT and histopathological correlates of the striped cortex

Given the shape and course of the striped cortex, we hypothesised that the observed MRI contrast changes may be caused by $\text{A}\beta$ depositions in the walls of perforating arteries, co-localizing with iron accumulation and calcifications.

Microscopic examination showed severe and widespread CAA in both HCHWA-D cases (Fig. 2C). The sCAA case was also characterised by severe and widespread CAA and more than 200 microbleeds on *ex vivo* 3T MRI (Fig. 3B). No noticeable differences in vessel wall morphology or $\text{A}\beta$ staining of angiopathic arterioles was observed between areas with and without the striped cortex. Old microhemorrhages in the form of focal hemosiderin deposits were not evident in the examined tissue sections.

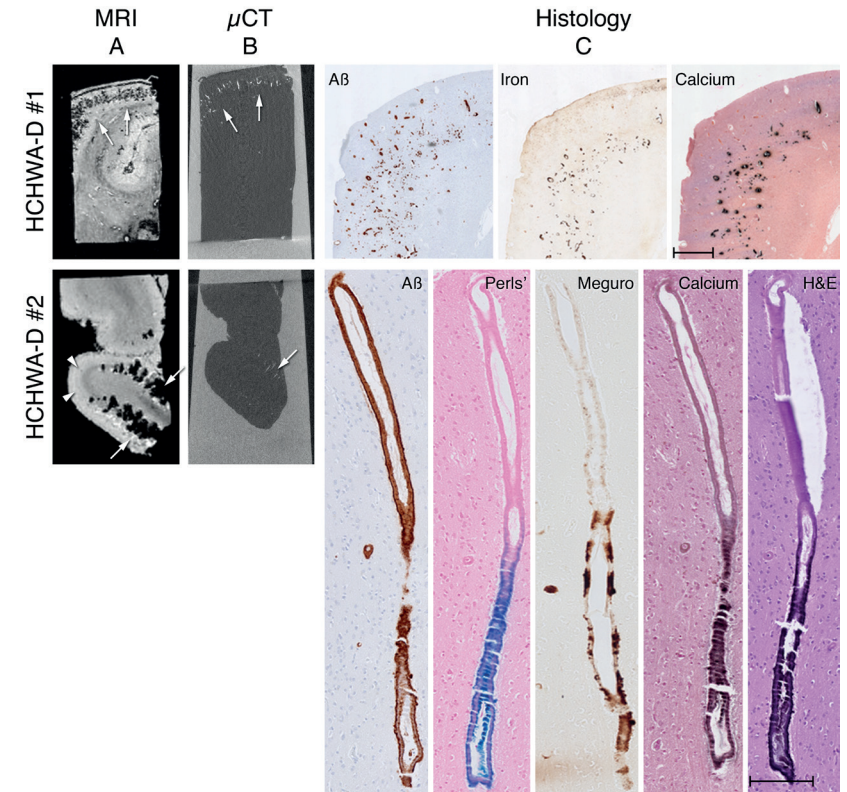


Figure 2: MRI, μCT and histology of the striped cortex in HCHWA-D. A striped pattern resembling the *in vivo* findings was found in the occipital lobe of HCHWA-D patient 1 (A, first row) and HCHWA-D patient 2 (A, second row). High-resolution 7T MRI (TE 12.5 ms) showed a striped pattern of the cortex (arrows) in addition to some parts of the cortical ribbon showing normal cortical contrast (arrowheads). (B) Vascular calcifications were confirmed by μCT (arrows). (C) Histopathological examination showed that the majority of the cortical vessels stained positive for $\text{A}\beta$. Interestingly, only vessels in the middle to deeper cortical layers stained positive for non-heme iron (Meguro) and calcium (Von Kossa), indicating iron accumulation and calcification of the vessel wall in specific cortical layers. In contrast to $\text{A}\beta$, which was observed over the full length of the perforating arteries, non-heme iron (Perls' and Meguro) and calcium (Von Kossa) was only observed in the lower part of the vessel. Calcification of the vessel wall was also visible on the H&E staining as deep purple depositions. C first row as well as C second row are consecutive slides. Orientation histology: top = leptomeninges; bottom = white matter. Scale bars in C first row = 1mm, C second row = 200 μm .

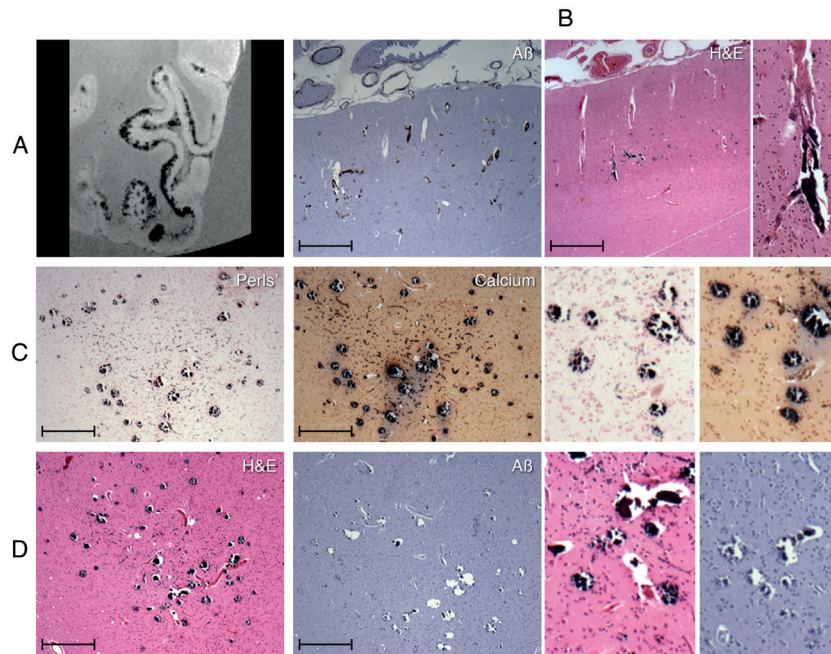


Figure 3: Striped cortex in a sporadic CAA case. (A) A similar striped pattern as in the HCHWA-D cases was observed in the occipital cortex of a sporadic CAA case on high-resolution 7T MRI. (B) This case was characterised by severe and widespread CAA and more than 200 microbleeds on ex vivo 3T MRI. (C) Histological examination showed the same co-localization in the vessel wall as observed in the HCHWA-D patients, namely: non-heme iron (Perls') and calcium (Von Kossa). Calcification of the vessel wall was also visible on the H&E staining as deep purple depositions. (D) Interestingly, in contrast with the HCHWA-D cases, iron accumulation and calcification was also observed in vessels without CAA. Scale bars = 500 μ m.

In both HCHWA-D cases and the sCAA case, co-localization of A β with non-heme iron and calcium in the vessel wall was found in areas containing the striped cortex (Fig. 2, 3, Suppl. Fig. I, Suppl. Fig. II, Suppl. Table I). In contrast to A β , which was observed over the full length of the perforating arteries, non-heme iron and calcium were only observed in the lower part of the vessel (Fig. 2C). Calcification of the vessel wall was also visible in the H&E staining as deep purple depositions and confirmed by μ CT (Fig. 2, 3). Interestingly, in contrast to the HCHWA-D cases, in sCAA, iron accumulation and calcification was also observed in vessels without CAA (Fig. 3D).

In addition, a hypointense line in the superficial cortical layers parallel to the cortical surface was observed in one of the HCHWA-D cases, resembling superficial siderosis. Histology showed co-localization with local iron accumulation in neurons in layer II of the cortex (Suppl. Fig. III).

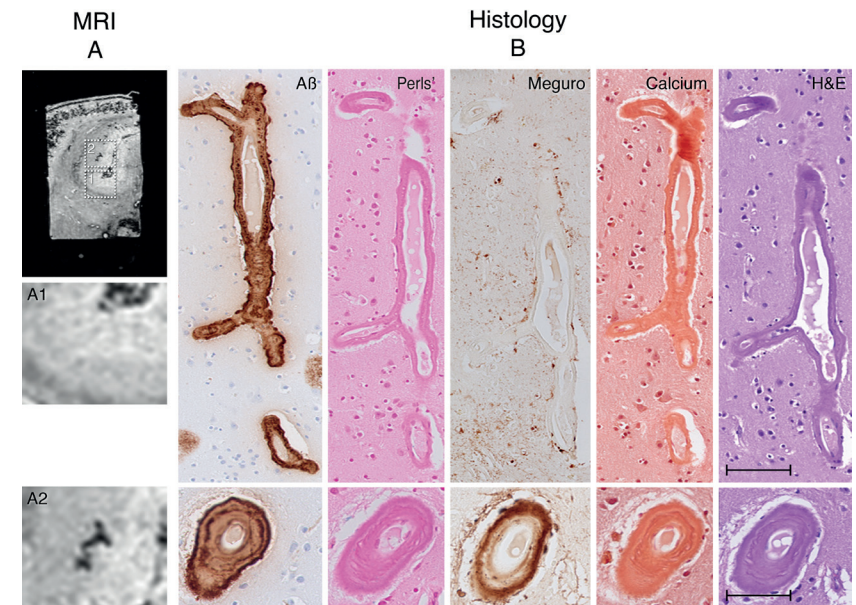


Figure 4: Zoomed MRI and histology of an area outside the 'striped cortex' in HCHWA-D patient 1. High-resolution 7T MRI (TE 12.5 ms) and zoom of an area without the striped cortex (A1) and an area with some contrast changes (A2). (B) Histopathological examination showed that most cortical vessels stained positive for A β in both areas. However, in areas without the striped cortex vessels were negative for non-heme iron (Perls' and Meguro) and calcium (Von Kossa). Also the H&E staining was negative. In areas with some contrast changes (A2), although less intense, these contrast changes correlated with an area where we found vessels positive for non-heme iron detected by the Meguro staining. The Perls', calcium and H&E stainings were negative. (B) are consecutive slides. Orientation histology: top = leptomeninges; bottom = white matter. Scale bars in B-F = 100 μ m; G-K = 50 μ m.

Histopathological correlate of areas outside the striped cortex

To confirm specificity of iron accumulation and calcification in the vessel wall as the histopathological correlate of the striped cortex, we further investigated other regions of the cortex in HCHWA-D tissue (Fig. 4A).

On histology, most cortical vessels stained positive for A β , also in areas without the striped pattern on MRI. However, these vessels were negative for non-heme iron and calcium (Fig. 4B, Suppl. Table I). We also noticed some areas outside the striped cortex with contrast changes on MRI which had a similar pattern, but that were less intense than the striped pattern described above. These MRI contrast changes may be due to vessels positive for A β and non-heme iron, but negative for calcium (Fig. 4B, Suppl. Table I). Calcification without iron accumulation was not observed.

Discussion

Our findings show that the recently observed striped pattern in the cortex of symptomatic HCHWA-D patients at 7T MRI is due to iron accumulation and calcification of A β positive penetrating arteries. The presence of both non-heme iron and calcification on penetrating arteries causes signal loss and hence abnormal cortical patterns on T₂*-weighted MRI.

As reported, on *in vivo* 7T MRI the striped cortex was found in 40% of the symptomatic HCHWA-D patients. Since the striped cortex was not found in presymptomatic mutation carriers, it might be associated with more advanced stages of the disease (3). Typically, the first stroke occurs between the ages of 39 and 76 years (mean 50 years) and is fatal for one-third of the patients. Those who survive suffer from recurrent strokes resulting in severe disabilities. In exceptional cases, people survive longer, with a maximum reported survival of 28 years (10). Histopathological examination showed that both the HCHWA-D cases and the sCAA case were characterized by a severe and widespread CAA. This suggests that the striped cortex may be a marker of advanced CAA.

Mineral substances such as iron and calcium are known as paramagnetic materials and have consistently been reported to cause hypointense signals on T₂*-weighted MRI images (5, 11). It is known that in patients with Alzheimer's disease and concomitant severe CAA have higher non-heme iron content in the temporal lobe than Alzheimer patients without CAA and that divalent iron accumulates within CAA-positive vessel walls (12). Iron-positive CAA vessels have also been reported in HCHWA-D patients (13, 14). Moreover, some of the largest cortical CAA vessels positive for iron were observed on histology and could be topographically matched with *ex vivo* high-resolution 9.4T MRI (13). Corresponding to our results, Nabuurs et al. showed that not all CAA-affected vessels resulted in a similar loss of MR signal (13). These different effects on MRI were thought to be caused by differences in the amount of A β , its positioning in the vessel wall or other associated microvasculopathies. Here we showed that A β depositions in and along the penetrating vessels are not in itself resulting in T₂*-weighted MRI contrast; CAA vessels without iron accumulation and calcification resulted in normal MRI signal, whereas the presence of iron alone or both iron and calcium resulted in the detection of hypointense signals on T₂*-weighted MRI.

These iron-sensitive MRI scans have been previously used to detect for example superficial siderosis, large intracerebral haemorrhage and (cortical) microbleeds. MRI-observed microbleeds, visible as small round hypointense lesions on T₂*-weighted MRI, correlate to acute microhaemorrhages or iron-positive old microhaemorrhages on histopathology (6). Of note, in our cases the observed striped cortex was not associated with acute or old haemorrhages on histopathology.

Apart from iron accumulation in CAA vessels, we also observed calcification of the vessel wall. Calcification of CAA vessels has been previously reported in very severe CAA cases; cortical calcifications were found using histopathology in p.Glu692 Gln (Dutch) patients (15) and using CT in patients with p.Glu693Lys (Italian) and p.Asp694Asn (Iowa) mutations (16). However, iron accumulation and calcifications as detected by 7T MRI in patients with the p.Glu693Gln mutation (Dutch) have not been reported previously and the underlying mechanisms of vascular iron accumulation and calcifications in APP mutation carriers are unknown. The striped cortex was found in the occipital cortex on *in vivo* MRI (3), which seems to be consistent with the posterior predominance of CAA severity. In addition, we showed that predominantly vessels in the middle cortical layers accumulated iron and calcium. Why specific regions and cortical layers are more affected than others remains to be elucidated. Lastly, we showed that some vessels only accumulated iron but no calcification, whereas we did not find any vessels with calcifications without iron. Based on these observations we speculate that in HCHWA-D A β depositions in the vessel wall are followed by iron accumulation, resulting eventually in calcifications of the vessel wall.

Conclusions

In conclusion, we identified iron accumulation and calcification of the vessel wall in HCHWA-D as the histopathological correlates of the striped cortex observed on *in vivo* 7T MRI. This novel MRI marker is of interest for clinical CAA severity evaluation as it was also observed in a case with severe sCAA. Associated mechanisms resulting in iron accumulation and calcification of CAA vessels will need further investigation.

Acknowledgement

The authors thank I. M. Hegeman-Kleinn for her technical assistance and Ernst Suidgeest for 7T MRI acquisition of the HCHWA-D brain slabs.

Sources of funding

SJvV receives funding from the Netherlands Organisation for Scientific Research (Rubicon fellowship grant # 019.153LW.014).

Disclosures

None

Supplementary Material

The Supplementary Material for this article can be found online at:

<https://www.ahajournals.org/doi/suppl/10.1161/STROKEAHA.118.021872>

References

1. Kamp JA, Moursel LG, Haan J, Terwindt GM, Lesnik Oberstein SA, van Duinen SG, et al. Amyloid beta in hereditary cerebral hemorrhage with amyloidosis-dutch type. *Rev Neurosci*. 2014;25:641-651
2. Luyendijk W, Bots GT, Vegter-van der Vlis M, Went LN, Frangione B. Hereditary cerebral haemorrhage caused by cortical amyloid angiopathy. *J Neurol Sci*. 1988;85:267-280
3. Koemans EA, van Etten ES, van Opstal AM, Labadie G, Terwindt GM, Wermer MJH, et al. Innovative mri markers of hereditary cerebral amyloid angiopathy at 7 tesla. *Stroke*. 2018;In press
4. Bulk M, Abdelmoula WM, Nabuurs RJA, van der Graaf LM, Mulders CWH, Mulder AA, et al. Postmortem mri and histology demonstrate differential iron accumulation and cortical myelin organization in early- and late-onset alzheimer's disease. *Neurobiol Aging*. 2017;62:231-242
5. Fukunaga M, Li TQ, van Gelderen P, de Zwart JA, Shmueli K, Yao B, et al. Layer-specific variation of iron content in cerebral cortex as a source of mri contrast. *Proc Natl Acad Sci U S A*. 2010;107:3834-3839
6. van Veluw SJ, Charidimou A, van der Kouwe AJ, Lauer A, Reijmer YD, Costantino I, et al. Microbleed and microinfarct detection in amyloid angiopathy: A high-resolution mri-histopathology study. *Brain*. 2016;139:3151-3162
7. Thompson BH, Stanford W. Imaging of coronary calcification by computed tomography. *J Magn Reson Imaging*. 2004;19:720-733
8. Shepherd TM, Thelwall PE, Stanisz GJ, Blackband SJ. Aldehyde fixative solutions alter the water relaxation and diffusion properties of nervous tissue. *Magn Reson Med*. 2009;62:26-34
9. van Duijn S, Nabuurs RJ, van Duinen SG, Natte R. Comparison of histological techniques to visualize iron in paraffin-embedded brain tissue of patients with alzheimer's disease. *J Histochem Cytochem*. 2013;61:785-792
10. Maat-Schieman M, Roos R, van Duinen S. Hereditary cerebral hemorrhage with amyloidosis-dutch type. *Neuropathology*. 2005;25:288-297
11. Langkammer C, Krebs N, Goessler W, Scheurer E, Ebner F, Yen K, et al. Quantitative mr imaging of brain iron: A postmortem validation study. *Radiology*. 2010;257:455-462
12. Schrag M, Crofton A, Zabel M, Jiffry A, Kirsch D, Dickson A, et al. Effect of cerebral amyloid angiopathy on brain iron, copper, and zinc in alzheimer's disease. *J Alzheimers Dis*. 2011;24:137-149
13. Nabuurs RJ, Natte R, de Ronde FM, Hegeman-Kleinn I, Dijkstra J, van Duinen SG, et al. Mr microscopy of human amyloid-beta deposits: Characterization of parenchymal amyloid, diffuse plaques, and vascular amyloid. *J Alzheimers Dis*. 2013;34:1037-1049
14. van Rooden S, Maat-Schieman ML, Nabuurs RJ, van der Weerd L, van Duijn S, van Duinen SG, et al. Cerebral amyloidosis: Postmortem detection with human 7.0-t mr imaging system. *Radiology*. 2009;253:788-796
15. Vinters HV, Natte R, Maat-Schieman ML, van Duinen SG, Hegeman-Kleinn I, Welling-Graafland C, et al. Secondary microvascular degeneration in amyloid angiopathy of patients with hereditary cerebral hemorrhage with amyloidosis, dutch type (hchwa-d). *Acta Neuropathol*. 1998;95:235-244
16. Sellal F, Wallon D, Martinez-Almoyna L, Marelli C, Dhar A, Oesterle H, et al. App mutations in cerebral amyloid angiopathy with or without cortical calcifications: Report of three families and a literature review. *J Alzheimers Dis*. 2017;56:37-46

Chapter 5

Osteopontin and phospho-SMAD2/3 are associated with calcification of vessels in D-CAA, an hereditary cerebral amyloid angiopathy

Laure Grand Moursel^{1,2}, Linda M. van der Graaf^{1,2}, Marjolein Bulk², Willeke M.C. van Roon-Mom¹, Louise van der Weerd^{1,2}

¹ Department of Human Genetics, Leiden University Medical Center

² Department of Radiology, Leiden University Medical Center

Adapted from Brain Pathol. (2019).

Abstract

In severe forms of cerebral amyloid angiopathy (CAA) pathology, vascular calcification has been observed in the cerebral cortex, both *in vivo* on MRI and CT, and *post mortem* using histopathology. However, the pathomechanisms leading to calcification of CAA-laden arteries are unknown. Therefore we investigated the correlation between calcification of cortical arterioles and several potential modulators of vascular calcification using immunohistochemistry in a unique collection of brain material of patients with a hereditary form of CAA, namely hereditary cerebral hemorrhage with amyloidosis-Dutch type (HCHWA-D or D-CAA).

We show a topographical association of osteopontin (OPN) and TGF β signaling factor phospho-SMAD2/3 (pSMAD2/3) in calcified CAA vessel walls. OPN and pSMAD2/3 gradually accumulate in vessels prior to calcification. Moreover we found that the vascular accumulation of Collagen 1 (Col1), OPN and pSMAD2/3 immunomarkers correlated with the CAA severity. This was independently of the vessel size, including capillaries in the most severe cases. We propose that calcification of CAA vessels in the observed HCHWA-D cases may be induced by extracellular OPN trapped in the fibrotic Col1 vessel wall, independently of the presence of vascular amyloid.

Introduction

Hereditary cerebral hemorrhage with amyloidosis-Dutch type (HCHWA-D) is an autosomal dominant genetic disorder caused by a missense mutation on chromosome 21 in the amyloid precursor protein (APP, NP_000475.1:p.Glu693Gln, known as APP E693Q) (29). This so-called Dutch variant, or D-CAA, is characterized by early onset cerebral amyloid angiopathy (CAA) defined by a progressive accumulation of Amyloid beta (A β) in the cerebral vasculature, resulting in acellular thickening of the vessel wall (1), leading to recurrent hemorrhagic strokes with midlife onset (15, 18). CAA pathology is also present in the majority of Alzheimer's Disease (AD) patients and is associated with intracerebral hemorrhages in the elderly.

Recently, a striped pattern of hypointense lines perpendicular to the pial surface was observed on *in vivo* 7T MRI in the occipital cortex of symptomatic D-CAA patients (17). Histopathological examination showed that the striped pattern in the cortex on 7T MRI is due to iron accumulation and calcification of penetrating arterioles (5, 39).

Similar calcifications have been observed in other hereditary CAA variants, such as the Iowa and Italian variants (26, 33, 44). In sporadic CAA, calcification of cortical areas involving CAA-affected vessels seems to be much rarer than in the familial cases; its has only been described in three cases of CAA-associated cerebral hemorrhage (5, 20, 28). Intracranial vascular calcifications in general aging and in neurodegenerative diseases are frequently found in the basal ganglia (23, 41), but cortical calcification has not been reported. Therefore, calcifications of the CAA-vessels are thought to be one of the CAA-associated microvasculopathies, secondary to CAA (22, 39). However, it is unknown why some CAA-vessels exhibit calcifications, whereas other vessels with similar CAA load do not.

In the current study we investigated if vascular calcification in HCHWA-D is linked to expression of several factors known to promote calcification, independent of CAA itself, namely transforming growth factor β (TGF β), osteopontin (OPN) and collagen1 (Col1), as detailed below. We previously reported an upregulation of the TGF β pathway in HCHWA-D *post mortem* brain tissue (9, 10). In particular, we described in angiopathic vessels a correlation between CAA severity and the accumulation of phosphoSMAD2/3 (pSMAD2/3), a direct TGF β 1 downstream signaling factor (9). Since, it is known that TGF β is a key factor in peripheral vascular calcifications (13, 40), we investigated the correlation between TGF β regulation and calcification in individual vessels.

A second known modulator of vascular calcification is OPN, also known as secreted phosphoprotein 1 (SPP1). It is a non-collagenous bone matrix protein induced by TGF β , leading to vessel calcification in a wide variety of peripheral disorders such as atherosclerosis, diabetes mellitus, and chronic renal failure (14). In the central nervous system, OPN is a constituent of the normal extracellular matrix (ECM), but in the context of neurodegenerative diseases, OPN has been described as a cytokine with a dual role in neuroinflammation and neuroprotection (4, 6, 43). Very little is known about the role of OPN in cerebrovascular calcification, though one previous study showed OPN associated with calcifications in the basal ganglia of AD patients (8).

Finally, ECM-related pathways are known to be upregulated in D-CAA (10). In particular collagen-1 (Col1), which is a pro-fibrotic gene induced by TGF β 1 signaling and an OPN binder, was found upregulated in D-CAA (9) and in an earlier study significantly increased quantities of Col1 were associated with vascular amyloid deposition (38). In atherosclerosis, Col1 is involved in vascular calcification through the binding of matrix vesicles, that act as nucleation foci for calcium deposits (11).

In order to unravel these pathomechanistic factors associated with cortical calcification, we used *post mortem* human brain material of D-CAA patients with well-characterized different levels of CAA load (9). We investigated the different layers (luminal, medial and abluminal) of calcified vessels with standard immunomarkers for these vascular components and assessed in cortical area the association of pSMAD2/3, Col1 and OPN with calcification and disease severity.

Material & Methods

Brain tissue

Occipital *post mortem* brain tissue from D-CAA patients was obtained from the Netherlands Brain Bank (NBB) and from our local neuropathology tissue collection (LUMC). Written informed consent was obtained for each donor and all material and data were handled in a coded fashion maintaining patient anonymity according to Dutch national ethical guidelines (Code for Proper Secondary Use of Human Tissue, Dutch Federation of Medical Scientific Societies, Rotterdam, the Netherlands). The study was approved by the local Ethics Committee.

Experimental design

Brain tissue from eight D-CAA patients, genetically tested for the presence of the mutation (NM_000484.3(APP):c.2077G>C), was used in this study as summarized in Table 1. In addition to the two cases previously described for the presence of calcifications (in (5); cases H2 and H14), six additional patients presenting a known range of CAA severity (based on (9)) were selected (H5, H6, H7, H8, H9 and H10 as shown in Table 1).

Table 1: Demographics of cases, patient code and CAA severity based on (9)

Diagnosis	Source	Age	Gender	PMDa	Codeb	CAA severity c
HCHWA-D	LUMC	70	F	5	H14*	n.a.
HCHWA-D	LUMC	57	M	3	H2*	+
HCHWA-D	LUMC	50	M	19	H5	+
HCHWA-D	LUMC	51	M	3	H8	+
HCHWA-D	NBB	61	M	7	H6	++
HCHWA-D	LUMC	71	M	n.a.	H10	++
HCHWA-D	LUMC	67	F	n.a.	H9	+++
HCHWA-D	NBB	71	M	6	H7	+++

Abbreviations: HCHWA-D = hereditary cerebral hemorrhage with amyloidosis-Dutch type, NBB = Netherlands Brain Bank, LUMC = Leiden University Medical Center, n.a.= not available.

a *Post mortem* delay (in hours)

b Patient code used in (9), (added material in italic)

c +: moderate, ++: high, +++: very high

* Patient material used in studies described in (5)

Tissue sectioning and staining

Formalin-fixed, paraffin-embedded blocks of brain tissue were cut into serial 5 μ m thick sections and mounted on coated glass slides (SuperFrost® Plus, VWR, Dietikon, Switzerland). Deparaffinization in xylene and rehydration through a series of ethanol concentrations was done. To detect calcification standard hematoxylin & eosin (HE) staining and the Von Kossa technique were included. For immunohistochemistry, the usage of an antigen retrieval procedure, a list of antibodies and their dilution are mentioned in Supporting information Table S1. After blocking steps for endogenous peroxidase (3 % H₂O₂ in dH₂O for 10 minutes) and for unspecific epitopes binding in blocking buffer (1 % BSA suspension in 0.1 % Tween 20, Phosphate Buffer Saline pH 7.4 for 1 hour at room temperature), the sections were incubated with primary antibody overnight at 4°C in the blocking buffer. Incubation with secondary HRP antibody was

followed by a DAB reaction (standard or enhanced using an avidin-biotin complex; details in Supporting information Table S1) and mounted with Entellan® New (107961, Merck, Darmstadt, Germany). An overview of the serial sectioning with the sequence of stainings is given in Supporting information Table S2. All slides were digitized using an automatic bright field microscope (Philips Ultra Fast Scanner 1.6 RA, Philips, Netherlands). All stained sections were independently evaluated by LvdG and LGM for the amount of different immunomarkers as described below.

Quantification of severity grade of calcification, Col1 load, CAA load (A β), osteopontin load and pSMAD2/3 load

On the HE stained sections, three cortical areas were delimited at low magnification (2.016 mm² per field of view), based on the presence of calcifications (deep purple color; (24)). The corresponding area on consecutive slides immunostained for OPN, pSMAD2/3, A β and Col1 was identified for each patient. Every area was counted twice at higher magnification (6.897 mm² per field view): one time for the total number of stained vessels and one time for the stained capillaries only. Subtraction of capillary number to total number of vessels gave the amount of intermediary size vessels. This group include all vessels larger than capillaries, with a typical external diameter between 10 and 300 μ m. Leptomeningeal vessels were excluded. Of note, only fully calcified vessels with a deep purple color in HE were counted.

Statistical analysis was done using GraphPad Prism v7.00 with a level of statistical significance set at $p < 0.05$. Normality of the distribution was assessed with a D'Agostino & Pearson test. Correlation matrices were computed with a two-tailed p -value using Pearson correlation or with Spearman correlation in case of non-parametric distribution.

Quantification of immunomarkers in calcified vessel:

Classic vascular immunomarkers were investigated in the calcified vessel layers (luminal, medial and abluminal). Vascular smooth muscle cells (VSMCs) are labeled with Smooth Muscle Actin (SMA) and the endothelial cells (ECs) with CD31, CD105, vWF and/or ICAM-1. The collagen composition of the ECM was determined by Col4 and Col1.

Intact calcified vessels that could be identified on consecutive sections were scored for SMA, CD31, ICAM-1, CD105, vWF, Col4 and Col1 in the luminal, medial and abluminal layers (examples are given in Supporting information Figure S1). A maximum of 10 vessels per patient was graded, given a total of 48 vessels scored in the different patients: 0 vessel for H5; 3 vessels for H8; 10 vessels for H10; 4 vessels for H2; 3 vessels for H9; 10 vessels for H6, 8 vessels for H14, and 10 vessels for H7.

Results

Calcified vessels and localization of immunomarkers

We expect the majority of stained vessels to be small arteries and arterioles (primarily affected in this disorder), but a specific distinction with veins and venules was not assessed; therefore we use the term of ‘‘medium to large vessels’’. Furthermore, we will employ the term calcification, more widely used than mineralization, with the understanding that the deposits may consist apart from calcium of several other co-aggregating minerals such as iron.

Calcification severity and occurrence of OPN and pSMAD2/3 labeling

Calcifications of angiopathic vessels were found in the occipital cortex of 7 out of 8 D-CAA cases. We observed different calcified vessel load between the D-CAA cases, expressed as the number of fully calcified vessels per mm², as shown in Figure 1. Within individuals, calcified vessels were clustering in specific part of the tissue section, and confined to the middle cortical layers (as also described in (5)). Calcified capillaries were A β -laden capillaries (capCAA), restricted to areas where bigger calcified vessels were present (data not shown) and only observed in those cases with the most severe calcification load in the medium to large vessels (Figure 1).

Calcified vessels showed a topographical co-localization with OPN and pSMAD2/3 staining in consecutive slides (Figure 2). Calcified vessels were always positive for both OPN and pSMAD2/3. Longitudinal sectioning of individual penetrating CAA-laden arterioles showed amyloid deposits along the entire vessel wall, but an absence of calcification along the leptomeninges

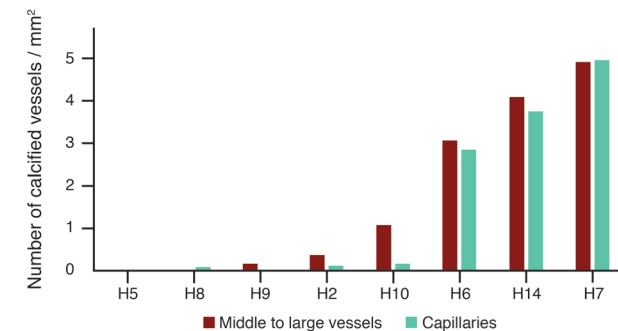


Figure 1: Calcification load (number of fully calcified vessels/mm²) in selected HCHWA-D material ranked from left to right on increased calcified vessel load. Calcification load range from: absent (in H5); low (in H8); mild (in H9, H2 and H10) to heavy (in H6, H14 and H7).

and the superficial cortical layers. Mid-way through the cortex, the gradual transition from non-calcified to calcified vessel wall was accompanied by the occurrence of OPN and pSMAD2/3 granules showing the same gradual transition (Figure 3). Within individual patients, CAA-laden vessels with different calcification load could be identified within one cortical region (Figure 4). Although calcified vessels were always OPN and pSMAD2/3 positive, the reverse is not the case: some OPN and pSMAD2/3 staining was detected in non-calcified angiopathic vessels as well.

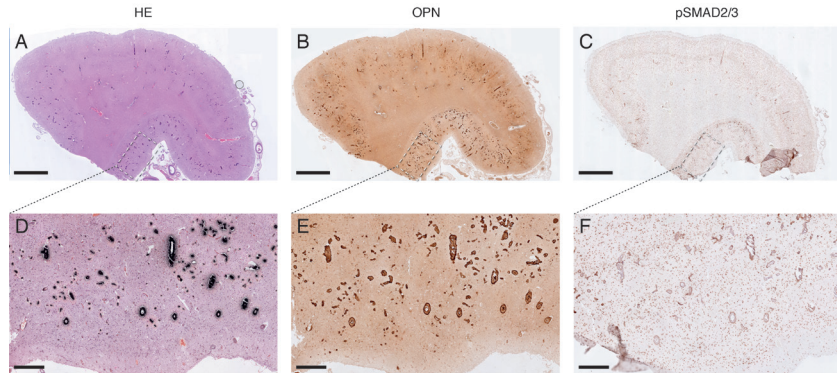


Figure 2: Topographical co-localization of OPN and pSMAD2/3 staining in calcified vessel already detectable at low and medium magnification; H7 patient. A, D. von Kossa staining. B, E. OPN staining. C, F. pSMAD2/3 staining. (A-C) Overview, scale bar 2mm; (D-F) Details of respectively (A-C); scale bar 400µm.

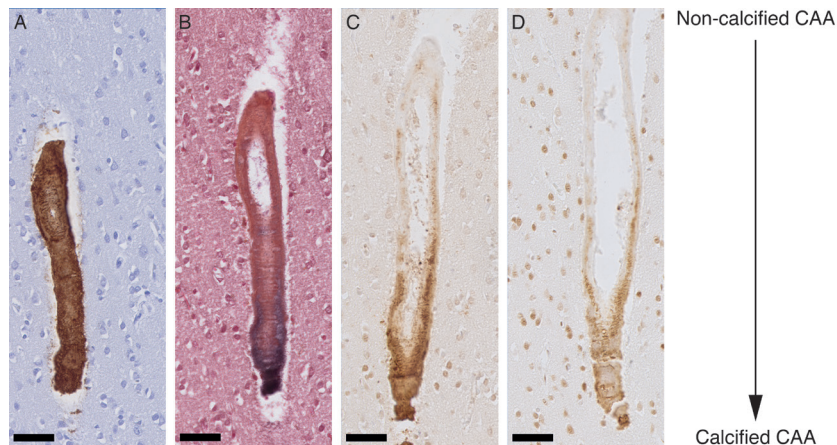


Figure 3: Transition CAA non-calcified to calcified vessel showing the gradual medial OPN and pSMAD2/3 accumulation. Longitudinal sectioning of a penetrating artery oriented leptomeninges (top) to white matter (bottom) side; H2 patient. A. Aβ staining. B. von Kossa staining. C. OPN staining. D. pSMAD2/3 staining. A-D. Consecutive slides; scale bar 50µm.

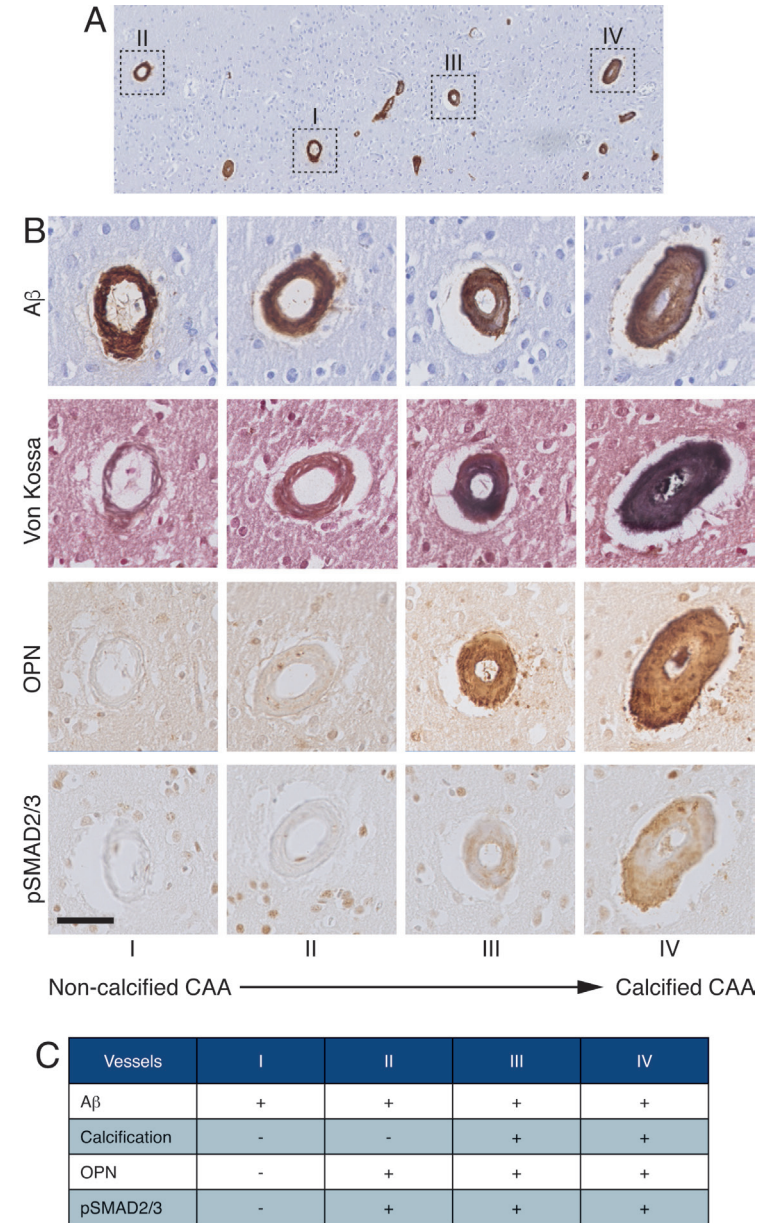


Figure 4: Adjacent cortical angiopathic vessels showing different degree of calcification and gradual accumulation of OPN and pSMAD2/3 in transversal sectioning, H2 patient. A. cortical area overview stained for Aβ; scale bar 200µm. B. details of vessels I to IV identified in (A) and consecutive slides labeling, scale bar 50µm. C. Table indicating the presence (+) or absence (-) of labelling on the vessel wall.

OPN also labeled the nuclei and cytoplasm of some glial cells and neurons. Notably, perivascular cells with a strong cytoplasmic OPN staining were detected in the proximity of vessels undergoing calcification (Supporting information Figure S2). In the parenchyma, pSMAD2/3 labeling was predominantly located in the nuclei of neurons, with little or no cytoplasmic staining, as previously described (9).

Characterization of the layers in the calcified vessels

Studies in peripheral vessels show that diverse mechanisms may trigger calcification, with different vascular components or cell types involved, such as the vascular smooth muscle cells (VSMCs), the endothelium or the extracellular matrix. Therefore we investigated the different layers (luminal, medial and abluminal) of the calcified vessels in more detail.

In D-CAA, the VSMCs have degenerated, as shown by the absence of SMA in the medial layer (Figure 5A). However, the endothelial layer is thought to remain intact (31). Nevertheless, a recent study assessing endothelial dysfunction in CAA showed a loss of CD31 in AD with CAA vessels compared to AD without CAA (21). As endothelial dysfunction may trigger inflammation and is closely linked with vascular pathology, including peripheral vascular calcification, we investigated normal (CD31, CD105, vWF) and activated (ICAM-1) endothelial markers.

Lumen were most frequently labeled for vWF (73% of calcified CAA vessels; Figure 5B). Classical endothelial labeling CD105 and CD31 remained positive in only 35% and 29% of the calcified CAA vessels, whereas luminal SMA staining was detected in 8% of the quantified vessels. An absence of luminal immunostaining was scored in 4% of the calcified vessels. The endothelial inflammation immunomarker ICAM-1 was present in 21% of the calcified lumens whereas ICAM-1 on astrocyte end foot was the major abluminal staining (96% of the scored calcified vessels; Figure 5B).

ECM remodeling of the basement membrane is known to occur in CAA, initially at the abluminal side. As Col1 is a known modulator of calcification, we investigated the presence of normal (Col 4) and fibrotic (Col 1) collagen. Col1 staining was more frequent than Col4 staining in abluminal (71% vs 10%) and medial layers (25% vs 2%) but not in luminal layers (58% vs 65%; Figure 5B).

In accordance with endothelial dysfunction and ECM remodeling, calcified vessels presented a reduction in classical luminal immunomarkers and an intensification in medial and abluminal fibrotic Col1. The above changes in the different layers were also observed in non-calcified CAA vessels but much less frequent.

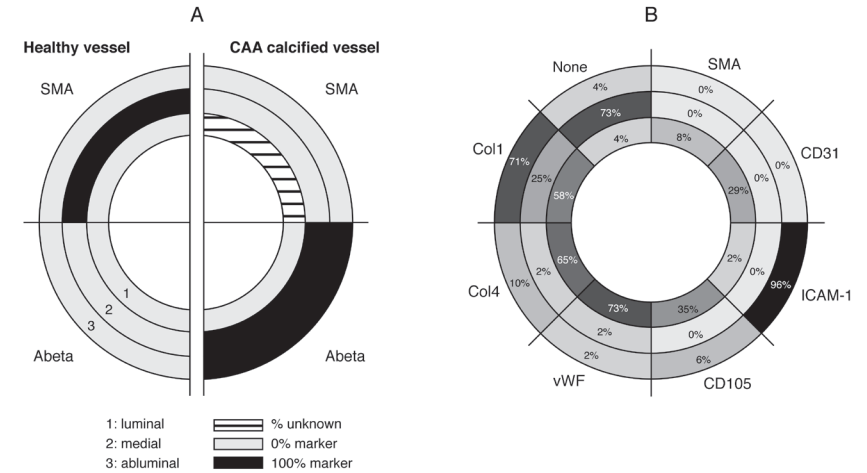


Figure 5: Characterization of calcified vessels. A. Representation of A β and SMA labeling in the luminal, medial and abluminal vascular layers in healthy and calcified CAA vessels in HCHWA-D. Luminal= endothelium; medial = VSMCs; abluminal = external basement membrane and astrocytic end feet. B. Representation of the proportion of each staining occurrence (or absence of) per vessel layers. Most of the vessel layers stained for multiple markers.

Vascular accumulation of Col1, OPN and pSMAD2/3 immunomarkers is related to disease severity

We observed that the majority of CAA vessels and capCAA (A β -laden capillaries) in D-CAA were Col1 positive; anatomically normal vessels were Col1 negative. An illustration of the topographical association between Col1 and A β in the angiopathic vessel wall is presented in Supporting information Figure S3 for two cases with different CAA and capCAA severity. CAA and CapCAA vessels were mostly OPN positive, but also frequently pSMAD2/3 positive.

Apart from a topographical association, we also investigated the accumulation of OPN, pSMAD2/3 and Col1 in the vessel wall in relation to disease severity as measured by CAA or capCAA load. Positive significant correlations between all immunomarkers studied and disease severity were found (Figure 6 and Supporting information Figure S4). Independently of the vessel size, the correlation of CAA/capCAA load with OPN, pSMAD2/3 and Col1 load was most significant.

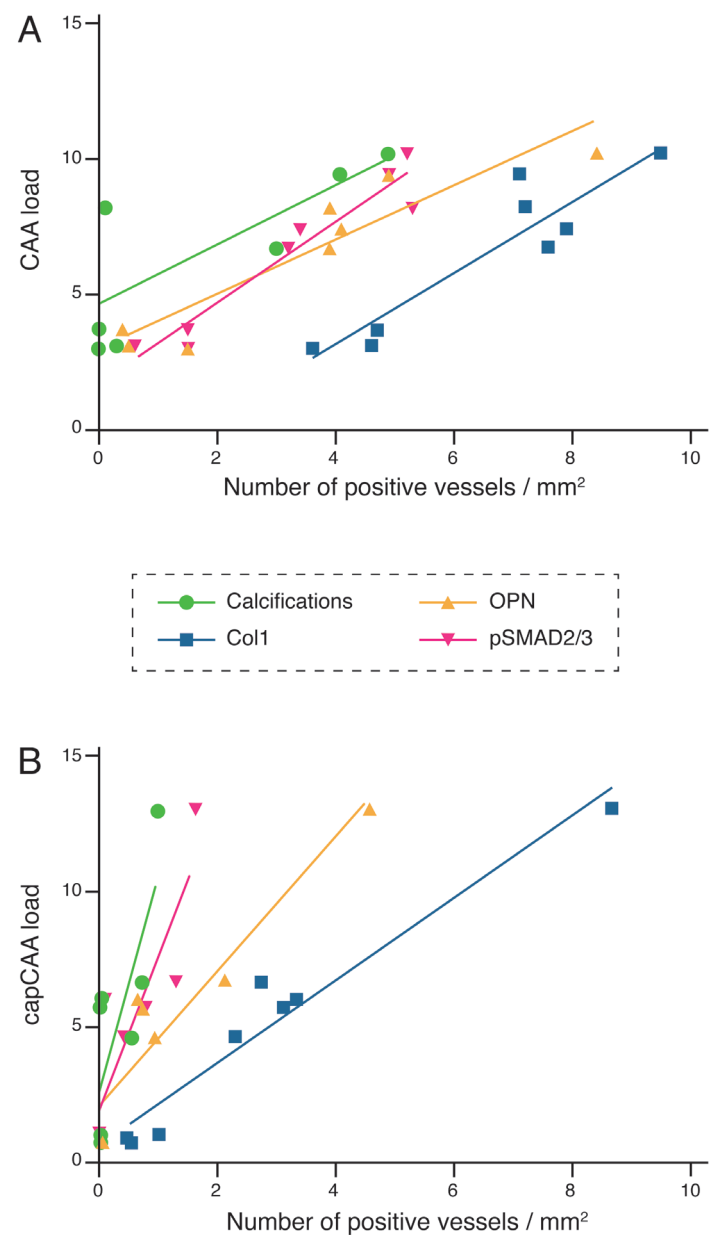


Figure 6: Graphical representation of the quantified OPN, pSMAD2/3 and Col1 immunomarkers and calcified vessels per patient plotted against the CAA load. A) in medium to large vessels and B) in capillaries. Highest correlation coefficient was obtained in A) between the CAA load and the pSMAD2/3 or OPN load (respectively Pearson $r=0.96$, $p=0.0001$ and $r=0.93$, $p=0.0009$). Details are given in Supporting information Figure S4.

Discussion

This study investigated OPN and Col1 immunomarkers though to promote calcification together with A β and pSMAD2/3 known immunomarkers associated with CAA severity, and proposes a mechanism of vascular calcification in HCHWA-D.

Calcifications are a feature of late stage CAA and capCAA pathology

In this study we found a significant correlation of the occurrence of vascular calcification with CAA severity, in line with a previous study on CAA-associated microvasculopathies (including calcifications) which also showed a correlation with CAA load (27).

Despite the spatial correlation between CAA load and vascular calcification, to date there is no proof for causality between the presence of the A β peptide per se, and calcification of the vessel wall (10,13). This is further supported by our previous finding where we observed calcification of non-CAA vessels in a sCAA case (6). Furthermore, we observed in the present and in previous studies very heterogeneous patterns of calcification in areas with comparable CAA load, even within the same patient. This suggests that vascular calcifications are most likely a secondary complication of the CAA pathology, but not directly caused by the deposition of amyloid.

As described in prior studies, capCAA is detected only in severely affected HCHWA-D patients and increases with CAA load (27,28). Calcifications of capCAA occurred mostly in subjects with the highest calcified vessel load and in proximity to other calcified vessels. This might either indicate a spreading of the calcification over the entire vascular tree, or it could be the result from surrounding parenchymal changes. Given the preferential occurrence of calcification in specific cortical lamina (6), local changes in the surrounding parenchyma are more plausible.

Col1, OPN and pSMAD2/3 accumulation might precede vessel wall calcification

To investigate the pathomechanism of vascular calcification in CAA, we investigated several potential modulators. pSMAD2/3 is a direct TGF β 1 downstream signaling factor which is known to modulate peripheral vascular calcification. OPN is a matrix protein induced by TGF β , also leading to peripheral vessel calcification and a central nervous system constituent of the ECM. Lastly, we stained for Col1, a pro-fibrotic gene induced by TGF β 1 signaling and an OPN binder, involved in ECM remodeling.

In Figure 6, the order of progression for each immunomarker is visualized as a function of increasing CAA severity. Interestingly, for the same scored area the number of vessels labeled by Col1 was often higher than the number of vessels stained for A β (Supporting information Figure S4B), indicating that the fibrosis of the vessel wall might precede the amyloid deposition. Alternatively, as the arterial system was not distinguished from the venous system, the fibrosis of veins and venules (usually spared from amyloid deposition) might contribute to the number of Col1-positive vessels as well. Both scenarios involve an early stage fibrosis of the vessel wall due to ECM remodeling regulated by TGF β as proposed in our previous work (16,17).

In addition, the topographical co-localization and gradual accumulation of OPN and pSMAD2/3 with calcification reveals that OPN and pSMAD2/3 accumulation are tightly linked to the calcification process. Moreover, the presence of OPN and pSMAD2/3 accumulation in non-calcified angiopathic vessels suggests an ongoing calcification process.

TGF β and OPN changes in calcified vessels

Besides having a role in excessive vascular fibrosis, prolonged chronic induction of TGF β might directly contribute to the calcification process in HCHWA-D. Evidence of TGF β -related induction of calcification genes were described in neuron-specific TGF β 1-overexpressing transgenic mice that presented with cerebral angiopathy. A microarray analysis of genes in the cortex identified upregulation of a group of genes involved in calcium homeostasis, tissue calcification and vascular calcification, including OPN (29).

In our studies, there was a topographical co-accumulation of OPN and pSMAD2/3 in pre-calcified vessels. This likely reflects a role for SMAD signaling in the vascular calcification. This is supported by Shi et al. who demonstrated that pSMAD3 can bind directly to the OPN promoter, activating OPN transcription (30). Furthermore SMAD3 overexpression in a mouse osteoblastic cell line was found to promote calcification via Col1 upregulation (31).

Calcification hypothesis in HCHWA-D

Many mechanisms have been proposed for vascular calcification in peripheral diseases. Cortical calcification in these paper resembles concentric medial artery calcification described in diabetes and chronic renal disease (32) and are different from intimal calcification as seen in atherosclerosis (eccentric; lumen deforming; (33)). In medial calcification, the proposed mechanisms are usually VSMCs mediated with vascular OPN production (34).

However, in this study, VSMCs are likely not responsible for the medial calcification. Firstly, VSMCs are not present in calcified, nor in pre-calcified OPN-positive vessels ((6) and this study) because CAA positive vessels usually do not have any VSMCs remaining. Furthermore, many CAA positive vessels were OPN-negative, suggesting that OPN and A β accumulation are caused by different mechanisms and vascular OPN does not have a vascular SMC origin.

This is based on our observation that there was local heterogeneity of vascular calcification, even within the same patient. We hypothesize that this variability may be due to tissue responses to local events such as microbleeds, micro-infarcts and hypoxia that are likely to occur in these patients. In this context, OPN is known to be upregulated and neuroprotective after ischemic events such as stroke (35) and local cortical injuries induce OPN increase in parenchymal cells as demonstrated in animal models of blood brain barrier damage in the context of ischemic (36) or hemorrhagic injuries (37). Furthermore, OPN is an immunomodulatory cytokine, upregulated in reaction to toxic amyloid species (38). Testing these hypotheses should be done in future studies using animal or cell models.

Lastly, it was demonstrated *in vitro*, that OPN could induce the calcification of Col1 fibers in the context of bone formation (39). In the current study the co-localization of OPN and Col1 in calcified vessels suggests a functional link between vascular OPN likely trapped into Col1 fibers and calcification of CAA vessel wall.

The clinical detection of potential biomarkers of vascular remodeling such as Col1 and OPN in blood or CSF, might give insight into the progression of CAA pathology in HCHWA-D. In addition, further investigations are required to determine whether OPN is a regulator of the early disease mechanism of interest as therapeutic target.

Acknowledgments

The authors thank S.G. van Duinen from the Department of Pathology, Leiden University Medical Center for supplying brain tissue. We acknowledge I.M. Hegeman for the preparation of sections and standard histological stainings and Y. Ramos for providing the osteopontin antibody. This work was supported by the Bontius stichting (Leiden, The Netherlands) and by the Netherlands Organisation for Scientific Research (NWO), under research program VIDI, project ‘‘Amyloid and vessels’’, number 864.13.014.

Compliance with ethical standards

Conflicts of interest: The authors declare they have no conflicts of interest.

Ethical approval: All procedures performed in this study involving human participants were in accordance with the ethical standards of the institutional and/or national research committee and with the 1964 Helsinki declaration and its later amendments or comparable ethical standards.

Informed consent: Informed consent was obtained from all individual participants included in the study.

Supporting material: The supporting information for this article can be found at <https://doi.org/10.1111/bpa.12721>.

References

- Attems J, Jellinger K, Thal DR, Van Nostrand W. (2011). Review: Sporadic cerebral amyloid angiopathy. *Neuropathol. Appl. Neurobiol.* 37:75–93
- Bidder M, Shao J-S, Charlton-Kachigian N, Loewy AP, Semenkovich CF, Towler DA. (2002). Osteopontin transcription in aortic vascular smooth muscle cells is controlled by glucose-regulated upstream stimulatory factor and activator protein-1 activities. *J. Biol. Chem.* 277:44485–96
- Bostrom KI. (2016). Where do we stand on vascular calcification? *Vascul. Pharmacol.* 84:8–14
- Brown A. (2012). Osteopontin: a Key Link Between Immunity, Inflammation and the Central Nervous System. *Transl. Neurosci.* 3:288–93
- Bulk M, Moursel LG, van der Graaf LM, van Veluw SJ, Greenberg SM, van Duinen SG, van Buchem MA, van Rooden S, van der Weerd L. (2018). Cerebral Amyloid Angiopathy With Vascular Iron Accumulation and Calcification. *Stroke.* 49:2081–87
- Carecchio M, Comi C. (2011). The role of osteopontin in neurodegenerative diseases. *J. Alzheimer's Dis.* 25:179–85
- Enkhjargal B, McBride DW, Manaenko A, Reis C, Sakai Y, Tang J, Zhang JH. (2017). Intranasal administration of vitamin D attenuates blood-brain barrier disruption through endogenous upregulation of osteopontin and activation of CD44/P-gp glycosylation signaling after subarachnoid hemorrhage in rats. *J. Cereb. Blood Flow Metab.* 37:2555–66
- Fujita D, Terada S, Ishizu H, Yokota O, Nakashima H, Ishihara T, Kuroda S. (2003). Immunohistochemical examination on intracranial calcification in neurodegenerative diseases. *Acta Neuropathol.* 105:259–64
- Grand Moursel L, Munting LP, van der Graaf LM, van Duinen SG, Goumans MJTH, Ueberham U, Natté R, van Buchem MA, van Roon-Mom WMC, van der Weerd L. (2018). TGFβ pathway deregulation and abnormal phospho-SMAD2/3 staining in hereditary cerebral hemorrhage with amyloidosis-Dutch type. *Brain Pathol.* 28:495–506
- Grand Moursel L, van Roon-Mom WMC, Kiełbasa SM, Mei H, Buermans HPJ, van der Graaf LM, Hettne KM, de Meijer EJ, van Duinen SG, Laros JFJ, van Buchem MA, 't Hoen PAC, van der Maarel SM, van der Weerd L. (2018). Brain transcriptomic analysis of hereditary cerebral hemorrhage with amyloidosis-Dutch type. *Front. Aging Neurosci.* 10:1–12
- Hodroge A, Trécherel E, Cornu M, Darwiche W, Mansour A, et al. (2017). Oligogalacturonic Acid Inhibits Vascular Calcification by Two Mechanisms: Inhibition of Vascular Smooth Muscle Cell Osteogenic Conversion and Interaction with Collagen. *Arterioscler. Thromb. Vasc. Biol.* 37:1391–1401
- Iwanaga Y, Ueno M, Ueki M, Huang CL, Tomita S, Okamoto Y, Ogawa T, Ueda N, Maekawa N, Sakamoto H. (2008). The expression of osteopontin is increased in vessels with blood-brain barrier impairment. *Neuropathol. Appl. Neurobiol.* 34:145–54
- Jian B, Narula N, Li QY, Mohler ER, Levy RJ. (2003). Progression of aortic valve stenosis: TGF-β1 is present in calcified aortic valve cusps and promotes aortic valve interstitial cell calcification via apoptosis. *Ann. Thorac. Surg.* 75:457–65
- Kahles F, Findeisen HM, Bruemmer D. (2014). Osteopontin: A novel regulator at the cross roads of inflammation, obesity and diabetes. *Mol. Metab.* 3:384–93

15. Kamp JA, Moursel LG, Haan J, Terwindt GM, Lesnik Oberstein SAMJ, Van Duinen SG, Van Roon-Mom WMC. (2014). Amyloid β in hereditary cerebral hemorrhage with amyloidosis-Dutch type. *Rev. Neurosci.* 25:641–51
16. Karwowski W, Naumnik B, Szczepański M, Myśliwiec M. (2012). The mechanism of vascular calcification – a systematic review. *Med. Sci. Monit.* 18:RA1-RA11
17. Koemans EA, van Etten ES, van Opstal AM, Labadie G, Terwindt GM, Wermer MJH, Webb AG, Gurol EM, Greenberg SM, van Buchem MA, van der Grond J, van Rooden S. (2018). Innovative Magnetic Resonance Imaging Markers of Hereditary Cerebral Amyloid Angiopathy at 7 Tesla. *Stroke.* 49:1518–20
18. Luyendijk W, Bots GT, Vegter-van der Vliet M, Went LN, Frangione B. (1988). Hereditary cerebral haemorrhage caused by cortical amyloid angiopathy. *J. Neurol. Sci.* 85:267–80
19. Maat-Schieman M, Roos R, van Duinen S. (2005). Hereditary cerebral hemorrhage with amyloidosis-Dutch type. *Neuropathology.* 25:288–97
20. Mackenzie IR. (1997). Cerebral amyloid angiopathy with extensive mineralization. *Clin. Neuropathol.* 16:209–13
21. Magaki S, Tang Z, Tung S, Williams CK, Lo D, Yong WH, Khanlou N, Vinters H V. (2018). The effects of cerebral amyloid angiopathy on integrity of the blood-brain barrier. *Neurobiol. Aging.* 70:70–77
22. Mandybur TI. (1986). Cerebral Amyloid Angiopathy: The Vascular Pathology and Complications. *J. Neuropathol. Exp. Neurol.* 45:79–90
23. Mann DM. (1988). Calcification of the basal ganglia in Down's syndrome and Alzheimer's disease. *Acta Neuropathol.* 76:595–98
24. McCartney E, Squier W. (2014). Patterns and pathways of calcification in the developing brain. *Dev. Med. Child Neurol.* 56:1009–15
25. Meller R, Stevens SL, Minami M, Cameron JA, King S, Rosenzweig H, Doyle K, Lessov NS, Simon RP, Stenzel-Poore MP. (2005). Neuroprotection by osteopontin in stroke. *J. Cereb. Blood Flow Metab.* 25:217–25
26. Mok T, Chalissery AJ, Byrne S, Costelloe L, Galvin L, Vinters H V., Farrell MA, Brett FM, Moroney JT. (2014). Familial cerebral amyloid angiopathy due to the iowa mutation in an Irish family. *Can. J. Neurol. Sci.* 41:512–17
27. Natté R, Maat-Schieman MLC, Haan J, Bornebroek M, Roos RAC, Van Duinen SG. (2001). Dementia in hereditary cerebral hemorrhage with amyloidosis-Dutch type is associated with cerebral amyloid angiopathy but is independent of plaques and neurofibrillary tangles. *Ann. Neurol.* 50:765–72
28. Nicolas G, Martinaud O. (2018). Sporadic Cerebral Amyloid Angiopathy with Cortical Occipital Calcifications in the Elderly. *Alzheimer Dis. Assoc. Disord.* 32:83–84
29. Prelli F, Levy E, van Duinen SG, Bots GTAM, Luyendijk W, Frangione B. (1990). Expression of a normal and variant Alzheimer's β -protein gene in amyloid of hereditary cerebral hemorrhage, Dutch type: DNA and protein diagnostic assays. *Biochem. Biophys. Res. Commun.* 170:301–7
30. Rentsendorj A, Sheyn J, Fuchs DT, Daley D, Salumbides BC, Schubloom HE, Hart NJ, Li S, Hayden EY, Teplow DB, Black KL, Koronyo Y, Koronyo-Hamaoui M. (2018). A novel role for osteopontin in macrophage-mediated amyloid- β clearance in Alzheimer's models. *Brain. Behav. Immun.* 67:163–80
31. Revesz T, Holton JL, Lashley T, Plant G, Rostagno A, Ghiso J, Frangione B. (2002). Sporadic and familial cerebral amyloid angiopathies. *Brain Pathol.* 12:343–57
32. Rodriguez DE, Thula-Mata T, Toro EJ, Yeh YW, Holt C, Holliday LS, Gower LB. (2014). Multifunctional role of osteopontin in directing intrafibrillar mineralization of collagen and activation of osteoclasts. *Acta Biomater.* 10:494–507
33. Sella F, Wallon D, Martinez-Almoyna L, Marelli C, Dhar A, et al. (2017). APP mutations in cerebral amyloid angiopathy with or without cortical calcifications: report of three families and a literature review. *J. Alzheimer's Dis.* 56:37–46
34. Shi X, Bai S, Li L, Cao X. (2001). Hoxa-9 represses transforming growth factor-beta-induced osteopontin gene transcription. *J. Biol. Chem.* 276:850–55
35. Sowa H, Kaji H, Yamaguchi T, Sugimoto T, Chihara K. (2002). Smad3 promotes alkaline phosphatase activity and mineralization of osteoblastic MC3T3-E1 cells. *J. Bone Miner. Res.* 17:1190–99
36. Thal DR, Ghebremedhin E, Rüb U, Yamaguchi H, Del Tredici K, Braak H. (2002). Two types of sporadic cerebral amyloid angiopathy. *J. Neuropathol. Exp. Neurol.* 61:282–93
37. Ueberham U, Zobiak B, Ueberham E, Brückner MK, Boriss H, Arendt T. (2006). Differentially expressed cortical genes contribute to perivascular deposition in transgenic mice with inducible neuron-specific expression of TGF- β 1. *Int. J. Dev. Neurosci.* 24:177–86
38. van Duinen SG, Maat-Schieman MLC, Buijn JA, Haan J, Roos RAC, Wattendorff AR, Frangione B, Luyendijk W. (1995). Cortical Tissue of Patients With Hereditary Cerebral-Hemorrhage With Amyloidosis (Dutch) Contains Various Extracellular-Matrix Deposits. *Lab. Invest.* 73:183–89
39. Vinters H V., Natté R, Maat-Schieman MLC, Van Duinen SG, Hegeman-Kleinn I, Welling-Graafland C, Haan J, Roos RAC. (1998). Secondary microvascular degeneration in amyloid angiopathy of patients with hereditary cerebral hemorrhage with amyloidosis, Dutch type (HCHWA-D). *Acta Neuropathol.* 95:235–44
40. Watson KE, Boström K, Ravindranath R, Lam T, Norton B, Demer LL. (1994). TGF- β 1 and 25-hydroxycholesterol stimulate osteoblast-like vascular cells to calcify. *J. Clin. Invest.* 93:2106–13
41. Wegiel J, Kuchna I, Wisniewski T, de Leon MJ, Reisberg B, Pirttila T, Kivimaki T, Lehtimaki T. (2002). Vascular fibrosis and calcification in the hippocampus in aging, Alzheimer disease, and Down syndrome. *Acta Neuropathol.* 103:333–43
42. Wegiel J, Kuchna I, Wisniewski T, de Leon MJ, Reisberg B, Pirttila T, Kivimaki T, Lehtimaki T. (2002). Vascular fibrosis and calcification in the hippocampus in aging, Alzheimer disease, and Down syndrome. *Acta Neuropathol.* 103:333–43
43. Yu H, Liu X, Zhong Y. (2017). The Effect of Osteopontin on Microglia. *Biomed Res. Int.* 2017:19–23
44. Zarranz JJ, Fernandez-Martinez M, Rodriguez O, Mateos B, Iglesias S, Baron JC. (2016). Iowa APP mutation-related hereditary cerebral amyloid angiopathy (CAA): A new family from Spain. *J. Neurol. Sci.* 363:55–56

Chapter 6

Brain transcriptomic analysis of hereditary cerebral hemorrhage with amyloidosis–Dutch type

Laure Grand Moursel^{1,2}, Willeke M.C. van Roon-Mom¹, Szymon M. Kielbasa⁴, Hailiang Mei⁴, Henk P.J. Buermans¹, Linda M. van der Graaf^{1,2}, Kristina M. Hettne¹, Emile J. de Meijer¹, Sjoerd G. van Duinen³, Jeroen F.J. Laros^{1,5}, Mark A. van Buchem², Peter A.C. 't Hoen¹, Silvère M. van der Maarel¹, Louise van der Weerd^{1,2}

¹ Department of Human Genetics, Leiden University Medical Center

² Department of Radiology, Leiden University Medical Center

³ Department of Pathology, Leiden University Medical Center

⁴ Department of Medical Statistics and Bioinformatics, Leiden University Medical Center

⁵ Department of Clinical Genetics, Leiden University Medical Center

Adapted from Front. Aging Neurosci. (2018).

Abstract

Hereditary cerebral hemorrhage with amyloidosis–Dutch type (HCHWA-D) is an early onset hereditary form of Cerebral Amyloid Angiopathy (CAA) caused by a point mutation resulting in an amino acid change (NP_000475.1:p.Glu693Gln) in the Amyloid Precursor Protein (APP). *Post mortem* frontal and occipital cortical brain tissue from 9 patients and 9 age-related controls was used for RNA sequencing to identify biological pathways affected in HCHWA-D. Although previous studies indicated that pathology is more severe in the occipital lobe in HCHWA-D compared to the frontal lobe, the current study showed similar changes in gene expression in frontal and occipital cortex and the two brain regions were pooled for further analysis. Significantly altered pathways were analyzed using Gene Set Enrichment Analysis (GSEA) on 2036 significantly differentially expressed genes. Main pathways overrepresented by down-regulated genes were related to cellular aerobic respiration (including ATP synthesis and carbon metabolism) indicating a mitochondrial dysfunction. Principal up-regulated pathways were Extra Cellular Matrix (ECM)-receptor interaction and ECM proteoglycans in relation with an increase in the Transforming Growth Factor beta (TGF β) signaling pathway. Comparison with the publicly available dataset from pre-symptomatic APP-E693Q transgenic mice identified overlap for the ECM-receptor interaction pathway, indicating that ECM modification is an early disease specific pathomechanism.

Introduction

Cerebral amyloid angiopathy (CAA) refers to the presence of amyloid, commonly Amyloid β (A β), in intracerebral vessels. CAA pathology is present in the majority of Alzheimer's Disease (AD) brains and is associated with intracerebral hemorrhages in the elderly.

Hereditary cerebral hemorrhage with amyloidosis-Dutch type (HCHWA-D) is a severe monogenic form of CAA with an autosomal dominant pattern of inheritance. A point mutation at codon 693 of the Amyloid Precursor protein (APP) located at chromosome 21 results in a glutamine for glutamic acid substitution (NP_000475.1:p.Glu693Gln) leading to the formation of the A β -E22Q peptide, a toxic variant of the A β peptide well-studied *in vitro* (1). Pathologically, HCHWA-D is characterized by severe amyloid angiopathy of meningo-cortical blood vessels; mutation carriers suffer from intracerebral hemorrhage, starting typically between the ages of 40 and 65.

Although previous radiological and neuropathological studies describe the disease in detail, the exact molecular processes causing A β accumulation in the vessel wall largely remain to be characterized. Some mechanisms have been already examined in HCHWA-D *post mortem* material, in particular extracellular matrix (ECM) remodeling in the angiopathic vessel wall. Changes in the basement membrane composition with accumulation of heparan sulfate proteoglycans (2) and activity of ECM-cross-linking enzymes like lysyl-oxidase (3) or tissue-transglutaminase (4) are processes known to promote A β aggregation. More recently, our group showed a phospho-Smad 2/3 dependent dysregulation in the TGF β pathway (5) with an increase in pro-fibrotic transcripts.

Genome wide gene expression studies are an unbiased approach to attain a comprehensive picture of dysregulated genes and pathways. RNA sequencing of *post mortem* human brain tissue is of particular interest to unravel complex mechanisms in neurodegenerative diseases (6), such as AD (7–9). In the current study, we perform a pathway analysis on differentially expressed protein-coding genes in brain tissue of HCHWA-D patients and age-matched controls to detect potential novel therapeutic targets and biomarkers of CAA pathology and to better comprehend the molecular pathology of HCHWA-D.

Recently, the brain transcriptome of the transgenic APP-E693Q mice was published (10), which allowed us to study overlapping pathways between our HCHWA-D patient data and pre-symptomatic APP-E693Q transgenic mice, in order to identify conserved and critical pathways in CAA.

Patients, materials and methods

Study design

This study was performed in 36 samples: frontal and occipital cortex samples from 9 HCHWA-D and 9 non-demented control (NDC) subjects. Patient material information can be found in Figure 1. Both frontal and occipital cortex were used, based on the previous finding that the CAA pathology is more severe in the occipital lobe in HCHWA-D compared to the frontal lobe (11). Written informed consent was obtained for each donor in accordance with the Declaration of Helsinki and all material and data were handled in a coded fashion maintaining patient anonymity according to Dutch national ethical guidelines (Code for Proper Secondary Use of Human Tissue, Dutch Federation of Medical Scientific Societies). The study was approved by the local Ethics Committee (Commissie Medische Ethiek, LUMC).

RNA isolation, library preparation and sequencing

Brain tissue processing, tissue homogenization and RNA extraction were done as described previously (5) (see Datasheet 1_Supplementary Method). Samples for RNA extraction were processed directly, whereas samples for protein extraction were stored at -80C prior to analysis. RNA content was measured with the Nanodrop at 260nm and evaluation of RNA Integrity was performed with on-chip electrophoresis using an RNA 6000 Nano kit and a Bio-Analyzer 2100 (Agilent). Samples with a RNA integrity number (RIN) value of <5 were excluded from the study.

RNA samples were depleted for ribosomal RNA (rRNA) with the Ribo Zero Gold Human kit (Illumina) and strand specific RNA-Seq libraries were generated as previously described (12), with minor modifications as defined in Datasheet 1_Supplementary Method. After amplification of the libraries, samples with unique sample indexes were pooled and sequenced paired-end 2x50bp on a HiSeq2500 system following standard Illumina guidelines.

Mapping reads, gene expression counts and quality controls

RNA-Seq files were processed using the BIOPET Gentrapp pipeline v0.6 developed at the LUMC¹ which performs FASTQ preprocessing (including quality control, quality trimming and adapter clipping), RNA-Seq alignment, read and base quantification, and optionally transcript assembly. FastQC (RRID:SCR_000141, v0.11.2) was used for checking raw read QC. Low quality read trimming was done using Sickle (RRID:SCR_006800, v1.33) with default settings. Adapter clipping was performed using Cutadapt (RRID:SCR_011841, v1.9.1) with default settings. RNA-Seq reads

alignment were performed using GSNAP (RRID:SCR_005483, v2014-12-23) with setting "--npaths 1" on GRCh38 reference genome without the alternative contigs. The gene read quantification was performed using HTSeq-count (RRID:SCR_011867, v0.6.1p1) with setting "--stranded reverse". The gene annotation used for quantification were UCSC RefSeq genes for GRCh38 downloaded on 2015-07-13.

SNPs and gender based quality controls as well as median 5'-3' bias methods are specified in Datasheet 1_Supplementary Method.

Normalization and differential expression analysis

CQN (RRID:SCR_001786, v1.22) was used to normalize the gene count table for library sizes, gene transcript lengths (sum of exons lengths) and gene transcript GC-contents (concatenated exon sequences). EdgeR (RRID:SCR_012802, v3.18.1) was used to perform differential gene expression analysis. An interaction model *group*area* was fit with two factors: *group* (two categories: HCHWA-D vs. control) and *area* (two categories: frontal vs. occipital). As offsets we used the normalization coefficients obtained from the CQN model. Benjamini & Hochberg FDR was computed to adjust *p*-values obtained for each differentially expressed gene (DEG). Finally, a table of raw and normalized expression levels of the genes was produced (not shown), and a table of gene expression levels fold changes (FC) and their significances for each gene and model component.

Validation of RNA-Seq data

Quantitative RT-PCR (qPCR) was performed with the same RNA extracts as were used for RNA-Seq analysis and the primers listed in Datasheet 2_Supplementary Table 1. Primer design, qPCR method and analysis were done as described previously (5) are provided in Datasheet 1_Supplementary Method. Correlation of expression levels between the RNA-Seq and the qPCR data was calculated from expression levels of selected genes extracted from the count matrix. The gene expression mean values per patient (log₂ transformed) of both the count matrix and the qPCR results were plotted.

Western Blot was performed from frozen brain sections as described in Datasheet 1_Supplementary Method with anti-HSP70 (1:1500, Santa Cruz Biotechnology Cat# sc-24, RRID:AB_627760) and anti-β-actin (1:5000, Abcam Cat# ab6276, RRID:AB_2223210).

All statistical analysis from the validation section were conducted in GraphPad Prism (RRID:SCR_002798, v7.00) with a level of statistical significance set at *p* <0.05.

¹ http://biopet-docs.readthedocs.io/en/latest/releasenotes/release_notes_0.6.0/

Pathway analysis

Gene Ontology (GO) annotations and significantly altered pathways in KEGG, Reactome and Wikipathways were analyzed using GeneTrail2 (13) (RRID:SCR_006250, v1.5; GO, KEGG, Reactome retrieved 11/01/2016; Wikipathways retrieved 18/02/2016) with the Gene Set Enrichment Analysis (GSEA) method. GSEA was performed using a Kolmogorov-Smirnov non-parametric rank statistic (14) with Benjamini and Yekutieli FDR multiple testing adjustment method. Gene lists were ranked based on either FC or FDR (top list with most significantly up-regulated and bottom list with most significantly down-regulated; keeping the dysregulation direction).

Analysis was performed on extended gene sets and most significant DEGs from HCHWA-D brains from the current study and from transgenic APP-E693Q mice (DEG WT vs. APP-E693Q mice, entorhinal cortex (10) as depicted in Figure 2. Subsequent known interactions between genes set were visualized with the STRING database (RRID:SCR_005223, v10.5).

Results

Quality checks of samples and RNA-Seq reads

Based on SNPs, gender and HCHWA-D mutation presence, all 36 samples were concordant and included in the analysis (Datasheet 3_Supplementary Figure 1). The average number of reads after sequencing was 19 578 485 for controls and 23 038 641 for HCHWA-D. The number of reads after alignment are depicted in Datasheet 3_Supplementary Figure 2. The count matrix was generated with uniquely mapped reads. On average, the HCHWA-D samples had a lower RIN value than control samples (6.50 ± 0.96 and 7.92 ± 0.78 respectively). The median 5'-3' bias (ratio of median 5'bias:3'bias) was calculated for each sample (samples code and details in Datasheet 2_Supplementary Table 2). High values (>5) were found for 3 control samples (S_7, S_17, S_18) and 8 HCHWA-D samples (S_19, S_21, S_22, S_23, S_24, S_28, S_32, S_36), but we did not find a significant correlation with a longer *post mortem* delay (PMD) or a lower RIN value (not shown). On another hand, there was a strong positive correlation between the median 5'-3' bias and the number of reads with GC-content $> 75\%$ (Datasheet 3_Supplementary Figure 3). This prompted us to apply a GC correction before analyzing differentially expressed genes.

Quality controls of differential gene expression and analysis

Because of large differences in the GC-content of samples, correction for GC bias was done with the CQN model. After GC correction, fold changes dependence of gene GC-contents were no longer observed (Figure 3). The

clustering of reads was examined with principal component analysis (PCA) and no clustering related to the gender or the origin of tissue (NBB vs. LUMC; data not shown) were identified. PCA showed a close clustering of the control samples with less homogeneity in the HCHWA-D samples. Most frontal and occipital samples from the same subject clustered together (Datasheet 3_Supplementary Figure 4).

Diagnosis	Source	Age range	PMDs ^a
NDC	LUMC	70-75	6
NDC	LUMC	65-69	4
NDC	NBB	60-64	6
NDC	NBB	60-64	10
NDC	NBB	55-60	8
NDC	NBB	55-60	9
NDC	NBB	55-60	8
NDC	NBB	50-54	8
NDC	LUMC	40-45	n.a.
HCHWA-D	NBB	70-75	6
HCHWA-D	NBB	60-64	7
HCHWA-D	LUMC	55-60	6
HCHWA-D	LUMC	55-60	3
HCHWA-D	LUMC	50-54	6
HCHWA-D	LUMC	50-54	3
HCHWA-D	LUMC	50-54	3
HCHWA-D	LUMC	50-54	19
HCHWA-D	LUMC	45-50	11

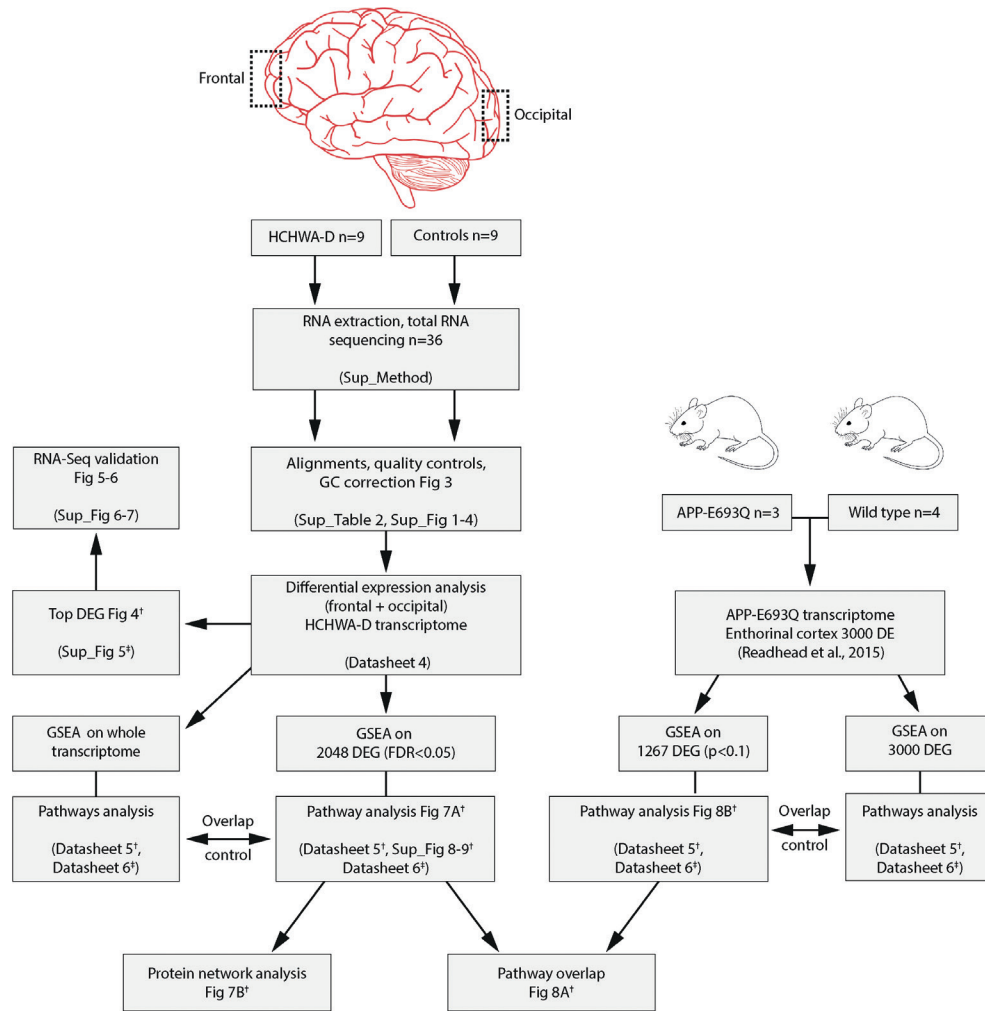
NDC non-demented control, HCHWA-D hereditary cerebral hemorrhage with amyloidosis-Dutch type, NBB Netherlands Brain Bank, LUMC Leiden University Medical Center, n.a. not available.

^a Post-mortem delay (in hours)

Figure 1: Patient material overview. Controls without stroke were age-matched [mean age \pm standard deviation (SD) HCHWA-D: 55.8 ± 7.1 ; NDC: 58.6 ± 8.4]; both gender were included in the two groups (%M, %F; HCHWA-D: 78, 22; NDC: 56, 44); and *post mortem* delay (PMD; in hours) were not significantly different (HCHWA-D: 7.1 ± 5.2 ; NDC: 7.2 ± 2.2). Frontal and occipital human *post mortem* brain tissue was obtained from the Netherlands Brain Bank (NBB) and from our hospital (LUMC).

When we analyzed DEG independently of cases, we found 380 genes differently expressed in frontal vs. occipital cortex, but in the HCHWA-D cortex we did not find evidence that the two brain regions were differently affected. Therefore, in all further analyses, frontal and cortical samples in each group were pooled (18 versus 18 samples). HCHWA-D whole dataset and subset of significantly altered genes (FDR < 0.05) with both FC and FDR

are provided in Datasheet 4_Supplementary Material 1. 2048 significant DEG were identified (Figure 3B) including 1201 (7.5%) up-regulated DEG and 847 (5.3%) down-regulated DEG. The top list of DEG, ranked on FC, is given in Figure 4A (down-regulated DEG with both FC and FDR) and Figure 4B (up-regulated DEG with both FC and FDR). Top DEG ranked on significance can be found in Datasheet 3_Supplementary Figure 5.



* FC ranking of genes; *FDR ranking of genes

Figure 2: Flow chart of the study and associated files.

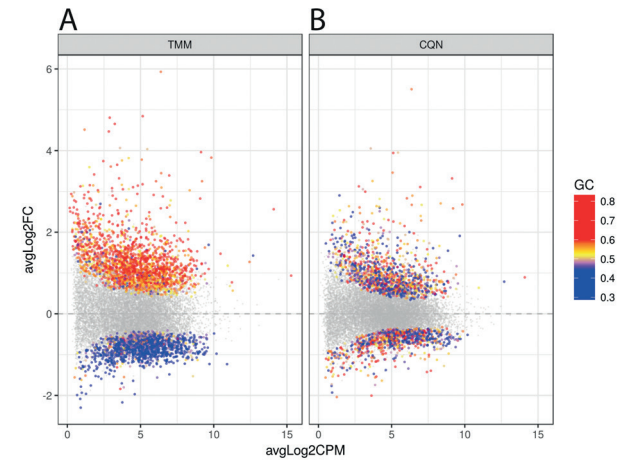


Figure 3: Dot plot of the differentially expressed genes (DEG) in HCHWA-D samples compared to the control samples with log2 fold change (log2FC) versus log2 counts per million (log2CPM) (A) without correction and (B) with CQN correction for GC bias. Significant DEG in both panels are highlighted by colored dots; colors in legend indicates the GC content.

Validation of top up-regulated and down-regulated genes

Five genes from the top DEG (up- and down-regulated) were selected based on FC, FDR and expression level. Three up-regulated genes (*HSPA1A*, *NPTX2* and *PDYN*) and two down-regulated genes (*GPD1* and *CX3CR1*) were validated by qPCR. The trend for up or down-regulation was confirmed, although statistical significance was not reached for every target principally due to high variability in patient samples (Figure 5). Nevertheless, the correlation of gene expression per patient between the count matrix (log2CPM) and the qPCR was highly significant for *NPTX2*, *PDYN* and *GPD1* and significant for *HSPA1* and *CX3CR1* (Datasheet 3_Supplementary Figure 6).

For protein level validation of these five genes, western blots were performed on brain homogenates. HSP70 protein was found to be up-regulated in occipital cortex of HCHWA-D, although the difference was not significant (Figure 6; original picture in Datasheet 3_Supplementary Figure 7).

Pathway analysis

We performed GSEA in Gene Trail2 on gene sets sorted by FC. GSEA tests per category whether the genes in the set are randomly distributed or accumulate at the top (“enriched” pathway) or the bottom (“depleted” pathway) of the sorted input list (14). Accordingly, “depleted” pathways

A

Gene name	Log2FC	adj.P.Val	Full name
DRD5	-2.04	1.058E-05	Dopamine Receptor D5
TMEM125	-2.01	0.008	Transmembrane protein 125
TSPAN8	-1.93	0.012	Tetraspanin 8
LOC101927641	-1.77	0.036	Non coding RNA
CX3CR1	-1.74	0.015	Chemokine (C-X3-C motif) receptor 1
LOC403323	-1.73	0.049	Non coding RNA
DNAH17	-1.64	0.004	Dynein, axonemal, heavy chain 17
SUSD3	-1.56	0.009	Sushi Domain Containing 3
GJB1	-1.56	0.047	Gap junction protein, beta 1, 32kDa
GPIHBP1	-1.54	0.015	Glycosylphosphatidylinositol anchored high density lipoprotein binding protein 1
TYMSOS	-1.54	0.015	TYMS Opposite Strand
NAPSB	-1.52	0.010	Napsin B Aspartic Peptidase, Pseudogene
GPD1	-1.51	0.019	Glycerol-3-phosphate dehydrogenase 1

B

Gene name	Log2FC	adj.P.Val	Full name
HSPA6	5.50	3.19E-06	Heat Shock Protein Family A (Hsp70) Member 6
INHBA	4.05	3.19E-05	Inhibin Beta A Subunit
PDYN	3.95	3.63E-04	Prodynorphin
RRAD	3.94	2.70E-04	Ras-related associated with diabetes
TIMP1	3.46	1.80E-04	TIMP metalloproteinase inhibitor 1
HSPA1A	3.32	1.63E-05	Heat shock 70kDa protein 1A
LINC01164	3.25	1.02E-02	Long Intergenic Non-Protein Coding RNA 1164
SECTM1	3.12	1.22E-02	Secreted And Transmembrane 1
HSPB1	3.11	1.75E-06	Heat shock 27kDa protein 1
CHI3L2	3.05	1.39E-02	Chitinase 3-like 2
SPOCD1	2.99	6.22E-03	SPOC domain containing 1
GNG10	2.90	1.11E-02	Guanine nucleotide binding protein (G protein), gamma 10
BAG3	2.90	8.73E-05	BCL2-associated athanogene 3
SERPINH1	2.83	1.85E-04	Serpin Family H Member 1
SERPINE1	2.82	3.76E-03	Serpin Family E Member 1
DNAJB1	2.71	8.13E-07	DnaJ (Hsp40) homolog
NPTX2	2.68	8.69E-03	Neuronal pentraxin II
LAMB3	2.67	1.14E-02	Laminin, beta 3
VEGFA	2.67	2.54E-07	Vascular endothelial growth factor A
PNOC	2.64	1.48E-02	Prepronociceptin
C7orf61	2.64	1.61E-03	Chromosome 7 open reading frame 61
LOXHD1	2.62	1.48E-03	Lipoxygenase homology domains 1
HSPA7	2.61	2.47E-03	Heat Shock Protein Family A (Hsp70) Member 7
GBP2	2.60	1.46E-04	Guanylate binding protein 2
HSPA1B	2.58	3.53E-04	Heat shock 70kDa protein 1B
ADM	2.56	3.20E-05	Adrenomedullin
C2CD4A	2.54	1.10E-02	C2 Calcium Dependent Domain Containing 4A
ACRC	2.51	1.30E-05	Acidic repeat containing

Figure 4: (A) Top list of down-regulated genes based on fold change (ranking based on $\log_2FC < -1.5$; 13 out of 847 genes shown); (B) Top list of up-regulated genes (ranking based on $\log_2FC > 2.5$; 28 out of 1201 genes shown).

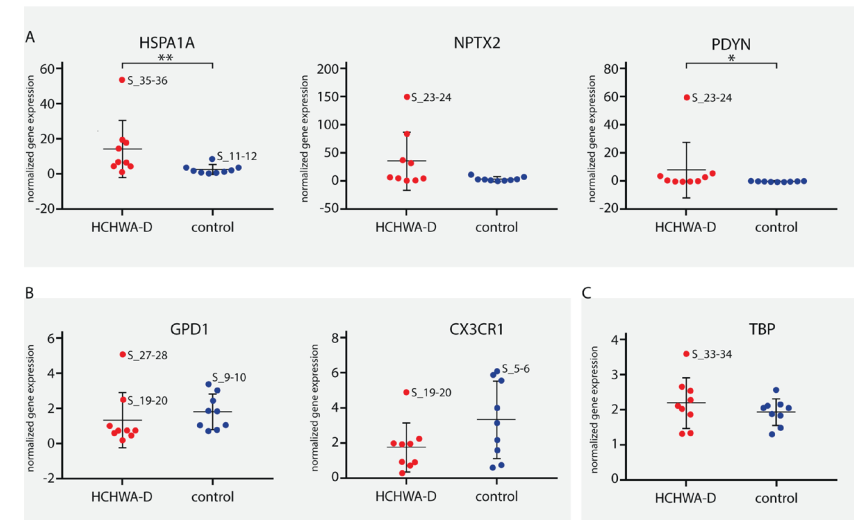


Figure 5: qPCR analysis of (A) 3 up-regulated genes (*HSPA1A*; *NPTX2* and *PDYN*) and (B) 2 down-regulated genes (*GPD1* and *CX3CR1*). Transcript levels of HCHWA-D samples were not following a normal distribution (data not shown). *HSPA1A* and *PDYN* were found significantly up-regulated (MW test, $p=0.006^{**}$ and $p=0.040^{*}$ respectively). For *GPD1* significance was reached upon removal of the greatest outlier (t -test, $p=0.030^{*}$; H3 outlier identified with ROUT method, $Q=1\%$; data not shown), no significant outliers found for *CX3CR1*. Transcript expression levels were normalized with two reference gene, $n=9$. (C) *TBP* normalization control was not significantly different (t -test, $p=0.32$). $^{*}p<0.05$, $^{**}p<0.01$.

are overrepresented by down-regulated genes and ‘‘enriched’’ pathways are overrepresented by up-regulated genes. Although GSEA doesn’t require pre-processed expression data, it has been used on thresholded data, for example to identify robust molecular signatures in tumor diagnosis (15). Similarly, in order to identify predominant pathways and genes dysregulation caused by the APP p.Glu693Gln substitution in HCHWA-D we conducted analysis both on the whole dataset and on the subset of significantly altered genes. Top annotated GO processes were similar in both analyses for the HCHWA-D dataset and for the murine dataset (exhaustive analysis in Datasheet 5_Supplementary Material 2 for genes ranked on FC). The GSEA on genes ranked on FDR is provided in Datasheet 6_Supplementary Material 3. The analysis of the subset of significantly altered genes (ranked on FC) is detailed below.

GSEA on HCHWA-D dataset

GSEA on the significant DEG subset (FDR <0.05; 2036 out of 2048 genes were recognized) was performed. Top annotated GO processes were associated to “depleted” mitochondria-related categories and “enriched” ECM-related categories. Major dysregulated pathways and identified genes in the DEG subset from Reactome and KEGG are summarized in Figure 7A.

Cellular respiration pathways (oxidative phosphorylation and respiratory electron transport) were “depleted” as well as the neurodegenerative diseases pathway in KEGG [Alzheimer disease (AD), Parkinson disease (PD) and Huntington disease (HD)]. As most genes from these pathways overlapped with the cellular respiration (Datasheet 3_Supplementary Figure 8), only the genes non-related to cellular respiration were included in the PD, AD and HD-categories on Figure 7A. Oxidative phosphorylation genes specific for HCHWA-D, i.e. not represented in the other neurodegenerative disease categories were the ATP6V subunits, *COX14*, *COX15*, *LRPPRC* and *TCIRG1*.

ECM-related pathways (ECM-receptor interaction and ECM proteoglycans) were significantly “enriched” pathways. Expression values boxplots (Datasheet 3_Supplementary Figure 9) show that many of these genes follow highly concordant trends. Four clusters were defined based on known interactions between genes in this group (Figure 7B). The main cluster (red) includes *CD44* and multiple collagen genes. *CD44* has direct interactions with the three other clusters: integrins and fibronectin (*FN1*) cluster (yellow), lamininB and SV2 cluster (green), and Transforming Growth Factor Beta (*TGFBI* and *TGFBI2*), Serpin Family E Member 1 (*SERPINE1*

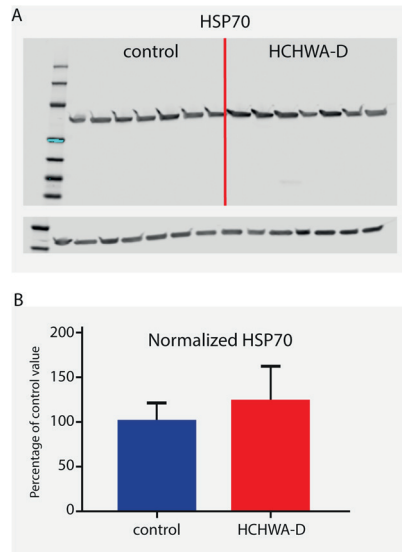


Figure 6: Western blot analysis of HSP70 (antibody detecting *HSPA1A* and *HSPA1B*). (A) Signals given by HSP70 antibody showing a band at 70kDa (with β -actin loading control under main blot). (B) Signal intensity quantification (n=7, β -actin normalized). Higher protein level in HCHWA-D occipital cortex compared to control occipital cortex was measured although not significantly different; $p=0.1888$ with a two-tailed unpaired Student's *t*-test.

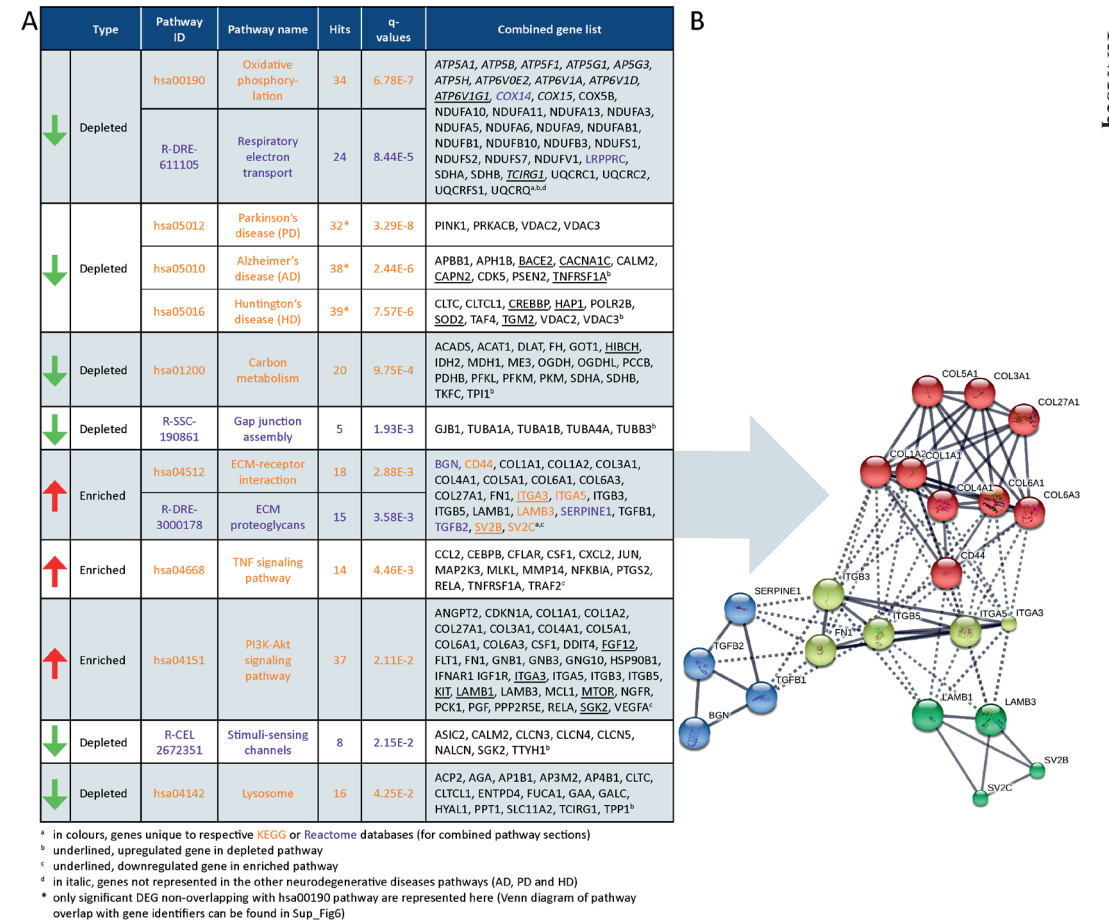


Figure 7: Dysregulated pathways in HCHWA-D. (A) Significantly dysregulated pathways in HCHWA-D DEG subset and associated genes identifiers in GeneTrail2 v1.5 (with fold change input; ranked on statistical significance except for the combined HD, AD and PD categories). Depleted pathways (green arrow) are overrepresented by downregulated genes and enriched pathways (red arrow) are overrepresented by upregulated genes. Text color code distinguish pathways originating from KEGG (orange) or Reactome (purple) databases. (B) Schematic representation of known interactions between genes of the ECM-related pathways. Representation of high confidence interactions with MCL clustering in String interaction database (line thickness indicates the strength of data support).

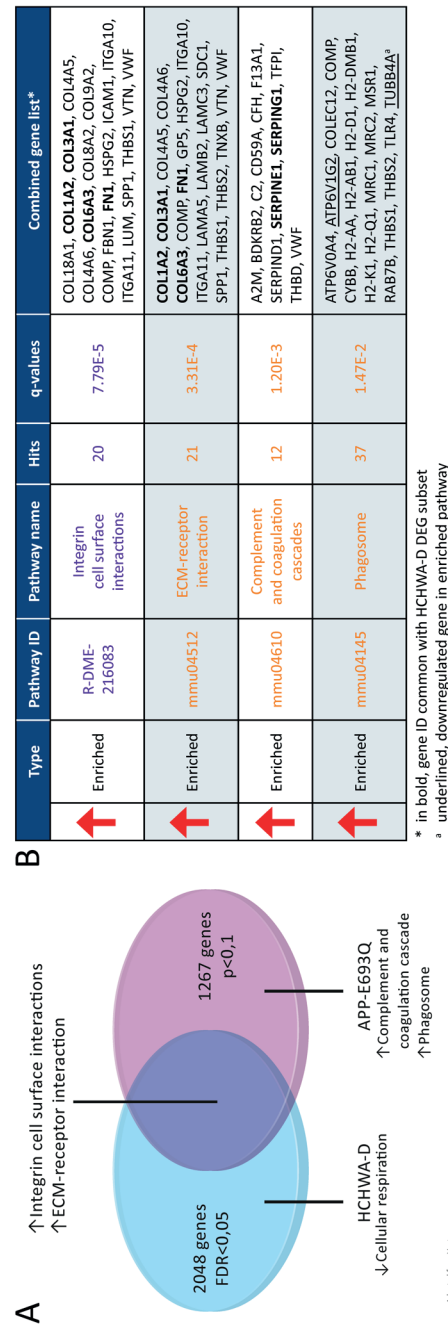


Figure 8: Transcriptome comparison of HCHWA-D and APP-E693Q mouse model (entorhinal cortex; APP-E693Q vs. WT; Readhead et al., 2015). (A) Venn diagram depicting major dysregulations and overlap in enriched pathway. (B) Significantly dysregulated pathways in APP-E693Q DEG subset and associated genes identifiers in GeneTrail2 v1.5 (with fold change input; ranked on statistical significance). Text color code distinguish pathways originating from KEGG (orange) or Reactome (purple) databases.

also known as Plasminogen activator inhibitor-1 or PAI-1) and biglycan (*BGN*) cluster (blue). The integrin and fibronectin group have a central role with interactions with the three other clusters. Additional correlation plots of the gene expression levels per patient between RNA-Seq and qPCR data are given for *TGFBI*, *TGFBR2*, *FNI*, *SERPINE1*, *TIMP-1* and *Col1A1* profibrotic genes (Datasheet 3_Supplementary Figure 10).

GSEA on APP-E693Q dataset and pathways comparison

Murine DEG (entorhinal cortex; APP-E693Q vs. WT (10)) were extracted and GSEA on a DEG subset ($p < 0.1$; 1088 out of 1267 genes were recognized) was performed. A transcriptomic comparison between HCHWA-D patients and APP-E693Q mice at the pathway level is schematically shown in Figure 8A. Major dysregulated pathways and identified genes in the APP-E693Q subset are summarized in Figure 8B.

Discussion

Our study provides a comprehensive transcriptome analysis of human HCHWA-D brain cortex. Using RNA-Seq, we identified oxidative phosphorylation dysfunction and enrichment in ECM-related pathways as major transcriptomic changes in HCHWA-D and we revealed an overlap in affected pathways with the APP-E693Q mouse model.

Homogeneity in gene expression between cortical regions

In the current report, we did not find evidence that frontal and occipital cortex of HCHWA-D were differently affected. This finding is in agreement with our previous study where we found no difference in CAA severity between occipital and frontal lobes, both area being similarly severely affected at pathological examination (5).

RNA quality in HCHWA-D group and corrections

Although the RIN values on average were lower in the HCHWA-D group, we did not observe an effect of the RIN value on the number of reads, and therefore no correction for RIN value was applied. This is supported by a study of human *post mortem* brain *ex vivo* degradation (mimicking PMD) where correcting for RIN value in data analysis did not remove the induced degradation bias (16). Nevertheless, a GC bias positively correlated with the median 5'-3' bias, and affecting the FC after normalization, was corrected. Additionally, GC-content of genes might be associated with RNA decay and genes playing regulatory function were found more unstable (16–18). Alternatively, lower RNA quality was recently associated with dementia

diagnostic (19), also occurring in HCHWA-D (20) (unknown dementia status here). Accordingly, an accelerated RNA degradation in HCHWA-D samples could reflect underlying pathogenesis and brain damage. We are confident that the GC correction rectified possible RNA integrity differences as we found a very high correlation with qPCR on random-primed cDNA, a technique that suffers much less from RNA degradation and GC bias.

Oxidative phosphorylation dysfunction in HCHWA-D

Cellular aerobic respiration, including ATP synthesis and carbon metabolism (TCA cycle, glycolysis/gluconeogenesis) were most significantly altered pathways, dominated by down-regulated genes, which indicates a mitochondrial dysfunction in HCHWA-D.

The mitochondrial respiratory chain complex I (NADH-Ubiquinone) and the ATP synthase complex V (F-type ATPase) were altered pathways in HCHWA-D like in other neurodegenerative diseases (AD, PD and HD). This cellular energy dysfunction is a common denominator in neurodegenerative diseases (21,22). Mostly studied in AD, in the context of neuronal mitochondrial dysfunction (23), oxidative injury has also been studied in endothelial and perivascular cells (24). In particular, *in vitro* studies have shown that especially the Dutch-A β -peptide (A β E22Q), via accelerated generation of toxic oligomeric species, could induce mitochondrial alteration of smooth muscle and endothelial cells, leading to induction of apoptosis (25). Although confirmed in the APP-E693Q mice, the presence of oligomeric A β species in HCHWA-D has not been demonstrated yet.

The vacuolar proton pumps (V-type ATPase), responsible for acidifying the vacuolar system and in particular in the phagosomal/lysosomal vesicles, was also part of the oxidative phosphorylation pathway affected in HCHWA-D (ATP6V subunits and *TCIRG1*). Since vacuolar proton pumps have a high ATP-demand, mitochondrial dysfunction thus could also impacts autophagocytosis and protein turnover, thereby contributing to pathogenic protein accumulation (26).

Enrichment in ECM-related pathways in HCHWA-D

In contrast, genes in the ECM-related pathways were mostly up-regulated in HCHWA-D brain samples. We showed differential expression of *CD44*, a cell-surface glycoprotein that acts as a principal receptor for ECM proteins such as hyaluronic acid, osteopontin, collagens and mediates the cell surface activation of matrix metalloproteinase. *CD44* has been implicated in several inflammatory diseases (27), as well as in AD pathology where an increase in reactive CD44-positive astrocytes was demonstrated (28). In addition, CD44v6 and CD44v10 splice variants were significantly higher in AD hippocampal neurons (29), and in lung fibrosis, CD44v6 is mediating

the induction of *COL1* pro-fibrotic action of TGF β 1 (30). In HCHWA-D, upregulation of *FNI*, *SERPINE1* and collagen genes also suggests TGF β 1-mediated fibrosis, as proposed in our recent study (5). The presence of *TIMP-1* among the top 5 up-regulated genes strengthens this hypothesis. *TIMP-1* is a strong inhibitor of matrix metalloproteinase thereby reducing ECM turnover and exacerbating the fibrosis. Of interest, *FNI*, which was commonly up-regulated in HCHWA-D and APP-E693Q mice, was also found up-regulated in plasma of both asymptomatic HCHWA-D and *PSEN1* mutation carriers (31) and was recently proposed as a blood-based biomarker for AD (32). Additionally, basement membrane thickening of the vessel wall by *FNI* was shown in early stages of AD before A β deposition (33). The use of ECM component detection in plasma, like *FNI*, as biomarkers to monitor early CAA-associated changes in the cerebrovasculature requires further investigation. Of therapeutic relevance, *PSTG2* (COX-2) inhibitor celecoxib was found to lower *FNI* and *COL1* expression and attenuate the vessel wall thickness in stroke-prone spontaneously hypertensive rats (34).

Other identified pathways in HCHWA-D

APP expression was not up-regulated, but some specific APP cleavage enzyme genes were altered, indicating disturbances in APP processing. *APHB1* and *PSEN2*, both functional component of the gamma-secretase complex (cleavage at A β C-terminal side) were down-regulated, possibly also affecting the Notch-signaling. *BACE2* (cleavage at β -site and within A β region), on the other hand was up-regulated. A β production by *BACE2* was increased by the Flemish mutation (p.AlaA692Gly) and *BACE2* is highly expressed in the vasculature (35). These findings are in accordance with earlier studies suggesting that APP-Dutch mutation pathogenic effect was due to an altered APP processing more than a global increase in A β production (36–39).

The inflammation component although not dominating, was represented in the TNF-signaling pathway, TNF being a potent pro-inflammatory cytokine. In particular the leukocytes activation and recruitment genes (*CCL2*, *CXCL2*, *CSF1*) are present and could indicate a vascular inflammation and endothelial cell activation, similarly to AD dysregulation (40). PI3k/Akt signaling, also part of the TNF super-family, is involved in AD affecting endothelial cell viability and angiogenesis (41).

Lastly, the Heat Shock Proteins (HSPs) family was highly represented in the top up-regulated genes, in particular HSP70 (HSPA family). HSP are commonly up-regulated in AD (42) but also in PD, PSP and FTLT-Tau (43). They are central to many mechanisms and likely involved in response to ER stress and protein misfolding but can also have an anti-apoptotic role (via JNK, MAPK, ERK and PARP-1 signaling) and modulate ECM (via focal

adhesion and Akt signaling). Small HSPs (sHSP, HSPB family) contribute to neuropathology by actively triggering inflammatory reactions in AD and in HCHWA-D (44,45). Noticeably the top up-regulated sHSPs in our study HSP27 (*HSPB1*) and α B-crystallin (*CRYAB*), were not associated with CAA in HCHWA-D but were already suggested to be efficient chaperone maintaining the peptide in an oligomeric state not trapped into aggregates (45,46).

Overlap with APP-E693Q mouse model pathways

We compared transcriptome changes in HCHWA-D human brain tissue and the APP-E693Q mouse model in order to isolate mutation-associated primary dysregulation with the mouse model representing an early stage of the disease before CAA appearance, while the human *post mortem* samples are the end stage of the disease. The identified ECM-related pathway overlap is striking.

Genes involved in cellular aerobic respiration were not affected in the transcriptome of 12-month APPE-693Q mice but phagosomal system genes were predominantly up-regulated, possibly indicating an early compensatory mechanism to remove the excess of toxic proteins. Consistently, an age-dependent lysosomal dysfunction was recently described in the APP-E693Q mice, with a higher lysosomal count in the entorhinal cortex of the 12-months mice and autophagosomal/autolysosomal protein level increases only in 24-month old mice, leading to an inflammatory reaction and neuronal loss (47). In HCHWA-D the lysosomal pathway was significantly down-regulated probably representing an end-stage state of the disease.

Although we did not find a significant overlap in the complement and coagulation cascades pathway, *SERPINE1* and *SERPING1* were commonly up-regulated in HCHWA-D and APP-E693Q indicating an early altered balance between thrombosis and fibrinolysis. *SERPING1* (C1-inhibitor) is controlling complement activation, blood coagulation, fibrinolysis and generation of kinins. C1-inhibitors are neuroprotective after ischemic stroke (48) and traumatic brain injury (49) via important anti-inflammatory and antithrombotic mechanisms. On the other hand, *SERPINE1* plays a major role in pro-thrombotic conditions, regulating tissue-type plasminogen activator (tPA) and urokinase-type plasminogen activator (uPA) activity. *SERPINE1* gene expression was found up-regulated in AD brain (7) as well and could be a plasmatic biomarker for the early detection and diagnosis of AD (50).

To conclude, an increase in ECM-related pathways was identified in HCHWA-D and could be, based on the APP-E693Q mice, involved in an early dysregulation inducing pro-fibrotic mechanisms. The mitochondrial dysfunction in HCHWA-D might be a consequence of impaired lysosomal/phagosomal function, in link with the proteinopathies. Alternatively, the

formation of toxic oligomeric A β species described in the APP-E693Q mice could trigger oxidative stress affecting the mitochondrial compartment. The formation of toxic oligomeric A β species in HCHWA-D and their role of oxidative stress on neuronal, vascular and perivascular cell, would require further investigations.

Conflict of interest

The authors declare no conflict of interest.

Author Contributions

LGM,WR, LW, SK, HM, HB and JL designed the experiments. LGM, LVG and EM performed the experiments. HB supervised the sequencing. HM and SK processed, controlled and generated the datasets. LGM interpreted the datasets and wrote the manuscript. WR and LW supervised and co-wrote the manuscript. KH, SD, MB, PH and SM critically revised the manuscript. All authors contributed to manuscript revision, read and approved the submitted version.

Funding

This work was supported by the Bontius stichting (Leiden, The Netherlands), the Dutch CAA foundation (Rotterdam, The Netherlands) and by the Netherlands Organization for Scientific Research (NWO, The Hague, The Netherlands), under research program VIDI, project ‘‘Amyloid and vessels’’, number 864.13.014.

Acknowledgements

The authors thank the Netherlands Brain Bank (Amsterdam, The Netherlands) for supplying brain tissue.

Supplementary Material

The Supplementary Material for this article can be found online at: <https://www.frontiersin.org/articles/10.3389/fnagi.2018.00102/full#supplementary-material>

Data availability

Sequence data and count table generated during the current study have been deposited at the European genome-phenome Archive (EGA, <http://www.ebi.ac.uk/ega/>) which is hosted at the European Bioinformatics Institute (EBI) under EGA accession number EGAD00001003806. Data are available upon approval of the Data Access Committees (EGAC00001000771).

References

- Kamp JA, Grand Moursel L, Haan J, Terwindt GM, Lesnik Oberstein SAMJ, van Duinen SG, et al. Amyloid β in hereditary cerebral hemorrhage with amyloidosis-Dutch type. *Rev Neurosci*. 2014 May 28;25(5):641–51.
- van Horssen J, Otte-Holler I, David G, Maat-Schieman ML, van den Heuvel LP, Wesseling P, et al. Heparan sulfate proteoglycan expression in cerebrovascular amyloid deposits in Alzheimer's disease and hereditary cerebral hemorrhage with amyloidosis (Dutch) brains. *Acta Neuropathol*. 2001 Dec;102(6):604–14.
- Wilhelmus MMM, Bol JGJM, van Duinen SG, Drukarch B. Extracellular matrix modulator lysyl oxidase colocalizes with amyloid-beta pathology in Alzheimer's disease and hereditary cerebral hemorrhage with amyloidosis-Dutch type. *Exp Gerontol*. 2013 Feb;48(2):109–14.
- De Jager M, van der Wildt B, Schul E, Bol JGJM, van Duinen SG, Drukarch B, et al. Tissue transglutaminase colocalizes with extracellular matrix proteins in cerebral amyloid angiopathy. *Neurobiol Aging*. 2013 Apr;34(4):1159–69.
- Grand Moursel L, Munting LP, van der Graaf LM, van Duinen SG, Goumans M-JTH, Ueberham U, et al. TGFbeta pathway deregulation and abnormal phospho-SMAD2/3 staining in hereditary cerebral hemorrhage with amyloidosis-Dutch type. *Brain Pathol*. 2017;1–12.
- Kavanagh T, Mills JD, Kim WS, Halliday GM, Janitz M. Pathway analysis of the human brain transcriptome in disease. *J Mol Neurosci*. 2013;51(1):28–36.
- Magistri M, Velmesshev D, Makhmutova M, Faghihi MA. Transcriptomics Profiling of Alzheimer's Disease Reveal Neurovascular Defects, Altered Amyloid- β Homeostasis, and Deregulated Expression of Long Noncoding RNAs. *J Alzheimer's Dis*. 2015;48(3):647–65.
- Mills JD, Nalpathamkalam T, Jacobs HIL, Janitz C, Merico D, Hu P, et al. RNA-Seq analysis of the parietal cortex in Alzheimer's disease reveals alternatively spliced isoforms related to lipid metabolism. *Neurosci Lett*. 2013;536(1):90–5.
- Twine NA, Janitz K, Wilkins MR, Janitz M. Whole Transcriptome Sequencing Reveals Gene Expression and Splicing Differences in Brain Regions Affected by Alzheimer's Disease. Preiss T, editor. Vol. 6, PLoS ONE. San Francisco, USA; 2011.
- Readhead B, Haure-Mirande J-V, Zhang B, Haroutunian V, Gandy S, Schadt EE, et al. Molecular systems evaluation of oligomerogenic APPE693Q and fibrillogenic APPKM670/671NL/PSEN1 Δ exon9 mouse models identifies shared features with human Alzheimer's brain molecular pathology. *Mol Psychiatry*. 2015 Aug;21(August):1–13.
- Maat-schieman M, Roos R, Duinen S Van, van Duinen S. Review Article Hereditary cerebral hemorrhage with amyloidosis- Dutch type. *Neuropathology*. 2005 Dec;25(February):288–97.
- Parkhomchuk D, Borodina T, Amstislavskiy V, Banaru M, Hallen L, Krobitch S, et al. Transcriptome analysis by strand-specific sequencing of complementary DNA. *Nucleic Acids Res*. 2009 Oct;37(18):e123.
- Stöckel D, Kehl T, Trampert P, Schneider L, Backes C, Ludwig N, et al. Multi-omics enrichment analysis using the GeneTrail2 web service. *Bioinformatics*. 2016;32(10):1502–8.
- Backes C, Keller A, Kuentzer J, Kneissl B, Comtesse N, Elnakady YA, et al. GeneTrail-advanced gene set enrichment analysis. *Nucleic Acids Res*. 2007;35(SUPPL.2):186–92.
- Monti S, Monti S, Savage KJ, Savage KJ, Kutok JL, Kutok JL, et al. Molecular profiling of diffuse large B-cell lymphoma identifies robust subtypes including one characterized by host inflammatory response. *Response*. 2005;105(5):1851–61.
- Jaffe AE, Tao R, Norris A, Kealhofer M, Nellore A, Jia Y, et al. A framework for RNA quality correction in differential expression analysis. *Hear Lung*. 2016;114(27):1–26.
- Feng H, Zhang X, Zhang C. mRIN for direct assessment of genome-wide and gene-specific mRNA integrity from large-scale RNA-sequencing data. *Nat Commun*. 2015;6(May):7816.
- Gallego Romero I, Pai A a, Tung J, Gilad Y. RNA-seq: impact of RNA degradation on transcript quantification. *BMC Biol*. 2014;12(1):42.
- Miller JA, Guillozet-Bongaarts A, Gibbons LE, Postupna N, Renz A, Beller AE, et al. Neuropathological and transcriptomic characteristics of the aged brain. Nelson SB, editor. *Elife*. 2017;6:e31126.
- Wattendorff AR, Frangione B, Luyendijk W, Bots GT, Wattendorff, Frangione, et al. Hereditary cerebral haemorrhage with amyloidosis, Dutch type (HCHWA-D): clinicopathological studies. *J Neurol Neurosurg Psychiatry*. 1995 Aug;58(6):699–705.
- Lin MT, Beal MF. Mitochondrial dysfunction and oxidative stress in neurodegenerative diseases. *Nature*. 2006 Oct;443(7113):787–95.
- Golpich M, Amini E, Mohamed Z, Azman Ali R, Mohamed Ibrahim N, Ahmadiani A. Mitochondrial Dysfunction and Biogenesis in Neurodegenerative diseases: Pathogenesis and Treatment. *CNS Neurosci Ther*. 2017;23(1):5–22.
- Costa RO, Ferreira E, Martins I, Santana I, Cardoso SM, Oliveira CR, et al. Amyloid beta-induced ER stress is enhanced under mitochondrial dysfunction conditions. *Neurobiol Aging*. 2012 Apr;33(4):824.e5-16.
- Di Marco LY, Venneri A, Farkas E, Evans PC, Marzo A, Frangi AF. Vascular dysfunction in the pathogenesis of Alzheimer's disease - A review of endothelium-mediated mechanisms and ensuing vicious circles. *Neurobiol Dis*. 2015;82:593–606.
- Ghiso J, Fossati S, Rostagno A. Amyloidosis Associated with Cerebral Amyloid Angiopathy: Cell Signaling Pathways Elicited in Cerebral Endothelial Cells. *J Alzheimers Dis*. 2014;42(03):S167-76.
- Ganguly G, Chakrabarti S, Chatterjee U, Saso L. Proteinopathy, oxidative stress and mitochondrial dysfunction: cross talk in Alzheimer's disease and Parkinson's disease. *Drug Des Devel Ther*. 2017;11:797–810.
- Misra S, Hascall VC, Markwald RR, Ghatak S. Interactions between Hyaluronan and Its Receptors (CD44, RHAMM) Regulate the Activities of Inflammation and Cancer. *Front Immunol*. 2015;6:201.
- Akiyama H, Tooyama I, Kawamata T, Ikeda K, McGeer PL. Morphological diversities of CD44 positive astrocytes in the cerebral cortex of normal subjects and patients with Alzheimer's disease. *Brain Res*. 1993;632:249–59.
- Pinner E, Gruper Y, Ben Zimra M, Kristt D, Laudon M, Naor D, et al. CD44 Splice Variants as Potential Players in Alzheimer's Disease Pathology. *J Alzheimer's Dis*. 2017;58(4):1137–49.
- Ghatak S, Bogatkevich GS, Atnelishvili I, Akter T, Feghali-Bostwick C, Hoffman S, et al. Overexpression of c-Met and CD44v6 receptors contributes to autocrine TGF-beta1 signaling in interstitial lung disease. *J Biol Chem*. 2014 Mar;289(11):7856–72.

31. Muenchhoff J, Poljak A, Thalamuthu A, Gupta VB, Chatterjee P, Raftery M, et al. Changes in the plasma proteome at asymptomatic and symptomatic stages of autosomal dominant Alzheimer's disease. *Sci Rep.* 2016;6(July):1–11.
32. Long J, Pan G, Ifeachor E, Belshaw R, Li X. Discovery of Novel Biomarkers for Alzheimer's Disease from Blood. *Dis Markers.* 2016;2016:4250480.
33. Lepelletier F-XF-X, Mann DMA, Robinson AC, Pinteaux E, Boutin H. Early changes in extracellular matrix in Alzheimer's disease. *Neuropathol Appl Neurobiol.* 2015 Feb;43(2):167–82.
34. Tang J, Xiao W, Li Q, Deng Q, Chu X, Chen Y, et al. A Cyclooxygenase-2 Inhibitor Reduces Vascular Wall Thickness and Ameliorates Cognitive Impairment in a Cerebral Small Vessel Diseases Rat Model. Vol. 12, *Current Alzheimer Research.* 2015. p. 704–10.
35. Farzan M, Schnitzler CE, Vasilieva N, Leung D, Choe H. BACE2, a beta -secretase homolog, cleaves at the beta site and within the amyloid-beta region of the amyloid-beta precursor protein. *Proc Natl Acad Sci U S A.* 2000;97(17):9712–7.
36. De Jonghe C, Zehr C, Yager D, Prada CM, Younkin S, Hendriks L, et al. Flemish and Dutch mutations in amyloid beta precursor protein have different effects on amyloid beta secretion. *Neurobiol Dis.* 1998 Oct;5(4):281–6.
37. Herzig MC, Winkler DT, Burgermeister P, Pfeifer M, Kohler E, Schmidt SD, et al. Abeta is targeted to the vasculature in a mouse model of hereditary cerebral hemorrhage with amyloidosis. *Nat Neurosci.* 2004 Oct;7(9):954–60.
38. Nilsberth C, Westlind-Danielsson a, Eckman CB, Condron MM, Axelman K, Forsell C, et al. The “Arctic” APP mutation (E693G) causes Alzheimer's disease by enhanced Abeta protofibril formation. *Nat Neurosci.* 2001;4(9):887–93.
39. Watson DJ, Selkoe DJ, Teplow DB. Effects of the amyloid precursor protein Glu693 →Gln ‘Dutch’ mutation on the production and stability of amyloid β-protein. 1999;709:703–9.
40. Grammas P, Ovase R. Inflammatory factors are elevated in brain microvessels in Alzheimer's disease. *Neurobiol Aging.* 2001;22(6):837–42.
41. Grammas P, Sanchez A, Tripathy D, Luo E, Martinez J. Vascular signaling abnormalities in Alzheimer disease. *Cleve Clin J Med.* 2011 Aug;78 Suppl 1:S50-3.
42. Koren J, Jinwal UK, Lee DC, Jones JR, Shults CL, Johnson AG, et al. Chaperone signalling complexes in Alzheimer's disease. *J Cell Mol Med.* 2009;13(4):619–30.
43. Milanesi E, Pilotto A. Microarray Gene and miRNA Expression Studies: Looking for New Therapeutic Targets for Frontotemporal Lobar Degeneration. *Drug Dev Res.* 2014;75(6):366–71.
44. Wilhelmus MMM, Boelens WC, Otte-Höller I, Kamps B, Kusters B, Maat-Schieman MLC, et al. Small heat shock protein HspB8: its distribution in Alzheimer's disease brains and its inhibition of amyloid-beta protein aggregation and cerebrovascular amyloid-beta toxicity. *Acta Neuropathol.* 2006 Feb;111(2):139–49.
45. Wilhelmus MMM, Boelens WC, Kox M, Maat-Schieman MLC, Veerhuis R, de Waal RMW, et al. Small heat shock proteins associated with cerebral amyloid angiopathy of hereditary cerebral hemorrhage with amyloidosis (Dutch type) induce interleukin-6 secretion. *Neurobiol Aging.* 2009 Feb;30(2):229–40.
46. Wilhelmus MMM, Boelens WC, Otte-Höller I, Kamps B, de Waal RMW, Verbeek MM. Small heat shock proteins inhibit amyloid-beta protein aggregation and cerebrovascular amyloid-beta protein toxicity. *Brain Res.* 2006 May 17;1089(1):67–78.
47. Kaur G, Pawlik M, Gandy SE, Ehrlich ME, Smiley JF, Levy E, et al. Lysosomal dysfunction in the brain of a mouse model with intraneuronal accumulation of carboxyl terminal fragments of the amyloid precursor protein. *Mol Psychiatry.* 2017 Jul;22(7):981–9.
48. Heydenreich N, Nolte MW, Gob E, Langhauser F, Hofmeister M, Kraft P, et al. C1-inhibitor protects from brain ischemia-reperfusion injury by combined antiinflammatory and antithrombotic mechanisms. *Stroke.* 2012 Sep;43(9):2457–67.
49. Albert-Weissenberger C, Mencl S, Schuhmann MK, Salur I, Göb E, Langhauser F, et al. C1-Inhibitor protects from focal brain trauma in a cortical cryolesion mice model by reducing thrombo-inflammation. Vol. 8, *Frontiers in Cellular Neuroscience.* 2014. p. 8–269.
50. Oh J, Lee H-J, Song J-H, Park SI, Kim H. Plasminogen activator inhibitor-1 as an early potential diagnostic marker for Alzheimer's disease. *Exp Gerontol.* 2014;60:87–91.

Chapter 7

Discussion

Aim of the study & central findings

The general aim of this thesis was to decipher the molecular pathogenesis of HCHWA-D. Since no proven therapeutic treatment exists to prevent or even delay the disease onset, the understanding of underlying pathomechanisms in HCHWA-D is important. It may help discovering new therapeutic targets and biomarkers that can be used to assess the efficacy of candidate drugs in treatment trials.

The main finding of the work presented in this thesis is that TGF β deregulation plays a central role in HCHWA-D pathology. This deregulation is demonstrated using HCHWA-D brain material. At the gene expression level, on individual genes, TGF β 1, its receptors and TGF β -induced genes are upregulated (chapter 3). At the pathway level, in the transcriptomic study, extracellular matrix (ECM)-pathways related to TGF β are increased (chapter 6). Lastly at the protein level using histology, we showed the actual activation of the TGF β signaling cascade. First by showing the accumulation of its activated transcription factor (pSMAD2/3; chapter 3) in some angiopathic vessels, then by identifying the presence of the pro-fibrotic collagen 1 (col1) protein, a major TGF β -induced genes, in amyloid-laden vessels (chapter 5). By selecting patients at different disease stages, we discovered that pSMAD2/3 and col1 accumulation in angiopathic vessel walls are correlated with CAA load (chapter 3 & 5).

We show that TGF β deregulation correlates with disease severity. However, disease severity in HCHWA-D is also characterized by the higher occurrence of secondary remodelling of angiopathic vessels (1). In an initial study, we identified vascular calcifications, a specific secondary vascular remodelling, to be the cause of a recently described neuroimaging feature of advanced disease stage in HCHWA-D (2). In the subsequent study, we assessed the presence of osteopontin (OPN) in these calcifications, as described in other non-A β related vasculopathies in link with TGF β increase (3). We further discovered a topographical association of pSMAD2/3 and OPN in these calcifications and we also linked their gradual accumulation with the calcification process (chapter 5).

Study of pathomechanisms in human brain tissue material

Advantages & Difficulties

The use of human brain material is undeniably a unique chance to study pathomechanisms in relevant tissue and has a high scientific value. Using patient tissue gives access to the whole complexity of the disease in comparison to pathological processes *in vitro* which lack the cellular and physiological context or *in vivo* studies in animal model which cannot fully recapitulate human brain diseases.

Despite these advantages, patient brain material is underused in research mostly because its utilization remains challenging (4). The principal drawback is the heterogeneity of samples due to individual differences (age, gender, health, body mass, life style), prior medication exposure and additional co-morbidities, which are confounding factors. Secondly, for gene expression analysis, the RNA quality is variable, mostly due to the circumstances of death (agonal stress, (5)) but other factors such as postmortem interval, dissection protocols and storage conditions can influence the RNA integrity as well. Because the RNA quality is generally lower than for RNA isolated from cell cultures or animal models, it requires testing and optimisation of standard procedures, as discussed in chapter 6. Thirdly, the material is scarce, which might be restrictive in experimental design. Lastly, postmortem human tissue reflects the end-stage of the disease and therefore cannot replace cellular and animal research models where early events in illness can be studied.

Frontal versus occipital pathology in HCHWA-D

Previous CAA neuropathological studies suggested that CAA pathology was more prominent in the occipital lobes than in the frontal lobes (chapter 1). We studied these two areas as they were presumed to represent different disease stages. Some histopathological findings (other than β -amyloid vascular accumulation) were indeed more prominent occipitally. We discovered both perivascular ring of pSMAD2/3 granules (chapter 3) and cortical calcifications of angiopathic vessels (which are a very advanced disease stage) predominantly occipitally (chapter 4), although a direct link between these two findings remain to be demonstrated. However, at the transcriptomic level, we did not find evidence that frontal and occipital cortexes of HCHWA-D were differently affected (chapter 6). Also the amount of angiopathic vessels showed no significant difference between the frontal and the occipital cortex (chapter 3). Nevertheless, one finding of this thesis is that the study of patients with different disease stages is more informative of pathomechanisms than the study of different brain areas.

The correlation of the different CAA load with pSMAD2/3 accumulation independently of the brain area, revealed TGF β -related pathomechanisms (chapter 3).

- Pathological disease severity in HCHWA-D is comprised of CAA load plus additional secondary vascular remodeling
- Gene expression in frontal and occipital cortex is similar but secondary vessel pathology showed more perivascular changes and vascular calcifications occipitally

Consequences of TGF β activation

TGF β s are pleiotropic cytokines involved in a variety of biological effects, modulating ECM metabolism, cell cycle as well as immune response (6). Transgenic mice overexpressing TGF β 1 in brain cells have been extensively studied to understand the influence of this cytokine on the vasculature, on neuroinflammation and on A β deposition (7,8). Results of this thesis, in light of knowledge from previous neuropathological and transgenic mice studies, further implicate TGF β in HCHWA-D phenotypic variability.

Effects of TGF β on the cerebrovasculature

Cerebrovascular fibrosis

The pathogenesis of cerebrovascular fibrosis has been studied in mouse model overexpressing TGF β 1 in astrocytes (GFAP-TGF β 1, (9)). It starts by a perivascular astrogliosis inducing an early thickening of vascular basement membranes (3-4 months) by ECM proteins, followed by the deposition of amyloid fibrils by 6 months of age. When these mice are crossed with mice overexpressing human APP (hAPP) in neurons (GFAP-TGF β 1/PDGF-hAPP), amyloid vascular deposits are detected even earlier (2-3 months). Remarkably, another mouse model with a neuron-specific TGF β 1 inducible overexpression, develop a similar angiopathic phenotype via induction of perivascular astrogliosis, confirming that astrocytes are major player in the cerebrovascular fibrosis (10).

Prior studies in HCHWA-D also described perivascular astrogliosis associated with arteriolar CAA (11) and perivascular ECM remodelling (12,13). Although the chronology of events is unknown, based on animal model studies, a TGF β 1-mediated fibrosis, preceding and triggering the CAA pathology might be an early event in HCHWA-D patients as well.

Accordingly, our transcriptomic study suggests an early TGF β 1-mediated fibrosis. By comparing the human transcriptome with the transcriptome of young APP-E693Q mice at the pathway level, we could identify an overlap

in the upregulation of ECM-related pathways, which is in mice prior to the onset of CAA pathology (chapter 6). Moreover, we confirmed in patient material the increase of TGF β -induced pro-fibrotic target genes such as plasminogen activator inhibitor-1 (PAI-1), fibronectin (FN1) and collagen (Type I Col1A1 and Type III Col3A1; chapter 3). We further proposed that the accumulation of Col1 protein in the vessel walls might be prior to amyloid deposition (chapter 5), suggesting a TGF β 1-mediated fibrosis triggering the CAA pathology.

Secondary vascular remodelling

Prolonged TGF β 1 overexpression in astrocytic-TGF β 1 mice results in degenerative changes in microvascular cells (at 9-18 month) and cerebral microhemorrhages at older age (18-24 month). Our results show that TGF β deregulation correlates with disease severity. As most severe cases are in general the oldest patients, it suggests that also in patients TGF β activation is prolonged, and is likely modulating the CAA pathology. The most severe cases also present with secondary vascular remodeling such as vascular calcifications studied in this thesis. Interestingly, in the neuronal-TGF β 1 mice, a microarray analysis of cortical gene expression showed upregulation of OPN as well as various genes also involved in tissue mineralization and vascular calcification, strengthening the influence of TGF β 1 on this type of vasculopathy.

Effect of TGF β on microglia / macrophages phenotype

TGF β is also a major player in the inflammatory phenotype of brain microglia and macrophages. The inflammatory response can present either two or three states: a pro-inflammatory state (M1) and a repair/resolution state (M2), which is sometimes subdivided into an alternative inflammation state (phagocytic, fibrotic) or an acquired deactivation state (immunosuppressive) (14). The M2 state is associated with, and induced by, a TGF β 1 increase (15). Although not extensively studied in this thesis, the immune response in HCHWA-D is thought to be influenced by TGF β 1 upregulation and to modulate the phenotype.

TGF β -promoted parenchymal clearance of A β by microglia activation is a probable underlying mechanism in HCHWA-D. Previous neuropathological studies in HCHWA-D described a tendency for a disappearance of parenchymal amyloid plaques with age (16) and identified microglial phagocytosis of non-fibrillar A β (11). In APP-overexpressing mice, in parallel to the increase of CAA pathology, additional TGF β 1 overexpression resulted in a microglial activation promoting the clearance of A β and reducing the amount of A β parenchymal plaques. It is suggested that TGF β 1 induces microglial phagocytosis (8) which is characteristic of M2 inflammatory

state. In HCHWA-D patients, typical M2 genes *Sphk1*, *TGFβ1* and *HO-1* (acquired deactivation) together with chitinase-Like Proteins genes *CHI3L2* and *CHI3L1* (alternative inflammatory, (14)) were significantly increased in our RNAseq study (chapter 6, supplementary tables).

Lastly, inflammatory CAA can also be induced by *TGFβ* pathway activation. Inflammatory CAA is characterized by the infiltration of macrophages and other blood-derived immune cells around and/or within the vessel walls of CAA-affected blood vessels. Perivascular macrophages have a function in the regulation of CAA (17) and *TGFβ1* is a central player in the modulation of the phenotype and brain infiltration of macrophages. Indeed, in APP and *TGFβ1*-overexpressing mice, induction of inflammatory CAA via activation of macrophages reduces the CAA pathology and is thus considered as beneficial (18,19). At histopathological examination, inflammatory CAA is common in HCHWA-D and is more frequently detected in patients with the most severe phenotype (20). Whether inflammatory CAA is beneficial or detrimental to the patients is a matter of debate. Although it is associated with diverse vasculopathies and increased risk of dementia (16), patients with inflammatory CAA survive on average longer and have smaller non-fatal hemorrhages (M. Maat Schieman, unpublished work). In conclusion, the exact contribution of these immune cells to the CAA pathology is unclear, limited to animal models studies and requires further investigations.

- The *TGFβ* pathway is activated in HCHWA-D, and contributes to the phenotypic variability
- *TGFβ* chronic overexpression aggravates the vascular fibrosis, is associated with the CAA pathology severity and might promote vascular calcification

Possible causes of *TGFβ* activation in HCHWA-D

TGFβ in the central nervous system (CNS) is induced upon injuries as part of the healing process. Independently of stroke-related brain injuries, we discuss below potential early *TGFβ* induction in HCHWA-D triggered by cellular stress or interference with *TGFβ* related processes.

Early response to cellular toxicity

Oligomeric *Aβ* species (o*Aβ*s) have been extensively studied and are the most toxic of the *Aβ* species accumulating in AD and in APP-overexpressing animal models. o*Aβ* are potent neurotoxins inducing a wide range of cellular

dysfunctions (oxidative and ER stress, calcium dyshomeostasis, cell cycle re-entry, mitochondrial dysfunction) as well as neurodegenerative reactions (21,22).

A higher stability of o*Aβ*s due to the E22Q mutation (chapter 1) have been predicted *in silico* (23), demonstrated *in vitro* (24–26) and further found *in vivo*, in APP-E693Q mice (27). In APP-E693Δ mice, a closely related animal model with a lack of glutamate at position 22 of *Aβ*, intraneuronal o*Aβ*s lead to mitochondrial dysfunction (28). Even though the actual existence of o*Aβ*s has never been proven in patients, we also found a mitochondrial dysfunction in our HCHWA-D transcriptomic study (chapter 6) indicating cellular stress, possibly triggered by toxic oligomeric species.

While less investigated, o*Aβ*s can elicit a stress response in other cell types than neurons. Particularly, endothelial cells (ECs) *in vitro* are highly susceptible to Dutch o*Aβ* peptide (29) and endothelial injuries lead to a CAA phenotype associated with *TGFβ1* upregulation (30). Nevertheless Dutch o*Aβ* addition to ECs in monoculture leads to a decrease in *TGFβ1* (31,32), and it is likely that the *TGFβ* response observed *in vivo* mostly comes from other cell type such as glial cells (33). Especially reactive astrocytes are susceptible to o*Aβ*s toxic species and can induce a neuroprotective *TGFβ* response. A recent study revealed that o*Aβ* can activate astrocytes; astrocyte-derived *TGFβ1* prevents synapse loss induced by o*Aβ* in AD mice (34). Such a protective astrocytic reaction to limit the level of neurotoxic soluble o*Aβ* was also suggested to occur in HCHWA-D (11).

Direct interferences with *TGFβ* activity

Finally, the Dutch mutation could directly interfere with *TGFβ*-related processes.

TGFβ1 co-aggregates with amyloid parenchymal plaques in AD and Down Syndrome, suggesting a neuroprotective *Aβ* sequestration (35). It was demonstrated that *Aβ* can bind to *TGFβ* (36) and to *TGFβ* receptors (*TGFβR*) (37). Although the effect of the Dutch *Aβ* peptide on the interaction with *TGFβ* is unknown, the FAQD Dutch *Aβ* motif was predicted to influence the *Aβ* binding to *TGFβ* receptors, meaning a putative direct interference with the signalling pathway.

Furthermore, Amyloid Precursor Protein (APP) and *TGFβ1* play a role in the coagulation cascade. APP is able to form complex with coagulation factors *in vivo*, and in blood of HCHWA-D patients the complex APP-factors XIa was slightly increased (38). Although the exact impact of the Dutch mutation on the coagulation cascade remains to be explored, APP is accumulating in HCHWA-D vascular amyloid (39) and might be blood-derived from platelets, which are rich in APP proteins. In transgenic CAA mouse models, platelet recruitment to vascular amyloid is prolonged (in

APP23 and APP Dutch mice (40)). Since TGF β 1 is also stored in large amount in platelets and Col1 particularly can induce platelet exocytosis (41), the presence of vascular Col1 in HCHWA-D (chapter 5) might enhance platelet recruitment and exocytosis, thereby providing local higher TGF β 1 and APP concentrations and further aggravating (or even initiating) the CAA pathology.

- Pathomechanisms such as enhanced formation of oA β , endothelial injuries or coagulation disorders could enhance endogenous TGF β response before stroke onset

Future perspectives

Pathomechanisms in HCHWA-D

A major question raised by this work is whether the Dutch mutation itself triggers an endogenous TGF β increase.

As described above, TGF β 1 cerebral overexpression in AD mice induces a CAA pathology increase and a parenchymal amyloid reduction. Intriguingly, a CAA phenotype is consistently induced in transgenic animals upon insertion of Dutch mutation in the APP sequence (APP Dutch (42), APP Dutch/ APP23 (43); APP Dutch/BACE1 (44); APP-E693Q/PS1 Δ exon9 (27); Knock-In model APP DSL (45)). TGF β 1 levels in those models would be interesting to measure in order to know whether the insertion of the Dutch mutation leads to an endogenous TGF β 1 increase as proposed in this thesis.

The direct effect of the Dutch A β peptide on TGF β -related mechanisms could be further tested experimentally. As described in this chapter, some biological processes might only be triggered by specific A β species such as oA β s. Obtaining specific A β species *in vitro* using synthetic A β is problematic because A β peptide is highly unstable (personal observations). Instead, endogenous A β produced by iPS patient-derived cells, combined with recent progress in organoids or organ-on-chip technologies, opens new possibilities. Once established, an endogenous TGF β increase, for example, in patient-derived astrocyte/neuronal cocultures would be an interesting phenotype for further studies into pathomechanisms or therapeutic targets.

Biomarkers of cerebrovascular fibrosis

New biomarkers of CAA pathology in blood and cerebrospinal fluid (CSF) would be highly valuable to detect the disease onset, improve the clinical diagnosis and understand underlying pathomechanisms.

Results from this thesis suggest that biomarkers of cerebrovascular fibrosis such as direct measure of TGF β levels or detection of downstream pro-fibrotic components (such as FN1, Serpine1 and OPN) could be of interest. Brain TGF β levels in asymptomatic mutation carriers and in post-stroke patients have not been determined to date. In mutation carriers, detection of TGF β levels might indicate the onset of brain injuries (see **Graphic summary**) and help in defining windows for therapeutic intervention. For clinical practice, biomarkers of cerebrovascular fibrosis could help to estimate disease severity and progression. Finally, monitoring such biomarkers in therapeutic intervention studies will add insight into safety, effect and effectiveness of drugs in clinical trials.

Developing biomarkers of cerebrovascular fibrosis would help to better estimate the onset and progression of CAA pathology in HCHWA-D but also in other CAA-related vasculopathy and small vessel diseases where TGF β plays a central role as well (46,47).

- Developing biomarkers of cerebrovascular fibrosis will help understanding the disease in its initial phase, improving diagnostic tools and defining the best therapeutic strategies for HCHWA-D
- Such biomarkers are of interest for other CAA pathologies

Therapeutics intervention

TGF β lowering therapies

TGF β pathway is a double-edged sword

TGF- β is key in tissue homeostasis and disruption of the TGF β pathway has been implicated in numerous human diseases. Activation of the TGF β pathway in systemic diseases (such as atherosclerosis) has beneficial anti-inflammatory properties as well as detrimental profibrotic effects. Similar dual effects have been observed in the CNS. In animal models, TGF β 1 increase is neuroprotective, especially acutely after injury (48–51). However, chronically high levels cause extensive cerebrovascular fibrosis as described in this thesis.

Considerations with TGF β lowering therapies

Given the short-term beneficial effect of TGF β on neuroprotection, TGF β lowering therapies should be considered with care. *In vivo* pharmacological tuning of TGF β in APP mice is feasible (52–54). In symptomatic patients, monitoring intracerebral TGF β to prevent high chronic levels could be beneficial. Indeed patients suffering from recurrent strokes most probably have higher TGF β levels than pre-symptomatic mutation carriers. In the

context of stroke, acute TGF β upregulation restricts the infarct size in mouse models (49,55). However, in ageing animals, the TGF β response is stronger and last longer (56,57) resulting in more long-term detrimental effects. Maintaining TGF β levels within a certain range might therefore slow down CAA severity and disease progression. In practice, strategies targeting the downstream ECM modulators and pro-fibrotic genes would be a safer option than interfering with the TGF β signaling. For example PSTG2 (COX-2) inhibitor celecoxib can lower FN1 and Col1 expression and attenuate the vessel wall thickness in stroke-prone spontaneously hypertensive rats (58).

Amyloid lowering therapy

Anti-A β immunotherapy

Two strategies of A β vaccination have been tried in AD clinical trial, either active immunization with A β species to trigger a host immune response, or passive immunization by direct infusion of anti-A β antibodies.

But although anti-A β immunotherapies are effective in removing parenchymal A β , an increase in CAA pathology is observed, implicating a TGF β upregulation. Amyloid-related imaging abnormalities (or ARIA) in amyloid-modifying therapeutic trials are a major concern and multiple studies indicate that vascular amyloid is the common pathophysiological mechanism behind ARIA (59). At autopsy, A β vaccination consistently induced a removal of parenchymal plaques and an increase in amyloid vascular deposition in brains of clinical trial participants (60,61). Anti-A β immunotherapy in old AD transgenic mice had similar effects, with a worsening in CAA pathology and hemorrhages with longer treatment. Interestingly this phenotype is again triggered by a change in the inflammatory state characterized by TGF β upregulation (62).

A first immunotherapy trial for probable CAA patients with Ponezumab, an antibody-targeting A β 40, was launched by Pfizer in 2013 (NCT01821118; <https://clinicaltrials.gov>). After promising results in mouse models with CAA pathology (63), infusions of humanized ponezumab or placebo were evaluated for changes in occipital vascular reactivity by BOLD fMRI (primary endpoint). Although Ponezumab was well tolerated and showed drug-placebo differences, it did not meet the primary endpoint and the trial was stopped in 2016 in phase II (results not yet published; (64)). The pathological effect of this therapy is unknown with the current biomarkers and understanding of pathomechanisms. Based on the loss of cerebrovascular reactivity in the treated patients (65) one might speculate that the treatment resulted in a possible aggravation of the CAA pathology similarly to the AD clinical trial observations. In the light of this thesis and previous literature (66), the loss of cerebrovascular reactivity could be associated with an increase in TGF β mediated vascular fibrosis.

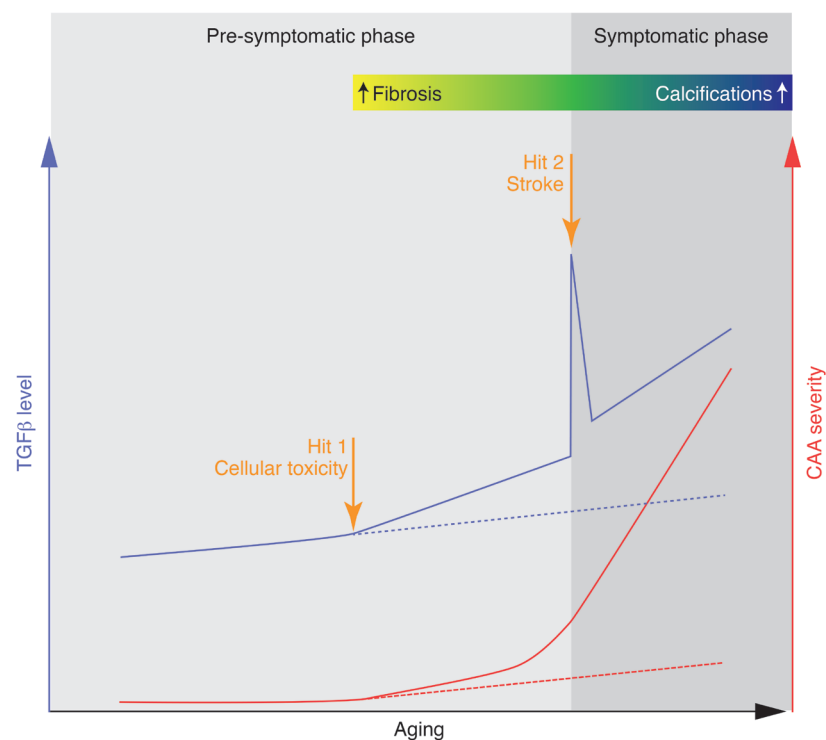
Other anti-A β strategies

Dutch amyloid seeds are harmful and irreversible due to a prion-like effect on WT A β (67), therefore an early intervention is preferable. One strategy, recently described for AD (68) and currently developed in our group for HCHWA-D, uses APP exon skipping to reduce the total A β secretion. Targeting cerebral genes with exon skipping is feasible and already in clinical trial for Huntington's Disease, where a recent clinical trial showed very promising results (69,70).

Alternative therapeutic strategies

Even though early anti-A β treatments are likely to be beneficial, therapeutic strategies uniquely focused on amyloid reduction will never completely prevent the CAA pathology in the context of vascular fibrosis. The complexity of CAA pathologies when amyloid deposition and cerebrovascular fibrosis are mixed is illustrated by studies in bitransgenic APP/TGF β (A/T) mice (71). Therapies which were beneficial in single APP or TGF β mice have a different outcome in A/T mice because vascular impairment caused by A β and TGF β are mechanistically different (72). In HCHWA-D and particularly in sporadic CAA, where ageing plays an important role, combinatorial therapeutic treatments simultaneously targeting soluble toxic amyloid species (such as Taxifolin targeting oA β s (73)) and preventing the cerebrovascular remodeling would in all likelihood be more effective than single target treatments.

- TGF β lowering therapies in brain should be considered with care
- Treatment to reduce the cerebrovascular fibrosis would be a safer option
- Early anti-A β intervention is preferable



Graphic summary: hypothetical pathomechanisms linking brain TGF β increase with CAA progression. An early response to cellular toxicity could initiate the TGF β increase (Hit 1) and trigger the vascular fibrosis in the pre-symptomatic phase. Acute stroke-related TGF β increase (Hit 2) could further accelerate the disease progression; leading in final stage to calcification of some angiopathic vessels.

References

- Vinters H V., Natté R, Maat-Schieman MLC, Van Duinen SG, Hegeman-Kleinn I, Welling-Graafland C, et al. Secondary microvascular degeneration in amyloid angiopathy of patients with hereditary cerebral hemorrhage with amyloidosis, Dutch type (HCHWA-D). *Acta Neuropathol.* 1998 Mar;95(3):235–44.
- Koemans EA, van Etten ES, van Opstal AM, Labadie G, Terwindt GM, Wermer MJH, et al. Innovative Magnetic Resonance Imaging Markers of Hereditary Cerebral Amyloid Angiopathy at 7 Tesla. *Stroke.* 2018 Apr; 49(6):1518–20.
- Mohler ER, Adam LP, McClelland P, Graham L, Hathaway DR. Detection of osteopontin in calcified human aortic valves. *Arterioscler Thromb Vasc Biol.* 1997 Mar;17(3):547–52.
- Mccullumsmith RE, Hammond JH, Shan D, Meador-Woodruff JH. Postmortem brain: An underutilized substrate for studying severe mental illness. *Neuropsychopharmacology.* 2014 Jan;39(1):65–87.
- Tomita H, Vawter MP, Walsh DM, Evans SJ, Choudary P V., Li J, et al. Effect of agonal and postmortem factors on gene expression profile: Quality control in microarray analyses of postmortem human brain. *Biol Psychiatry.* 2004 Feb 15;55(4):346–52.
- Vivien D, Ali C. Transforming growth factor- β signalling in brain disorders. *Cytokine Growth Factor Rev.* 2006;17(1–2):121–8.
- Buckwalter M, Pepper JP, Gaertner RF, Von Euw D, Lacombe P, Wyss-Coray T. Molecular and functional dissection of TGF- β 1-induced cerebrovascular abnormalities in transgenic mice. In: *Annals of the New York Academy of Sciences.* 2002. p. 87–95.
- Buckwalter MS, Wyss-Coray T. Modelling neuroinflammatory phenotypes in vivo. *J Neuroinflammation.* 2004 Jul 1;1(1):10.
- Wyss-Coray T, Lin C, Sanan DA, Mucke L, Masliah E. Chronic overproduction of transforming growth factor- β 1 by astrocytes promotes Alzheimer's disease-like microvascular degeneration in transgenic mice. *Am J Pathol.* 2000 Jan;156(1):139–50.
- Ueberham U, Ueberham E, Brückner MK, Seeger G, Gärtner U, Gruschka H, et al. Inducible neuronal expression of transgenic TGF- β 1 in vivo: Dissection of short-term and long-term effects. *Eur J Neurosci.* 2005 Jul;22(1):50–64.
- Maat-Schieman MLC, Yamaguchi H, Hegeman-Kleinn IM, Welling-Graafland C, Natté R, Roos RAC, et al. Glial reactions and the clearance of amyloid β protein in the brains of patients with hereditary cerebral hemorrhage with amyloidosis-Dutch type. *Acta Neuropathol.* 2004 May;107(5):389–98.
- van Duinen SG, Maat-Schieman MLC, Buijn JA, Haan J, Roos RAC, Wattendorff AR, et al. Cortical Tissue of Patients With Hereditary Cerebral-Hemorrhage With Amyloidosis (Dutch) Contains Various Extracellular-Matrix Deposits. *Lab Invest.* 1995 Aug;73(2):183–9.
- Wilhelmus MMM, Bol JGJM, van Duinen SG, Drukarch B. Extracellular matrix modulator lysyl oxidase colocalizes with amyloid-beta pathology in Alzheimer's disease and hereditary cerebral hemorrhage with amyloidosis-Dutch type. *Exp Gerontol.* 2013 Feb;48(2):109–14.
- Colton CA. Heterogeneity of microglial activation in the innate immune response in the brain. *J Neuroimmune Pharmacol.* 2009 Dec;4(4):399–418.

15. Heneka MT, Carson MJ, Khoury J El, Landreth GE, Brosseron F, Feinstein DL, et al. Neuroinflammation in Alzheimer's disease. *Lancet Neurol.* 2015;14(4):388–405.
16. Natté R, Maat-Schieman MLC, Haan J, Bornebroek M, Roos RAC, Van Duinen SG. Dementia in hereditary cerebral hemorrhage with amyloidosis-Dutch type is associated with cerebral amyloid angiopathy but is independent of plaques and neurofibrillary tangles. *Ann Neurol.* 2001 Dec;50(6):765–72.
17. Hawkes CA, McLaurin J. Selective targeting of perivascular macrophages for clearance of β -amyloid in cerebral amyloid angiopathy. *Proc Natl Acad Sci.* 2009;106(4):1261–6.
18. Town T, Laouar Y, Pittenger C, Mori T, Szekely CA, Tan J, et al. Blocking TGF- β -Smad2/3 innate immune signaling mitigates Alzheimer-like pathology. *Nat Med.* 2008;14(6):681–7.
19. Lifshitz V, Weiss R, Benromano T, Kfir E, Blumenfeld-Katzir T, Tempel-Brami C, et al. Immunotherapy of cerebrovascular amyloidosis in a transgenic mouse model. *Neurobiol Aging.* 2012 Feb;33(2):432.e1-432.e13.
20. Vinters H V. Inflammation complicates an “age-related” cerebral microangiopathy. *Can J Neurol Sci.* 2011 Jul;38(4):543–4.
21. Viola KL, Klein WL. Amyloid β oligomers in Alzheimer's disease pathogenesis, treatment, and diagnosis. *Acta Neuropathol.* 2015;129(2):183–206.
22. DiChiara T, DiNunno N, Clark J, Bu R Lo, Cline EN, Rollins MG, et al. Alzheimer's Toxic Amyloid Beta Oligomers: Unwelcome Visitors to the Na/K ATPase α 3 Docking Station. *Yale J Biol Med.* 2017 Mar;90(1):45–61.
23. Kassler K, Horn AHC, Sticht H. Effect of pathogenic mutations on the structure and dynamics of Alzheimer's A β 42-amyloid oligomers. *J Mol Model.* 2010 May;16(5):1011–20.
24. Miravalle L, Tokuda T, Chiarle R, Giaccone G, Bugiani O, Tagliavini F, et al. Substitutions at codon 22 of Alzheimer's β peptide induce diverse conformational changes and apoptotic effects in human cerebral endothelial cells. *J Biol Chem.* 2000 Sep 1;275(35):27110–6.
25. Ohshima Y, Taguchi K, Mizuta I, Tanaka M, Tomiyama T, Kametani F, et al. Mutations in the β -amyloid precursor protein in familial Alzheimer's disease increase A β oligomer production in cellular models. *Heliyon.* 2018;(October 2017):e00511.
26. Sian a K, Frears ER, El-Agnaf OM, Patel BP, Manca MF, Siligardi G, et al. Oligomerization of β -amyloid of the Alzheimer's and the Dutch-cerebral-haemorrhage types. *Biochem J.* 2000;349:299–308.
27. Gandy S, Simon AJ, Steele JW, Lublin AL, Lah JJ, Walker LC, et al. Days to criterion as an indicator of toxicity associated with human Alzheimer amyloid- β oligomers. *Ann Neurol.* 2010 Aug;68(2):220–30.
28. Umeda T, Tomiyama T, Sakama N, Tanaka S, Lambert MP, Klein WL, et al. Intraneuronal amyloid β oligomers cause cell death via endoplasmic reticulum stress, endosomal/lysosomal leakage, and mitochondrial dysfunction in vivo. *J Neurosci Res.* 2011 Jul;89(7):1031–42.
29. Viana RJS, Nunes a F, Castro RE, Ramalho RM, Meyerson J, Fossati S, et al. Tauroursodeoxycholic acid prevents E22Q Alzheimer's A β toxicity in human cerebral endothelial cells. *Cell Mol Life Sci.* 2009;66(6):1094–104.
30. Tan X-L, Xue Y-Q, Ma T, Wang X, Li JJ, Lan L, et al. Partial eNOS deficiency causes spontaneous thrombotic cerebral infarction, amyloid angiopathy and cognitive impairment. *Mol Neurodegener.* 2015;10(1):24.
31. Paris D, Ait-Ghezala G, Mathura VS, Patel N, Quadros A, Laporte V, et al. Anti-angiogenic activity of the mutant Dutch A(β) peptide on human brain microvascular endothelial cells. *Brain Res Mol Brain Res.* 2005 May 20;136(1–2):212–30.
32. Solito R, Corti F, Fossati S, Mezhericher E, Donnini S, Ghiso J, et al. Dutch and Arctic mutant peptides of β amyloid(1-40) differentially affect the FGF-2 pathway in brain endothelium. *Exp Cell Res.* 2009 Mar 1;315(3):385–95.
33. Liddel SA, Guttenplan KA, Clarke LE, Bennett FC, Bohlen CJ, Schirmer L, et al. Neurotoxic reactive astrocytes are induced by activated microglia. *Nature.* 2017;541(7638):481–7.
34. Diniz LP, Tortelli V, Matias I, Morgado J, Bergamo Araujo AP, Melo HM, et al. Astrocyte Transforming Growth Factor Beta 1 Protects Synapses against A β Oligomers in Alzheimer's Disease Model. *J Neurosci.* 2017 Jul;37(28):6797–809.
35. van der Wal EA, Gomez-Pinilla F, Cotman CW. Transforming growth factor- β 1 is in plaques in Alzheimer and Down pathologies. *Neuroreport.* 1993 Jan;4(1):69–72.
36. Mousseau DD, Chapelsky S, De Crescenzo G, Kirkitadze MD, Magoon J, Inoue S, et al. A direct interaction between transforming growth factor (TGF)- β s and amyloid- β protein affects fibrillogenesis in a TGF- β receptor-independent manner. *J Biol Chem.* 2003 Oct 3;278(40):38715–22.
37. Huang SS, Huang FW, Xu J, Chen S, Hsu CY. Amyloid β -Peptide Possesses a Transforming Growth Factor- β Activity *. *J Biol Chem.* 1998;273(42):27640–4.
38. Bornebroek M, Von Dem Borne PAK, Haan J, Meijers JCM, Van Nostrand WE, Roos RAC. Binding of amyloid β precursor protein to coagulation factor XIa in vivo may favour haemorrhagic stroke. *J Neurol.* 1998 Feb;245(2):111–5.
39. Rozemuller AJ, Roos RA, Bots GT, Kamphorst W, Eikelenboom P, Van Nostrand WE. Distribution of β A4 protein and amyloid precursor protein in hereditary cerebral hemorrhage with amyloidosis-Dutch type and Alzheimer's disease. *Am J Pathol.* 1993;142(5):1449–57.
40. Gowert NS, Donner L, Chatterjee M, Eisele YS, Towhid ST, Münzer P, et al. Blood platelets in the progression of Alzheimer's disease. *PLoS One.* 2014;9(2).
41. Alberio L, Dale GL. Flow cytometric analysis of platelet activation by different collagen types present in the vessel wall. *Br J Haematol.* 1998 Sep;102(5):1212–8.
42. Herzig MC, Winkler DT, Burgermeister P, Pfeifer M, Kohler E, Schmidt SD, et al. A β is targeted to the vasculature in a mouse model of hereditary cerebral hemorrhage with amyloidosis. *Nat Neurosci.* 2004 Oct;7(9):954–60.
43. Herzig MC, Eisele YS, Staufienbiel M, Jucker M. E22Q-mutant A β peptide (A β Dutch) increases vascular but reduces parenchymal A β deposition. *Am J Pathol.* 2009 Mar;174(3):722–6.
44. Herzig MC, Paganetti P, Staufienbiel M, Jucker M. BACE1 and mutated presenilin-1 differently modulate A β 40 and A β 42 levels and cerebral amyloidosis in APPDutch transgenic mice. *Neurodegener Dis.* 2007 Jan;4(2–3):127–35.
45. Li H, Guo Q, Inoue T, Polito V a, Tabuchi K, Hammer RE, et al. Vascular and parenchymal amyloid pathology in an Alzheimer disease knock-in mouse model: interplay with cerebral blood flow. *Mol Neurodegener.* 2014;9:28.
46. Pezzini A, Del Zotto E, Volonghi I, Giossi A, Costa P, Padovani A. Cerebral Amyloid Angiopathy: A Common Cause of Cerebral Hemorrhage. *Curr Med Chem.* 2009 Jul;16(20):2498–513.

47. Müller K, Courtois G, Ursini MV, Schwaninger M. New Insight Into the Pathogenesis of Cerebral Small-Vessel Diseases. *Stroke*. 2017;STROKEAHA.116.012888.
48. Flanders KC, Ren RF, Lippa CF. Transforming growth factor-betas in neurodegenerative disease. *Prog Neurobiol*. 1998;54(1):71–85.
49. Doyle KP, Cekanaviciute E, Mamer LE, Buckwalter MS. TGF β signaling in the brain increases with aging and signals to astrocytes and innate immune cells in the weeks after stroke. *J Neuroinflammation*. 2010 Jan;7(1):62.
50. Cekanaviciute E, Fathali N, Doyle KP, Williams AM, Han J, Buckwalter MS. Astrocytic transforming growth factor-beta signaling reduces subacute neuroinflammation after stroke in mice. *Glia*. 2014;62(8):1227–40.
51. Dobolyi A, Vincze C, Pál G, Lovas G. The neuroprotective functions of transforming growth factor Beta proteins. *Int J Mol Sci*. 2012 Jan;13(7):8219–58.
52. Zhang ZY, Li C, Zug C, Schluesener HJ. Icaritin ameliorates neuropathological changes, TGF- β 1 accumulation and behavioral deficits in a mouse model of cerebral amyloidosis. *PLoS One*. 2014;9(8).
53. Sachdeva AK, Chopra K. Lycopene abrogates A β (1-42)-mediated neuroinflammatory cascade in an experimental model of Alzheimer's disease. *J Nutr Biochem*. 2015;26(7):736–44.
54. Li C, Zug C, Qu H, Schluesener H, Zhang Z. Hesperidin ameliorates behavioral impairments and neuropathology of transgenic APP/PS1 mice. *Behav Brain Res*. 2015;281:32–42.
55. Song L, Liu F, Liu C, Li X, Zheng S, Li Q, et al. Neuroprotective effects of SMADs in a rat model of cerebral ischemia/reperfusion. *Neural Regen Res*. 2015;10(3):438.
56. Lively S, Schlichter LC. Age-Related Comparisons of Evolution of the Inflammatory Response After Intracerebral Hemorrhage in Rats. *Transl Stroke Res*. 2012;3(SUPPL. 1):132–46.
57. Buga AM, Margaritescu C, Scholz CJ, Radu E, Zelenak C, Popa-Wagner A. Transcriptomics of post-stroke angiogenesis in the aged brain. *Front Aging Neurosci*. 2014;6(MAR):1–20.
58. Tang J, Xiao W, Li Q, Deng Q, Chu X, Chen Y, et al. A Cyclooxygenase-2 Inhibitor Reduces Vascular Wall Thickness and Ameliorates Cognitive Impairment in a Cerebral Small Vessel Diseases Rat Model. Vol. 12, *Current Alzheimer Research*. 2015. p. 704–10.
59. Sperling RA, Jack CRJ, Black SE, Frosch MP, Greenberg SM, Hyman BT, et al. Amyloid-related imaging abnormalities in amyloid-modifying therapeutic trials: recommendations from the Alzheimer's Association Research Roundtable Workgroup. *Alzheimers Dement*. 2011 Jul;7(4):367–85.
60. Zotova E, Bharambe V, Cheaveau M, Morgan W, Holmes C, Harris S, et al. Inflammatory components in human Alzheimer's disease and after active amyloid-42 immunization. *Brain*. 2013 Aug 13;
61. Boche D, Zotova E, Weller RO, Love S, Neal JW, Pickering RM, et al. Consequence of A β immunization on the vasculature of human Alzheimer's disease brain. *Brain*. 2008 Dec;131(Pt 12):3299–310.
62. Wilcock DM, Rojiani A, Rosenthal A, Subbarao S, Freeman MJ, Gordon MN, et al. Passive immunotherapy against A β in aged APP-transgenic mice reverses cognitive deficits and depletes parenchymal amyloid deposits in spite of increased vascular amyloid and microhemorrhage. Vol. 1, *Journal of Neuroinflammation*. London; 2004. p. 24.
63. Bales KR, O'Neill SM, Pozdnyakov N, Pan F, Caouette D, Pi Y, et al. Passive immunotherapy targeting amyloid- β reduces cerebral amyloid angiopathy and improves vascular reactivity. *Brain*. 2016;139(2):563–77.
64. Banerjee G, Carare R, Cordonnier C, Greenberg SM, Schneider JA, Smith EE, et al. The increasing impact of cerebral amyloid angiopathy: Essential new insights for clinical practice. *J Neurol Neurosurg Psychiatry*. 2017;88(11):982–94.
65. Leurent C, Goodman JA, Zhang Y, He P, Polimeni JR, Gurol ME, et al. Immunotherapy with ponezumab for probable cerebral amyloid angiopathy. *Ann Clin Transl Neurol*. 2019;6(4):795–806.
66. Tong X-K. Vascular Remodeling versus Amyloid β -Induced Oxidative Stress in the Cerebrovascular Dysfunctions Associated with Alzheimer's Disease. *J Neurosci*. 2005 Nov 30;25(48):11165–74.
67. Condello C, Lemmin T, Stöhr J, Nick M, Wu Y, Maxwell AM, et al. Structural heterogeneity and intersubject variability of A β in familial and sporadic Alzheimer's disease. *Proc Natl Acad Sci*. 2018;201714966.
68. Chang JL, Hinrich AJ, Roman B, Norrbom M, Rigo F, Marr RA, et al. Targeting Amyloid-beta Precursor Protein, APP, Splicing with Antisense Oligonucleotides Reduces Toxic Amyloid-beta Production. *Mol Ther*. 2018 Jun;26(6):1539–51.
69. Rutten JW, Dauwerse HG, Peters DJM, Goldfarb A, Venselaar H, Haffner C, et al. Therapeutic NOTCH3 cysteine correction in CADASIL using exon skipping: In vitro proof of concept. *Brain*. 2016 Apr;139(4):1123–35.
70. Toonen LJA, Rigo F, van Attikum H, van Roon-Mom WMC. Antisense Oligonucleotide-Mediated Removal of the Polyglutamine Repeat in Spinocerebellar Ataxia Type 3 Mice. *Mol Ther Nucleic Acids*. 2017 Sep;8:232–42.
71. Ongali B, Nicolakakis N, Lecrux C, Aboukassim T, Rosa-Neto P, Papadopoulos P, et al. Transgenic mice overexpressing APP and transforming growth factor- β 1 feature cognitive and vascular hallmarks of Alzheimer's disease. *Am J Pathol*. 2010 Dec;177(6):3071–80.
72. Hamel E. Cerebral Circulation: Function and Dysfunction in Alzheimer's Disease. *J Cardiovasc Pharmacol*. 2015;65(4):317–24.
73. Saito S, Yamamoto Y, Maki T, Hattori Y, Ito H, Mizuno K, et al. Taxifolin inhibits amyloid- β oligomer formation and fully restores vascular integrity and memory in cerebral amyloid angiopathy. *Acta Neuropathol Commun*. 2017;5(1):26.

Summary

Hereditary cerebral hemorrhage with amyloidosis–Dutch type (HCHWA-D) is an early onset hereditary form of Cerebral amyloid angiopathy (CAA) caused by a point mutation of the Amyloid Precursor protein (APP). CAA refers to the accumulation of amyloid β ($A\beta$) peptide, resulting from APP protein cleavage, in intracerebral vessels. CAA pathology is present in the majority of Alzheimer's disease (AD) brains and is associated with intracerebral hemorrhages in the elderly. The general aim of this thesis is to decipher the molecular pathogenesis of HCHWA-D. Since no proven therapeutic treatment exists to prevent or even delay the disease onset, the understanding of underlying pathomechanisms in HCHWA-D is important. It may help discovering new therapeutic targets and biomarkers that can be used to assess the efficacy of candidate drugs in treatment trials.

Chapter 1 is a general introduction of HCHWA-D covering the clinicopathological and neuropathological aspects of the disease as well as the known pathogenesis and the importance of HCHWA-D studies for the CAA field. **Chapter 2** reviews other hereditary APP mutations and describes how the $A\beta$ mutation of HCHWA-D patients modifies $A\beta$ properties regarding aggregation, binding to cerebral vessel wall cells, interplay with extracellular matrix, proteolysis, and clearance, and how these altered characteristics lead to HCHWA-D pathogenesis.

Former research in the CAA field indicates the existence of factors able to influence $A\beta$ accumulation predominantly in vessels rather than in brain parenchyma, such as $TGF\beta$. Identification of aggravating factors of CAA pathology are therapeutic target of interest and therefore we explored in **Chapter 3** the $TGF\beta$ pathway deregulation in HCHWA-D. We discovered that in HCHWA-D brain material $TGF\beta 1$, its receptors and $TGF\beta$ -induced genes are upregulated. Using histology and compared to sporadic CAA, the actual activation of the $TGF\beta$ signaling cascade in the hereditary form is confirmed by the accumulation of its activated transcription factor phospho-SMAD2/3 (pSMAD2/3) in some angiopathic vessels which also correlates with the disease severity.

Understanding the underlying pathology of neuroimaging features in patients is essential for a precise diagnostic and follow-up of the disease. Therefore we investigated a recently described MRI neuroimaging feature of advanced disease stage in HCHWA-D. We used an histopathologic correlates in **Chapter 4** to reveal that cerebrovascular iron accumulation and calcification are the cause of the *in vivo* observed MRI abnormalities. We identified calcifications as a novel MRI marker of interest for clinical CAA severity evaluation in hereditary as well as sporadic CAA patients.

Because calcifications are a feature of severe CAA pathology (Chapter 4) and CAA severity is linked with TGF β deregulation (Chapter 3), we investigated in **Chapter 5** the calcified CAA vessels in HCHWA-D with a focus on TGF β -related disease progression. Besides pSMAD2/3 immunomarker, we quantified in patients with different severity the presence of osteopontin (OPN) and collagen 1 (col1), potential modulators of vascular calcification responsive to TGF β . We described an accumulation of OPN and pSMAD2/3 in calcified CAA vessels as well as the association of col1 protein, a fibrotic protein with vascular amyloid load. Chapter 5 tightly link the TGF β pathway deregulation to CAA progression and calcification in HCHWA-D.

Finally, **Chapter 6** is an transcriptomic study in human *post mortem* brain to identify major deregulated pathways in HCHWA-D and broaden our comprehension of molecular pathogenesis. By comparing the changes that we found in the human transcriptome with the transcriptome of young APP-E693Q mice at the pathway level, we could identify an overlap in the upregulation of ECM-related pathways, which is in mice prior to the onset of CAA pathology and suggests an early TGF β 1-mediated fibrosis. In addition, we identified a mitochondrial dysfunction, a feature of neurodegenerative diseases not yet described in HCHWA-D.

The discussion in **Chapter 7** summarizes the main finding of this thesis namely that TGF β deregulation plays a central role in HCHWA-D pathogenesis. Therefore the beneficial and detrimental aspects of TGF β on the vascular and parenchymal brain components are reviewed and the possible causes of TGF β activation in HCHWA-D as well as its implication for future studies and therapeutic intervention are discussed.

Nederlandse samenvatting

Hereditary cerebral hemorrhage with amyloidosis (Dutch) (HCHWA-D) is een erfelijke vorm van cerebrale amyloid angiopathie (CAA) die relatief vroeg in het leven ontstaat en veroorzaakt wordt door een puntmutatie in het amyloid precursor eiwit (APP). Doordat APP door enzymen wordt geknipt, wordt het kleinere amyloid β ($A\beta$) eiwit gevormd. Bij CAA hoopt dit eiwit op in bloedvaten in de hersenen. Naast deze erfelijke vorm is CAA ook aanwezig in de meeste patiënten met de ziekte van Alzheimer. CAA wordt gezien als een belangrijke oorzaak van hersenbloedingen bij ouderen. Het doel van dit proefschrift is om de moleculaire pathogenese van CAA in HCHWA-D patiënten in kaart te brengen. Omdat er nog geen behandeling bestaat om deze ziekte te voorkomen of zelfs te vertragen, is het belangrijk om de onderliggende mechanismen van HCHWA-D te begrijpen. Deze kennis kan helpen om nieuwe therapeutische aangrijpingspunten te vinden en biomarkers te onderzoeken die gebruikt kunnen worden om de werking van mogelijke geneesmiddelen te bekijken.

Hoofdstuk 1 is een algemene introductie over HCHWA-D, waarin de klinische, pathologische en neuropathologische aspecten van de ziekte worden beschreven. Daarnaast is gekeken naar wat bekend is over de pathogenese en naar het belang van HCHWA-D studies voor onderzoek naar CAA in het algemeen.

Hoofdstuk 2 geeft een overzicht van andere erfelijke APP-mutaties en beschrijft hoe de mutatie van HCHWA-D-patiënten de $A\beta$ -eigenschappen verandert met betrekking tot aggregatie, binding aan cerebrale bloedvaten, wisselwerking met extracellulaire matrix, proteolyse en klaring, en hoe deze veranderde kenmerken tot de HCHWA-D pathogenese leiden.

Uit eerder onderzoek naar CAA bleek al dat er factoren zijn die er voor zorgen dat $A\beta$ hoofdzakelijk ophoopt in de bloedvaten en niet in het hersenparenchym. Een voorbeeld hiervan is TGF β . Zulke factoren zijn interessante therapeutische targets en daarom hebben we in **hoofdstuk 3** de deregulatie van de TGF β cascade in HCHWA-D onderzocht. In HCHWA-D breinmateriaal hebben we gevonden dat TGF β 1, de receptoren hiervan en TGF β -geïnduceerde genen zijn verhoogd. De activatie van de TGF β cascade in erfelijke CAA blijkt ook uit de ophoping van de geactiveerde transcriptiefactor phospho-SMAD2/3 (pSMAD2/3) in sommige angiopathische bloedvaten, wat ook correleert met de ernst van de ziekte.

Het begrijpen van de onderliggende pathologie van kenmerkende verschijnselen op MRI beelden van patiënten zijn essentieel voor een goede diagnostiek en het volgen van de ziekte over de tijd. Daarom hebben we een recent beschreven MRI verschijnsel van een gevorderd stadium van de ziekte in HCHWA-D onderzocht. Hiervoor hebben we in **hoofdstuk 4**

histopathologische correlaties gebruikt om aan te tonen dat cerebrovasculaire ijzerophoping en calcificatie de oorzaak zijn van veranderingen in de MRI-beelden van patiënten. Hierdoor zijn calcificaties een nieuwe interessante MRI-marker voor evaluatie van de ernst van CAA in erfelijke, maar ook in sporadische CAA patiënten.

In **hoofdstuk 5** hebben we de mechanismen onderzocht van de calcificatie van CAA vaten in HCHWA-D. In patiënten met verschillende stadia van CAA hebben we de aanwezigheid van osteopontin (OPN) en collageen 1 (col1) gekwantificeerd. Dit zijn potentiële regelaars van calcificatie in de bloedvaten, bekend van perifere vasculaire calcificatie. De ophoping van OPN en col1 is sterk geassocieerd met pSMAD2/3 in gecalcificeerde CAA vaten, waardoor calcificatie nu gelinkt kan worden aan de eerder gevonden deregulatie van de TGF β pathway.

Tenslotte hebben we in **hoofdstuk 6** een transcriptoom studie gedaan om belangrijke ontregelingen van moleculaire routes in HCHWA-D te identificeren en de pathogenese beter te begrijpen. Door het menselijk transcriptoom te vergelijken met dat van jonge APP-E693Q muizen op het niveau van ontregelde moleculaire routes, konden we een overlap vinden in de activering van routes die gerelateerd zijn aan de extracellulaire matrix. In muizen zijn deze routes al bij het begin van de CAA pathologie afwijkend, wat suggereert dat TGF β 1-gemedieerde fibrose een vroeg proces is in het verloop van de ziekte. Daarnaast hebben we gezien dat mitochondriale disfunctie een belangrijk ziekteverschijnsel is, wat nog niet eerder beschreven was in HCHWA-D.

De discussie in **hoofdstuk 7** geeft een samenvatting van de belangrijkste bevindingen in dit proefschrift, namelijk dat TGF β -verstoring een centrale rol speelt in de HCHWA-D pathogenese. Daarom worden de gunstige en nadelige aspecten van TGF β op de vasculaire en parenchymale hersencomponenten besproken en worden de mogelijke oorzaken van TGF β -activering in HCHWA-D en de implicatie daarvan voor toekomstige studies en therapeutische interventie besproken.

List of publications

Grand Moursel L, van der Graaf, LM, Bulk M, van Roon-Mom WMC and van der Weerd L. Osteopontin and pSMAD2/3 are associated with calcification of vessels in hereditary cerebral amyloid angiopathy. *Brain Pathol.* (2019).

Grand Moursel L, van Roon-Mom WMC, Kielbasa SM, Mei H, Buermans HPJ, van der Graaf LM, Hettne KM, de Meijer EJ, van Duinen SG, Laros JFJ, van Buchem MA, 't Hoen PAC, van der Maarel SM and van der Weerd L. Brain Transcriptomic Analysis of Hereditary Cerebral Hemorrhage With Amyloidosis-Dutch Type. *Front. Aging Neurosci.* (2018).

Grand Moursel L, Munting LP, van der Graaf LM, van Duinen SG, Goumans M-JTH, Ueberham U, Natté R, van Buchem MA, van Roon-Mom WMC, van der Weerd L. TGFbeta pathway deregulation and abnormal phospho-SMAD2/3 staining in hereditary cerebral hemorrhage with amyloidosis-Dutch type. *Brain Pathol.* (2017).

Bulk M, **Grand Moursel L**, van der Graaf, LM, Van der Veluw SJ, Greenberg SM, van Duinen SG, van Buchem MA, van Rooden S, van der Weerd L. Cerebral Amyloid Angiopathy With Vascular Iron Accumulation and Calcification A High-Resolution Magnetic Resonance Imaging Histopathology Study. (2018).

Bossoni L, **Grand Moursel L**, Bulk M, Simon BG, Webb A, van der Weerd L et al. Human-brain ferritin studied by muon spin rotation: a pilot study. *J. Phys. Condens. Matter.* (2017).

Rotman M, Welling MM, van den Boogaard ML, **Grand Moursel L**, van der Graaf LM, van Buchem MA, van der Maarel SM, van der Weerd L. Fusion of hIgG1-Fc to 111 in-anti-amyloid single domain antibody fragment VHH-pa2H prolongs blood residential time in APP/PS1 mice but does not increase brain uptake. *Nucl Med Biol.* (2015).

Kamp JA, **Grand Moursel L**, Haan J, Terwindt GM, Lesnik Oberstein SA, van Duinen SG, van Roon-Mom WM, Amyloid β in hereditary cerebral hemorrhage with amyloidosis-Dutch type. *Rev. Neurosci.* (2014).

De Morrée A, Flix B, Bagaric I, Wang J, van den Boogaard M, **Grand Moursel L**, Frants RR, Illa I, Gallardo E, Toes R, van der Maarel SM, Dysferlin regulates cell adhesion in human monocytes. *J Biol Chem.*(2013).

De Morrée A, Droog M, **Grand Moursel L**, Bisschop IJ, Impagliazzo A, Frants RR, Klooster R, van der Maarel SM, Self-regulated alternative splicing at the AHNAK locus. *FASEB J.* (2012).

Chautard H, Blas-Galindo E., Menguy T, **Grand Moursel L**, Cava F, Berenguer J & Delcourt M, An activity-independent selection system of thermostable protein variants. *Nat Methods.* (2007).

List of abbreviations

AD	Alzheimer's disease
ApoE	Apolipoprotein E
APP	Amyloid precursor protein
A β	Amyloid beta
ARIA	Amyloid-related imaging abnormalities
BACE	Beta-secretase
BOLD fMRI	Blood-Oxygen-Level Dependent functional MRI
BSA	Bovine serum albumin
CAA	Cerebral amyloid angiopathy
CADASIL	Cerebral autosomal dominant arteriopathy with subcortical infarcts and leukoencephalopathy
capCAA	Capillary cerebral amyloid angiopathy
CARASIL	Cerebral autosomal recessive arteriopathy with subcortical infarcts and leukoencephalopathy
CNS	Central nervous system
Col	Collagen
CR1	Complement component receptor 1 gene
CSF	Cerebrospinal fluid
DAB	3,3'-Diaminobenzidine
DEG	differentially expressed gene
E	Acid glutamic
ECM	Extracellular matrix
ECs	endothelial cells
EGCG	Epigallocatechin-gallate
ER	Endoplasmic reticulum
FC	Fold change
FDR	False discovery rate
FN1	Fibronectin
FN1	Fibronectin
GAG	Glycosaminoglycan
GFAP	Glial fibrillary acidic protein
Gln	Glutamine
Glu	Acid glutamic
GSEA	Gene Set Enrichment Analysis
HCHWA-D	Hereditary cerebral hemorrhage with amyloidosis-Dutch type
HD	Parkinson disease

HE	Hematoxylin & eosin
HRP	Horseradish peroxidase
HSP	Heat Shock Protein
HSPG	Heparan sulphate proteoglycan
ICH	Intracerebral hemorrhages
LOX	Lysyl oxidase
MGE	Multiple Gradient Echo
MMP	Matrix Metalloproteinase
MRI	Magnetic resonance imaging
NBB	Netherlands Brain Bank
NDC	Non-demented control
NVU	Neurovascular unit
oA β s	Oligomeric A β species
OPN	Osteopontin
PAI-1	Plasminogen activator inhibitor-1
PCA	Principal component analysis
PD	Parkinson disease
PiB	Pittsburgh compound B
PMD	<i>Post mortem</i> delay
PS	Presenilin
pSMAD2/3	phosphoSMAD2/3
pTau	Hyperphosphorylated Tau
Q	Glutamine
qPCR	Quantitative reverse transcriptase-PCR
RIN	RNA integrity number
rRNA	Ribosomal RNA
RT	Room temperature
sCAA	Sporadic Cerebral amyloid angiopathy
SD	Standard deviation
SMAD	Homolog of Drosophila mothers against decapentaplegic
SMA	Smooth muscle actin
SMC	Smooth muscle cells
SPP1	Secreted phosphoprotein 1
T	Tesla
TE	Echo time
TGFBRs	TGF β receptors
TGF β	Transforming growth factor β
TOMM40	Translocase of outer mitochondrial membrane 40

TR	Repetition time
TSA	Tyramide Signal Amplification
tTG	Tissue transglutaminase
TUDCA	Tauroursodeoxycholic acid
uPA	Urokinase-type plasminogen activator
VSMCs	Vascular smooth muscle cells
WMHs	White matter hyperintensities
μ CT	Micro computed tomography

Curriculum vitae

Laure Grand Moursel was born on the 18th of March, 1979, in Angouleme, France. She completed her education in France (Master of science degree at Paris 7 University in 2003) and worked five years at Biomethodes (Evry, France), a biotechnology company specialized in the directed evolution of proteins. In 2009 she moved to the Netherlands where she started to work at the Leiden University Medical Center, in the Proteomics group of professor Silvére van der Maarel (Human Genetics department) where she specialized in the development of Heavy Chain antibodies (also known as VHH). In January 2013, she started a PhD in Neurosciences with a focus on Hereditary cerebral hemorrhage with amyloidosis–Dutch type (HCHWA-D) under the combined guidance of associate professor Louise van der Weerd (Radiology department) and associate professor Willeke van Roon-Mom (Human Genetics department) and under the lead of Professor Mark van Buchem, MD (Chair of Radiology department). In November 2018, she started as a senior scientist at Charles River Laboratories in Leiden.

Acknowledgements

Writing the last chapter of this PhD thesis feels like turning a chapter in my life. Both exciting and frightening, both a relief and a sorrow... It is time to say goodbye and thank everybody!

First of all, this thesis would not have been possible without Louise, my co-promotor, who offered me the opportunity to graduate while already working in her group. Although challenging, I had the chance to meet and collaborate with international researchers in the CAA field which was totally new to me. Louise, thank you for your support in all my projects over the years, I particularly appreciated your scientific curiosity and your enthusiasm to explore new fields.

Then, these years of graduation and this thesis would not have been the same without the essential contribution of Willeke, my second co-promotor. Willeke, thank you for your continuous encouragements, your responsiveness and your positive thinking! I learnt a lot from you and I'm deeply grateful!

Next I'm thankful to actual and former colleagues, mostly from human genetics at lab-f and lab-j who are too many to be named here, for their contribution to such a friendly working environment. I especially thank the Huntington group: Melvin, Lodewijk, Barry and Elena, thank you for your help and the nice co-working in the lab. I also warmly thank our radiology team, more specially Marjolein for her concern, help and wise advices, and Marc, Leon, Maarten, Tien, Boyd, Bauke and Ernst for having been such amazing colleagues!

Of course I do not forget Linda for her essential contribution to this work, her good mood and fantastic organization skills "You're so fast!!!". Linda, thank you for these years where we shared more than the daily work.

I also want to warmly thank Gerrit Kracht who worked on all the illustrations of this thesis.

Most importantly, my gratitude goes to Remy, my husband, who encouraged me in this adventure from its start and to Estelle, our daughter, to who I can finally answer "yes, I finished my book"! Their constant support is invaluable. I also want to thank here my family and friends for their encouragements.

Last but not least, I acknowledge the patients and their families for consenting to the use of autopsy material and I thank all the internal and external collaborators who contributed to this thesis and graduation, the co-authors for their advices and the improvements they brought to the published articles, but also the reading and opposing committee for taking the time to assess this work.

